AD_____

Award Number: DAMD17-02-1-0685

TITLE: Gene Therapy for Fracture Repair

PRINCIPAL INVESTIGATOR: William Lau, Ph.D.

CONTRACTING ORGANIZATION: Loma Linda Veterans Association
for Research and Education
Loma Linda, California 92357

REPORT DATE: May 2007

TYPE OF REPORT: Final

PREPARED FOR: U.S. Army Medical Research and Materiel Command
Fort Detrick, Maryland 21702-5012

DISTRIBUTION STATEMENT: Approved for Public Release;
Distribution Unlimited

REPORT DOCUMENTATION PAGE

Form Approved
OMB No. 0704-0188

1. REPORT DATE *(DD-MM-YYYY)* 01-05-2007	2. REPORT TYPE Final	3. DATES COVERED *(From - To)* 15 Nov 2002 – 14 Apr 2007
4. TITLE AND SUBTITLE Gene Therapy for Fracture Repair		**5a. CONTRACT NUMBER**
		5b. GRANT NUMBER DAMD17-02-1-0685
		5c. PROGRAM ELEMENT NUMBER
6. AUTHOR(S) William Lau, Ph.D. E-Mail: william.lau@va.gov		**5d. PROJECT NUMBER**
		5e. TASK NUMBER
		5f. WORK UNIT NUMBER
7. PERFORMING ORGANIZATION NAME(S) AND ADDRESS(ES) Loma Linda Veterans Association for Research and Education Loma Linda, California 92357		**8. PERFORMING ORGANIZATION REPORT NUMBER**
9. SPONSORING / MONITORING AGENCY NAME(S) AND ADDRESS(ES) U.S. Army Medical Research and Materiel Command Fort Detrick, Maryland 21702-5012		**10. SPONSOR/MONITOR'S ACRONYM(S)**
		11. SPONSOR/MONITOR'S REPORT NUMBER(S)

12. DISTRIBUTION / AVAILABILITY STATEMENT
Approved for Public Release; Distribution Unlimited

13. SUPPLEMENTARY NOTES

14. ABSTRACT

These studies examined approaches to optimize gene therapy for the repair of endochondral bone fractures. Several components of a gene therapy approach were examined, including viral vectors and associated regulatory elements, vector delivery to the fracture tissues, and the application of a combination of genes with different functions in bone formation and tissue repair. It was found that the murine leukemia-based viral vector, with transgene expression mediated by the long terminal repeat, provided more robust, though unregulated, gene expression than the lentiviral vector transgenes expressed from either non-specific or bone-specific promoters. Viral vector delivery was important in promoting fracture healing, as demonstrated through an intramedullary technique for vector application. The application of a combination of fibroblast growth factor-2 and bone morphogenetic protein-4 transgenes, that mediate proliferation and osteogenesis, respectively, suggested that combination gene therapy could be an important clinical approach for bone healing. Microarray studies also characterized global gene expression during the early inflammation phase and the later endochondral bone formation phase of normal fracture healing fracture healing. Several thousand genes displayed expression changes during fracture healing, including genes that have been associated with tissue regeneration, and identified candidates for future fracture repair studies using optimized vectors and delivery techniques.

15. SUBJECT TERMS
Wound Regeneration; Gene Therapy; MLV-based vector; Fracture Healing; BMP-4

16. SECURITY CLASSIFICATION OF:			17. LIMITATION OF ABSTRACT	18. NUMBER OF PAGES	19a. NAME OF RESPONSIBLE PERSON USAMRMC
a. REPORT U	**b. ABSTRACT** U	**c. THIS PAGE** U	UU	73	**19b. TELEPHONE NUMBER** *(include area code)*

Table of Contents

INTRODUCTION

Bone fracture is one of the most frequent injuries occurring during military training and in battle. Recent conflicts have suggested that while survival rates among wounded personnel have increased, battlefield injuries to the extremities have tended to be quite severe, often requiring extensive therapy for the repair of the wounded musculoskeletal tissues (Blanck, 1999; AAOS, 2007). However, even relatively minor but frequent minor fractures to bone can result in a loss of function with significant reductions in military preparedness. These injuries would also benefit from a therapeutic approach that produces rapid tissue repair. Any improvement in fracture therapy could yield substantial military benefits, as well as significant humanitarian and economic benefits in civilian applications (Einhorn, 1995).

Fracture repair requires a complex series of molecular events that coordinate the proliferation and differentiation of diverse periosteal tissues and bridge the injury with bone that is identical to the native bone (Bolander, 1992). Bone healing is unique in that bone normally heals without the production of a scar so common in the healing of most tissues, and is therefore more characteristic of a regenerative process. Growth factors are involved in all of these regenerative processes. To identify the molecular pathways that mediate the repair of the diverse tissues that develop in the fracture callus, the expression of growth factors and their receptors during fracture repair must first be characterized. Accordingly, different families of growth factors have been implicated that mediate diverse pathways of cell chemotaxis and tissue proliferation and differentiation during fracture repair (reviewed by Bolander, 1992, Andrew et al., 1993, Andrew et al., 1995, Barnes et al., 1999, Beasley and Einhorn, 2000). Normal endochondral bone repair is evaluated in the context of fracture tissue development (Bolander, 1992). The physiological and morphological effects following local or systemic administration of exogenous therapeutic genes can then be tested and novel therapies developed to enhance normal and impaired bone healing.

Gene therapy has tremendous potential to optimize healing in skeletal tissue injuries by delivering and expressing bone growth-promoting therapeutic genes identified in fracture and soft tissue healing expression studies. However, approaches employing gene therapy have only started to develop systems that deliver growth factor genes to injured tissues and efficiently regulate their expression in those tissues using engineered vectors. We propose to develop approaches to gene therapy that maximize the efficiency of delivery and expression of selected transgenes and thereby enhance fracture healing.

Currently, our gene therapy approach has the potential to repair large skeletal defects, certainly an advantage for the repair of severe battlefield injuries of the musculoskeletal system. Our initial studies utilized an exogenous bone morphogenetic protein (BMP)-2/4 hybrid transgene, expressed in a constitutive manner by a Murine leukemia virus (MLV)-based vector, to augment bone formation during repair in the rat femur fracture model (Rundle et al., 2003). We propose that more efficient delivery and expression of a selected growth factor gene(s) would further enhance fracture healing. Surgical techniques need to optimize the delivery of viral vectors to the periosteal tissues of healing fractures in small animals, and allow more accurate evaluation of the effects of the fracture therapy (Rundle et al., 2003). However, we also anticipate that to truly optimize gene therapy for fracture healing, multiple therapeutic genes that

modulate different cellular functions will be required to enhance fracture healing, and the expression of those therapeutic genes will need to be regulated in a gene-specific manner. It is therefore essential to have both an appropriate viral vector and an effective promoter to transduce tissues and to drive expression of therapeutic genes at the fracture site. Additionally, we have undertaken microarray studies of the fracture callus of multiple individual animal subjects to understand gene expression in the healing response to bone injury and identify novel genes that might accelerate or delay the healing of such injuries. The combination of optimal surgical delivery, efficient regulation of expression, and an optimized combination of therapeutic genes in the fracture by the appropriate viral vector will maximize the therapeutic effect for accurate measurement. These studies were undertaken to elucidate such approaches for gene therapy for musculoskeletal healing.

This project has two Technical Objectives and their respective Specific Objectives. All of the Specific Objectives of this project have largely been completed:

1. TECHNICAL OBJECTIVE 1: TO OPTIMIZE A GENE THERAPY FOR FRACTURE HEALING
    a) Specific Objective 1: To Optimize Gene Expression and Protein Production of Growth Factor genes from Periosteal Cells Transduced with MLV-based or Lentiviral-based Vectors.
    b) Specific Objective 2: To Compare the Local Periosteal Injection of the Virus at the Fracture Site with the Intramedullary Inoculation Procedure.
    c) Specific Objective 3: To Compare the Superiority of the MLV-based Versus the Lentiviral-based Vector Systems for the BMP-2/4 Transgene.
    d) Specific Objective 4: To Compare the Efficacy of the BMP-2/4 Transgene in the Optimized Vector System with that of the Combination of BMP-2/4 Transgene Plus Another Growth Factor Candidate Gene Identified by Microarray (Technical Objective 2) or Another Potent Bone Growth Factor.

2. TECHNICAL OBJECTIVE 2: TO APPLY MICROARRAY TO STUDY FRACTURE HEALING
    a) Specific Objective 1: To Extend the Number of Genes in Our Current In-house Micro-array Procedure.
    b) Specific Objective 2: To Apply Our Extended In-house Microarray to Study Gene Expression in the Fracture Callus at 3 Days After Fracture.
    c) Specific Objective 3: To Evaluate the Reproducibility and To Analyze the Data from the Extended Microarray.
    d) A Specific Objective 4 was added during the investigation: To evaluate the functional role of one or more Expressed Sequence Tags (ESTs) with altered expression during fracture healing by inhibition or augmentation of its expression *in vitro,* followed by identification of the resulting changes cellular phenotype and gene expression.

Ultimately, these findings could not only generally produce useful information to enhance fracture repair, but also help to develop genetic approaches to predict the response of individual military personnel to battlefield injury and subsequently individualize their musculoskeletal therapy.
This final report summarizes the results of all of these studies.

BODY

TECHNICAL OBJECTIVE 1: TO OPTIMIZE A GENE THERAPY FOR FRACTURE HEALING
<u>Specific Objective 1: To Optimize Gene Expression and Protein Production of Growth Factor genes from Periosteal Cells Transduced with MLV-based or HIV-based Vectors</u>

Objective:
    This goal of this study is to identify the optimum viral-based vector and regulatory (promoter) elements for fracture gene therapy by comparing transfection and expression frequencies of Murine Leukemia virus (MLV)-based and Human Immunodeficiency virus (HIV)-based gene therapy vectors and promoters in bone cells isolated from both periosteal bone surfaces.
    We focused on these two retroviral vector systems because each of these two vector systems has the capacity to accommodate large inserts that might be necessary for larger genes-of-interest, or the inclusion of regulatory elements to control expression. Both stably integrate into the host genome and can provide more prolonged transgene expression as compared to the transient transduction mediated by adenoviral and adeno-associated viral vectors. MLV-based vectors have been used extensively in gene transfer studies, and have the advantages of: 1) high viral titers that can be obtained due to their ability to withstand shearing forces encountered during ultracentrifugation; and 2) a broadened host-cell range. Their most obvious limitation is their requirement for actively proliferating cells for transduction. Another major disadvantage of MLV-based vectors is that expression from MLV-based vectors is controlled by the viral long terminal repeat (LTR) not suitable for the use of other promoters. The LTR provides very robust expression of gene inserts, but is too powerful to include any gene-specific regulatory promoter elements in the same vector, as they are simply overwhelmed by LTR-driven gene expression. This would preclude the use of tissue-specific promoters to target tissue-specific transgene expression. In contrast, the more recently developed HIV vectors have three distinct advantages over the MLV-based vectors: 1) they are capable of transducing both proliferating and non-proliferating cell types and are therefore not limited to injuries with proliferating cells; 2) because HIV LTRs are inherently less transcriptionally active than MLV LTRs, they allow regulation of the transgene expression using gene-specific and/or regulatory promoters; and 3) third-generation HIV vector LTRs are far less susceptible to transcriptional silencing as MLV LTRs. The obvious disadvantage of HIV-based vectors compared to MLV-based vectors is that the promoters of HIV-based vectors are much less potent compared to the LTRs of MLV-based vectors. Additionally, the viral titers that can be obtained with HIV-based vectors are lower than those of MLV-based vectors. The first Specific Objective of this project compared the efficiencies of various tissue-specific promoters in driving transgene expression from HIV-based vectors in the fracture repair model.


Materials and Methods:
    Periosteal and endosteal bone cells were aseptically isolated from the unfractured hindlimb bones of Sprague-Dawley rats. The femurs and tibias were removed at sacrifice, the epiphyses removed and the diaphyseal marrow ablated with saline. The diaphyses were digested with 0.25% trypsin and 0.20% collagenase II. The digests separated the periosteal and endosteal cells

from the cortical bone surfaces and yielded dispersed and heterogeneous populations of the fibroblastic and cambial cells. These adherent cells were retained in culture while nonadherent contaminating marrow cells were discarded. Cell preparations of periosteal and endosteal origins provided a representative population of cells to be targeted for viral transduction by external or internal injection techniques. These cells were cultured at a low passage number (i.e., less than passage 5) for the subsequent comparison of transgene expression from transfected MLV-based or the HIV-based vectors.

To obtain optimal estimates of the relative transgene expression efficiencies for the MLV-based and HIV-based vectors, the Enhanced Green Fluorescent Protein (EGFP) was used as a marker transgene. Vector efficiency was established by target cell EGFP expression (by FACS analysis using a FACSCalibur from BD BioSciences), which was regulated by the viral long terminal repeat (LTR) promoter in the case of the MLV-based vector, or by one of five test gene-specific promoters in the case of the HIV-based vector. These five gene-specific promoters were derived from the cytomegalovirus (CMV) (a non-specific viral promoter), elongation factor 1-α (EF-1α) (a non-specific mammalian cell promoter), collagen 1, collagen 2.3 (specific for osteoblastic cells) and core-binding factor alpha-1 (cbfa-1, runx-2) (specific for differentiated osteoblasts) genes.

Each vector and promoter-EGFP combination was transduced into the primary rat bone cell cultures in duplicate (n = 2). Additionally, the mouse osteoblast MC3T3-E1 cell line was included for comparison. Because variable transgene expression from different promoters makes the virus difficult to titer, fixed volumes (i.e., 10 µl and 50 µl) rather than fixed titers of each viral vector stock were compared for transfection and expression frequencies. The numbers of cells expressing EGFP were quantified by fluorescent cell sorting following 48 hours of culture.
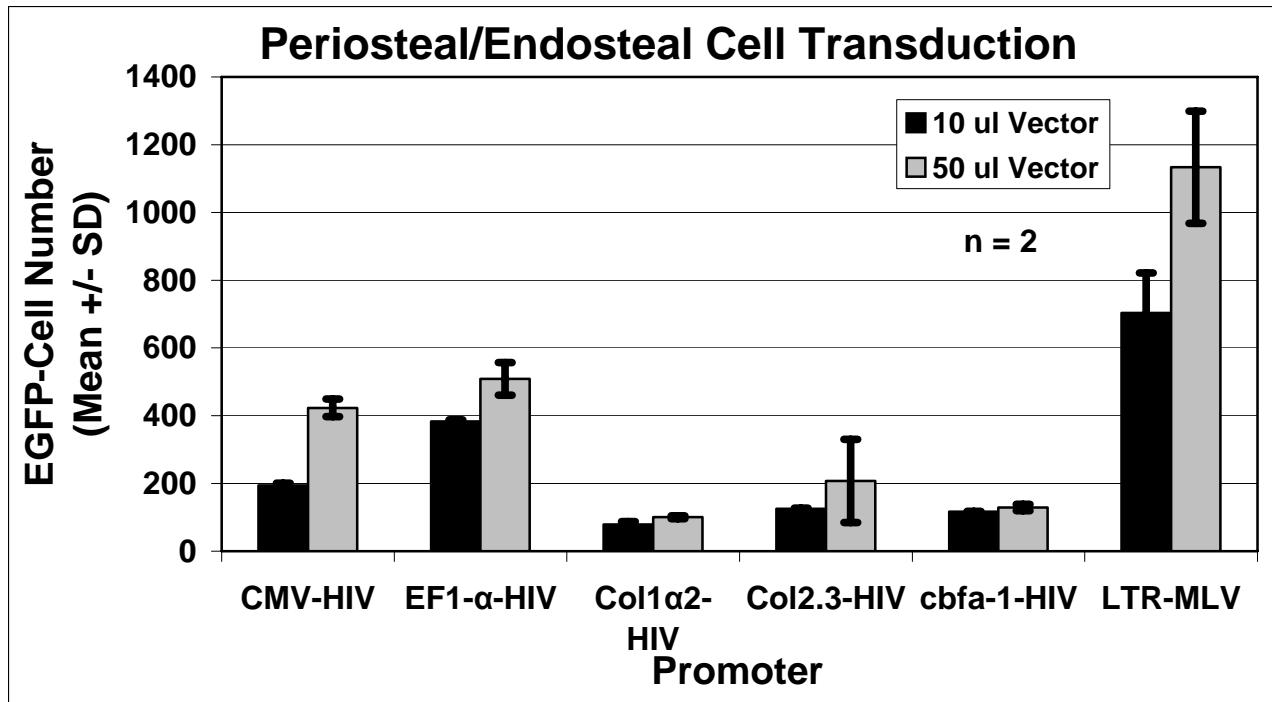
Periosteal/Endosteal Cell Transduction
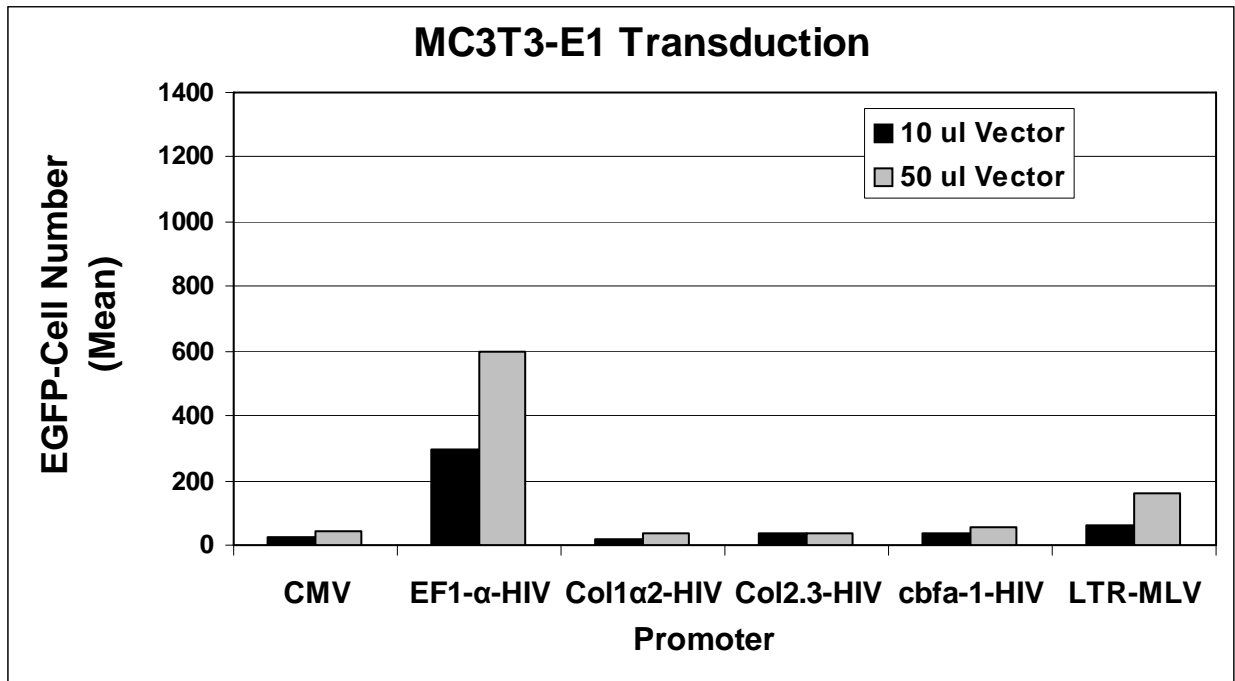
Figure 1. Mean EGFP expression in MC3T3-E1 osteoblastic cells (top) or in primary rat periosteal/endosteal bone cells (bottom) from the LTR promoter in an MLV vector, or other promoters (CMV, EF1-α, Col Iα2, Col 2.3, cbfa-1) in a HIV-based vector.

Results:

As expected, the powerful LTR promoter of the MLV-based vector provided the greatest numbers of EGFP-expressing cells in the endosteal/periosteal bone cells (Figure 1). Among the HIV-based vector promoters, the EF-1α promoter provided the best expression, with expression of the transgene than even the very robust viral CMV promoter. Surprisingly, and intriguingly, the promoters derived from genes normally associated with bone cells, but most notably the collagen 2.3 and the cbfa-1 displayed several-fold weaker transfection and expression frequencies. Similar results were also seen with the mouse osteoblastic MC3T3-E1 cells. The reason why the efficiency of transgene expression with the osteoblastic promoters in osteoblastic cells was significantly lower than those with the non-specific promoter, such as EF1-α, in the HIV-based vector backbone is not clear. However, because the exact titer of these vectors was not determined, we cannot rule out the unlikely possibility that the lower transgene expression with the osteoblastic promoter could be the results of a lower titer.

Conclusions:

These studies have confirmed that physiologically relevant regulatory and/or tissue-specific promoters can be used to drive transgene expression in the HIV-based vector. A surprising finding of these studies was that the efficiency of osteoblastic-specific promoters appeared to be less effective than the physiologically relevant, non-tissue specific promoter, EF-1α, in driving transgene expression in HIV-based vector in osteoblastic cells. The objective of this study has been achieved, as gene expression from the various vector-promoter combinations has been quantified. However, because 1) the titer of MLV-based vectors is usually much greater than that

of HIV-based vectors, 2) the LTR promoter of MLV vectors is much more potent than that of HIV-based vectors, and 3) we have much more experience with MLV-based viral vectors in fracture therapy, MLV-based vectors were used in subsequent studies, The HIV-based vector will be used for the vector comparison (Specific Objective 3). In this case, expression of the transgene will be driven by the nonspecific CMV promoter normally present in this vector. We plan to use the HIV-based vectors with tissue-specific and regulated promoters to develop and optimize gene therapy of fracture repair in which transgene expression can be regulated in the future.

Specific Objective 2: To Compare the Local Periosteal Injection of the Virus at the Fracture Site with the Intramedullary Inoculation Procedure

Objective:

This Specific Objective sought to develop surgical and injection techniques for the evaluation of gene therapy. Surgical techniques have been adapted to apply the viral-based vector gene therapies from either the exterior aspects of the rat femur fracture tissues, or to the interior of the fracture callus through the intramedullary space. Though either technique can be used to apply single or multiple injections of fracture gene therapy, we have previously demonstrated that percutaneous applications to the very thin layer of cells of the periosteum immediately post-fracture is difficult and inefficient in delivery, and the effect was less than optimal in that it transfected cells only around the injection sites. Intramedullary injection techniques have been developed to facilitate the delivery to the subperiosteal tissues that mediate fracture healing and maximize the propagation and local expression of growth factor expression in the tissues of the developing fracture callus. Though technically more difficult in both the surgery and the post-fracture injections, we hypothesized that the intramedullary injection technique would provide a more symmetric distribution of the therapy to the fracture and a more accurate evaluation of its therapeutic benefits. It is reasoned that viral vectors introduced through the intramedullary technique would seep out at the fracture site and accordingly would uniformly transfect cells around the fracture site. Therefore, the primary purpose of this Specific Objective was to compare the efficiency of the intramedullary application procedure with that of the local periosteal injection method. Because of our experience with its robust in vivo effects, our BMP-2/4 hybrid transgene was chosen for this comparison of application techniques for their ability to maximize expression of the growth factor.

Materials and Methods:
Fracture Surgery:

The fracture surgery for exterior injections is as previously described in the rat femur fracture model (Bonnerans and Einhorn, 1984). A stainless steel Kirschner wire (K-wire, or "pin") is inserted into the femoral medullary canal to stabilize the fracture, which is produced immediately after surgery by the three-point bending technique (Figure 2). Post-fracture injections are performed from the exterior lateral or medial aspects of the leg. However, for applications of intramedullary gene therapy, we have adapted this surgery by aseptically inserting and securing a 20G catheter into the medullary canal of the femur alongside the stabilizing pin (Figure 3). This indwelling catheter permits the post-fracture anterograde insertion of a needle into the medullary canal through the greater trochanter. The delivery of vectors expressing growth factor genes to the interior of the fracture can be attempted after various post-fracture interval at multiple times,

if necessary, depending on the growth factor, but we injected the MLV-based vector at one day post-fracture for reasons stated above in the Materials and Methods. However, because the fracture periosteum is a highly mitotic tissue after fracture, and the MLV-based vector requires actively proliferating cells for efficient cell target transduction, our approach routinely applies the therapy at one day post-fracture. This application is also relevant to fracture treatment in a clinical setting.

Rat Femur Fracture Model

Procedures:
1. Surgically insert a 0.89-mm steel K-wire in rat femur.
2. Create femur fracture by three point bending using an Instron mechanical tester.
3. Suture the surgical wound.

Figure 2. The rat femur fracture model.

Fracture Injection:

The therapeutic gene chosen was the "BMP-2/4" hybrid gene; the β-galactosidase marker gene was chosen as the control gene. Each was expressed from the MLV-based vector (Figure 4). In the BMP-2/4 hybrid gene, with the exception of 20 amino acids, the native BMP-4 signaling peptide sequence in the BMP-4 gene was replaced by the complete signaling peptide of BMP-2 gene. This substitution greatly enhanced the secretion of BMP-4 proteins (Peng et al., 2001), and most importantly, had no effect on the post-translational processing of the mature BMP-4 protein.

Surgical techniques were adapted to apply the viral-based vectors from either the exterior aspects of the rat femur fracture periosteum, in a percutaneous injection, or through the intramedullary space to the interior of the fracture callus. Multiple exterior injection or intramedullary injection techniques have been developed to maximize the symmetry of growth

factor expression to the fracture site and compared for their ability to maximize the therapeutic benefit of the growth factor. For this study, we hypothesized that a single medullary injection would provide a much more symmetric distribution of the therapy to the fracture.
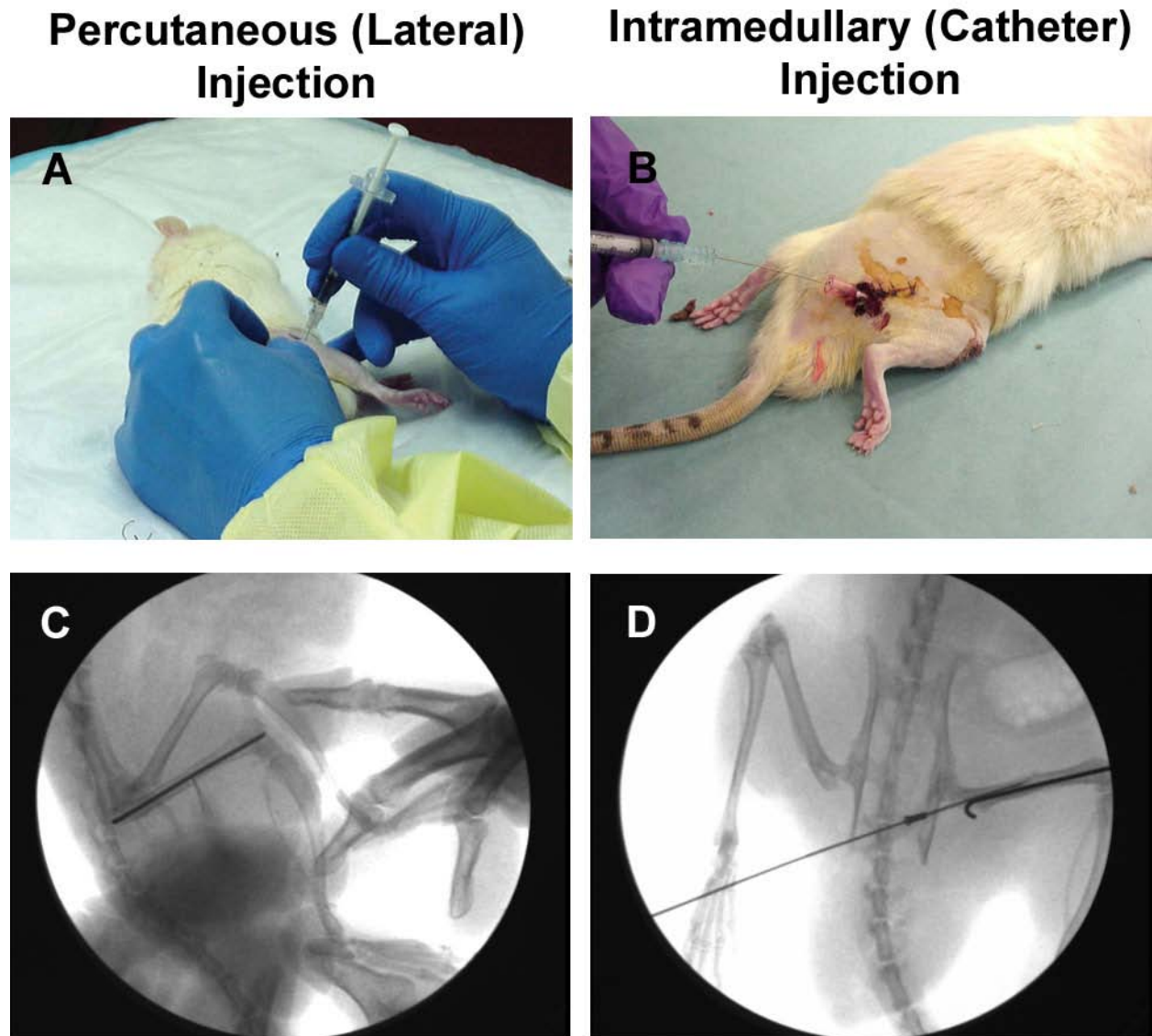
Figure 3. The usual femur fracture surgery (left, A and C) and intramedullary catheter modification (right, B and D). In both techniques, a stabilizing Kirschner wire is inserted into the medullary space, hooked, seated at the greater trochanter and cut flush with the condyle prior to fracture by three-point bending. In the catheter insertion modification, a 20 gauge catheter is inserted from the greater trochanter beside the wire inside the medullary space. Injections are performed under fluoroscopy (C, D), either from a percutaneous approach to the periosteal surface (A) or to the intramedullary space through the catheter (B). In the latter case, the external catheter hub is visible (D), though the internal tubing cannot be visualized by X-Ray.

MLV-based vector with BMP-2/4 therapeutic transgene.

MLV-based vector with β-galactosidase marker transgene.

Figure 4. MLV-based therapeutic gene vector constructs used to compare percutaneous and intramedullary gene therapy application techniques.

Fracture Callus Analysis:

The effects of the percutaneous and intramedullary injections were evaluated by various means. Gross anatomy of the fracture callus was examined at times when the effects of β-galactosidase marker and BMP-4 expression were expected to be maximal, at 7 days and 14 days, respectively. X-ray analysis was performed 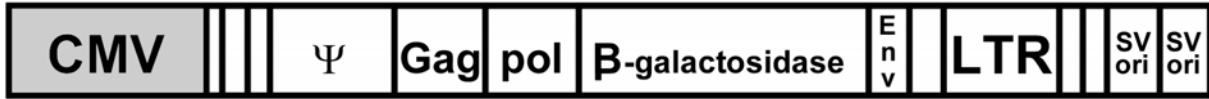throughout healing, and compared with histology at 14 days post-fracture, when fracture callus size is maximum, and 28 days, just prior to bony bridging of the fracture gap in the rat femur fracture model (normally 35 days), and when improved healing is expected to be most obvious. Mechanical testing was also performed at 28 days post-fracture, when augmented bone formation would be expected to accelerate the healing (i.e., bony bridging of the fracture) that normally occurs by 35 days in the rat femur fracture model.

Torsional Mechanical Test:

Torsion testing is the preferred method of mechanical strength testing for fracture healing, because unlike three-point or four-point bending techniques that measure mechanical strength in one orientation, it can test the different tissue orientations of the fracture callus. We have adapted an Instron DynaMite 8841 materials testing apparatus using Single Axis MAX32 software (Instron) to torsion test rodent femurs for mechanical strength. In this testing model, the femoral epiphyses are cast into dental epoxy resin using a custom mold that allowed them to be securely fastened and the diaphysis (with the fracture) aligned in the testing device for rotation around its vertical axis; the shape of the mold is designed to fit the jaws of the chuck of the torsion apparatus so the epiphyses are totally immobilized and the diaphysis can be accurately aligned. By this approach the bone is twisted about its axis and fails at the weakest point of the diaphysis, expected to be at the fracture. The strength of the fracture callus is determined by the ultimate load at failure, and the stiffness determined by comparing the load (force) to the torsional angle (i.e., stiffness is the slope of the relationship of load vs. the angle of twist). Testing is conducted at 28 days healing using a rotational speed of 2.5^o per second; 28 days is approximately one week before the normal bridging of the fracture gap with bony tissue. This time point is substituted for the originally proposed 21-day fracture strength analysis, based upon the mineralized tissue and bone formation produced by BMP-2/4 transgene expression at this time observed in earlier studies in this Specific Objective. The ultimate load (force in Newton-meters) to bone failure is determined as a measurement of the return to mechanical strength provided by each vector, as

defined by torsional testing of the unfractured contralateral femur of the same animal. The stiffness was calculated from this force-torsional displacement slope.

Results:
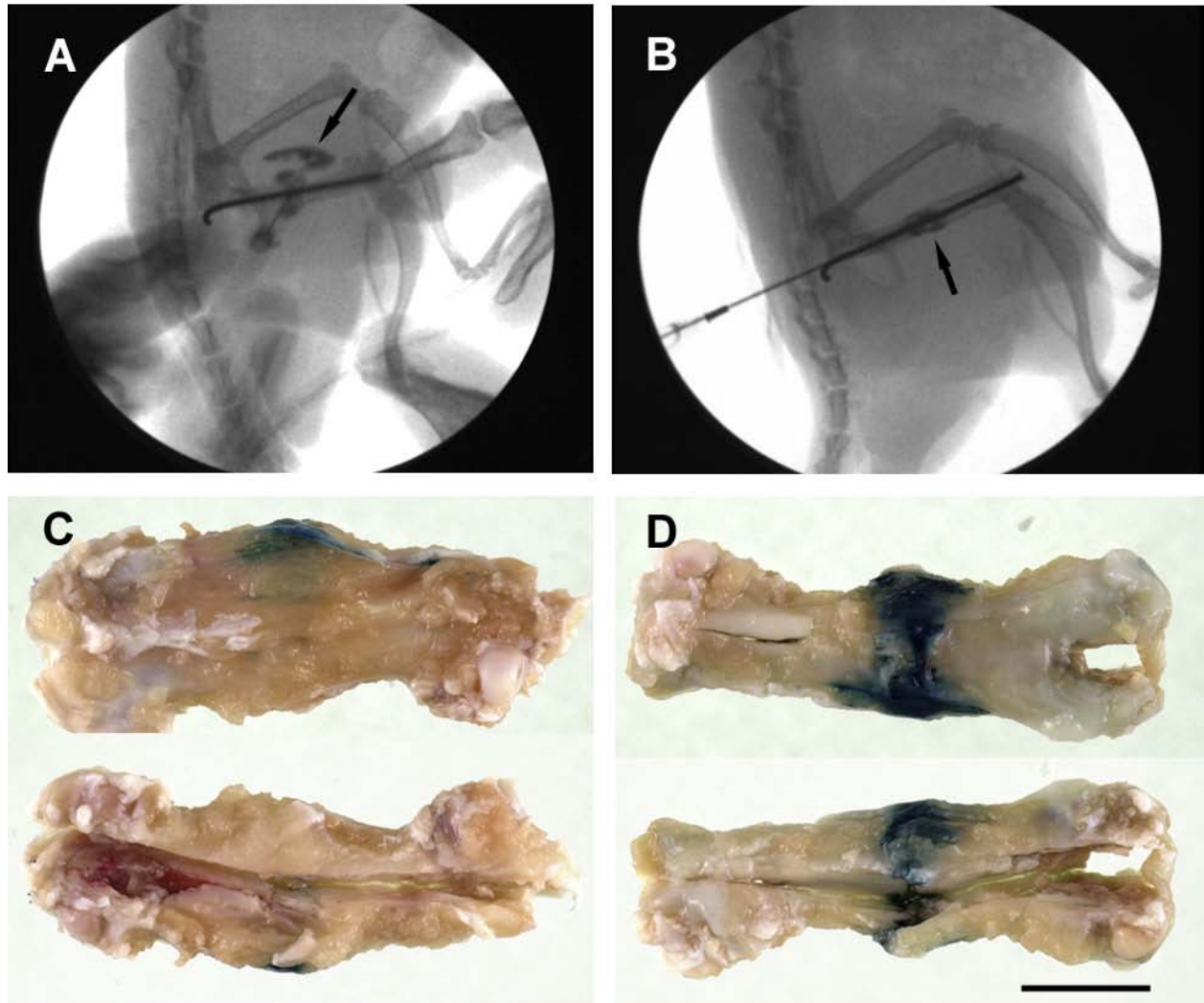
Figure 5. Marker localization in fractures injected from the percutaneous (lateral) aspect or through the intramedullary (catheter) injection. Top: A fluoroscope was used to visualize a radio-opaque contrast dye during a percutaneous injection from the lateral aspect (A) or an intramedullary catheter injection (B). Despite best efforts, the dye immediately distributed in the leg muscles when injected from the exterior (A, arrow). When injected through the catheter, the contrast dye was retained in the medullary space (B) close to the fracture site. Bottom: The MLV-based vector expressing the β-galactosidase marker transgene was injected at one day post-fracture and the femurs harvested at 7 days post-fracture, split open and stained for marker expression. The intramedullary injection (C, D) produced more extensive and symmetric marker expression in the exterior (D, top) and interior (D, bottom) of the fracture than the lateral injection exterior (C, top) or interior (D, bottom).

In Figures 5A and 5B, an injection of a radio-opaque contrast dye tracks the injection through the tissues when viewed through a fluoroscope. The dye volume was identical to that of the therapy applications. When injected percutaneously, much of it fails to penetrate the periosteum, which is a very thin target layer at one day post-fracture. Moreover, it spreads through the muscle tissues (Figure 5A). The intramedullary technique can distribute the injection at the fracture site but restrict penetration to the subperiosteal layers, where it should be most effective for fracture healing. When the β-galactosidase marker gene is injected at 1 day post-fracture and localized at 7 days post-fracture, (Figures 5C and 5D), the results reflect the observations with the contrast dye. The percutaneous injection provides localized marker transgene expression largely outside of the bulk of the fracture callus. However, the intramedullary injection has distributed the marker gene symmetrically and propagated it throughout the interior and exterior fracture tissues adjacent to the fracture site. This result is impressive, as the β-galactosidase marker expression is intracellular; a transgene that is secreted would be expected to exhibit even more extensive expression through the developing callus.
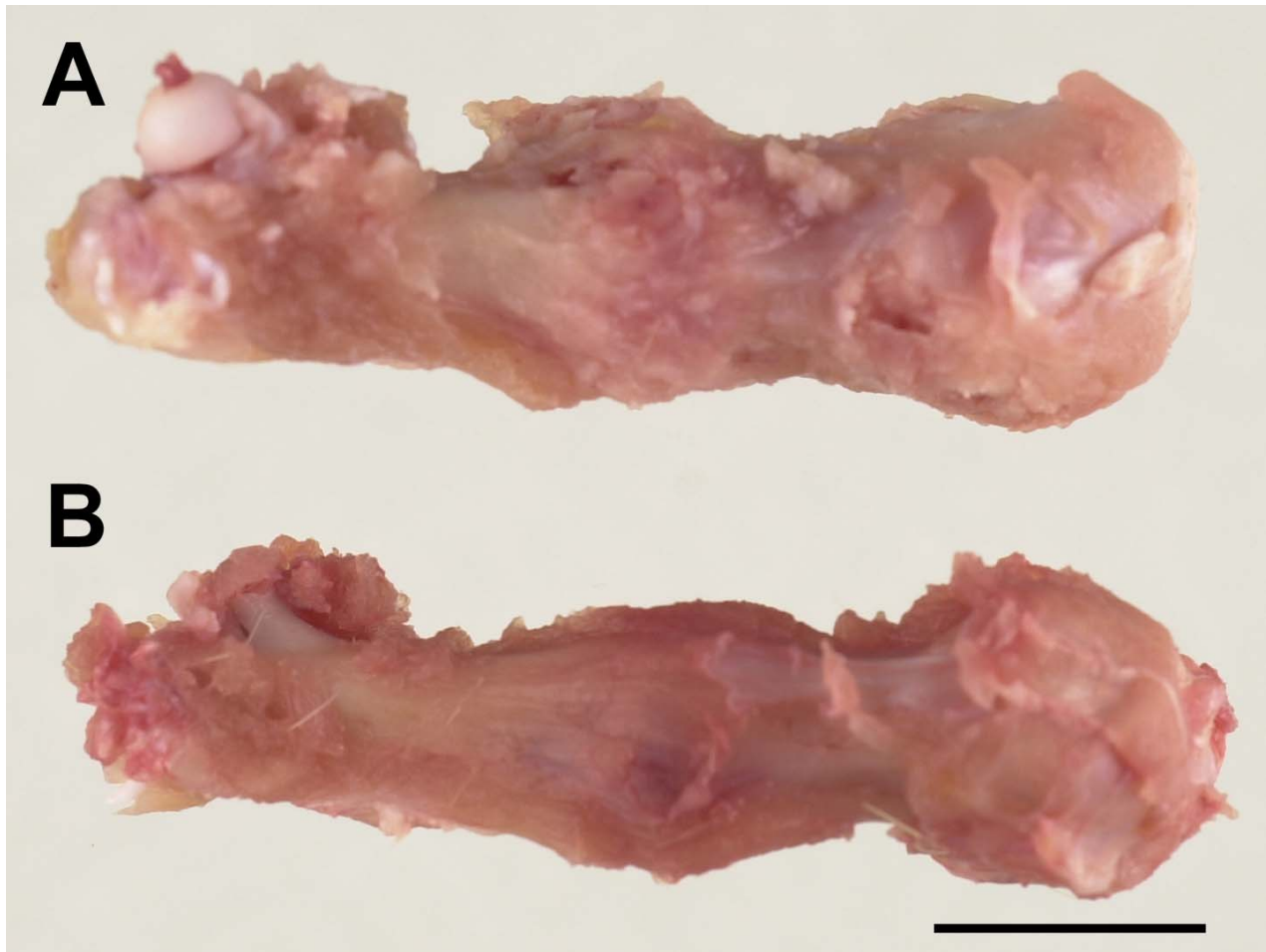

Figure 6. MLV-BMP-4 gene therapy at 14 days healing. (A) the percutaneous (lateral) injection method results in supraperiosteal bone, visible as a rough exterior to the fracture callus. This appearance contrasts with the smooth appearance produced by the intramedullary (catheter) injection (B) in which bone formation does not involve muscle tissues outside of the fracture. Scale bar = 1 cm.

When the BMP-2/4 hybrid therapeutic transgene was applied to the fracture by each of these injection techniques, the effects of osteogenic transgene expression in the supraperiosteal layers became apparent (Figure 6). In Figure 6A, the femur fractures were harvested at 14 days post-fracture, when BMP-4 gene expression has previously been observed to produce the greatest amount of bone. At this time, the rough appearance of the callus indicates that muscle has become ossified from the percutaneous injection. In our experience, BMP-4 expression commits interstitial fibroblastic cells to the osteogenic lineage, although the muscle fibers themselves are refractory to transduction. In contrast, as shown in Figure 6B, this effect is not observed for the intramedullary injection, as BMP-4 gene expression is confined to the subperiosteal layers and the external callus surface remains smooth in appearance.

To more accurately characterize the osteogenic effects of BMP-2/4 transgene expression throughout healing following each injection approach, mineralized fracture tissues were monitored throughout healing by X-ray fluoroscopy (Figure 7). Individual animals receiving the MLV-BMP-2/4 gene therapy by either the percutaneous injection or the intramedullary injection were observed weekly from 7 through 28 days. It was indeed confirmed that the muscle surrounding the femur became extensively ossified following the percutaneous injection, while the fracture itself received minimal therapeutic benefit. The intramedullary injection kept the osteogenic effects of BMP-4 expression confined to the subperiosteal layers, except for some leakage from the condyle (presumably through the hole through with the stabilizing K-wire was introduced. This effect was observable early in fracture healing but was most obvious by 28 days. It was very infrequent, especially as we became more proficient at the surgical technique.

Histology was also compared to the X-ray results at 14 days and 28 days post-fracture (Figure 8), when increases in callus bone and any accelerated improvements in bony bridging, respectively, would be expected to be most obvious. Trichrome stains of the fracture callus (which stains collagen tissues) established that, in agreement with the respective X-rays, the percutaneous injection produced supraperiosteal ectopic bone formation at 14 and 28 days post-fracture (Figures 8A and C). The X-rays further reveal that the percutaneous injection and BMP-4 expression produced bony tissue at some distance from the fracture. In the case of the intramedullary injection, lightly mineralized callus material bridges the fracture gap, but the entire mineralized area remained subperiosteal (Figures 8B and D). It appears that the bony material in the fracture gap is the result of bone growth radiating from the center of the fracture callus, most obvious in the 14 day post-fracture X-ray in Figure 8D. Thus the subperiosteal confinement of the BMP-4 therapy with the intramedullary approach has produced bone in the fracture gap that eventually bridges with the opposing distal and lateral sides of the normal bony callus. It did not accelerate the approach of each side of the bony callus toward the middle of the fracture callus. Accordingly, bony bridging in this case can be deemed unusual.

Figure 7. X-Ray comparison of mineralized tissue during healing. The injection was performed from the exterior (percutaneous, left) or through the catheter (intramedullary, right) and monitored at 7 days (A,B), 14 days (C,D), 21 days (E,F) and 28 days (G,H) healing. These X-rays follow the healing in the same animal for each injection technique. Some supraperiosteal bone has developed from leakage of the therapy at the condyle, most obvious in H (arrow), but it is not nearly as extensive as that of the percutaneous injection in G (arrow).
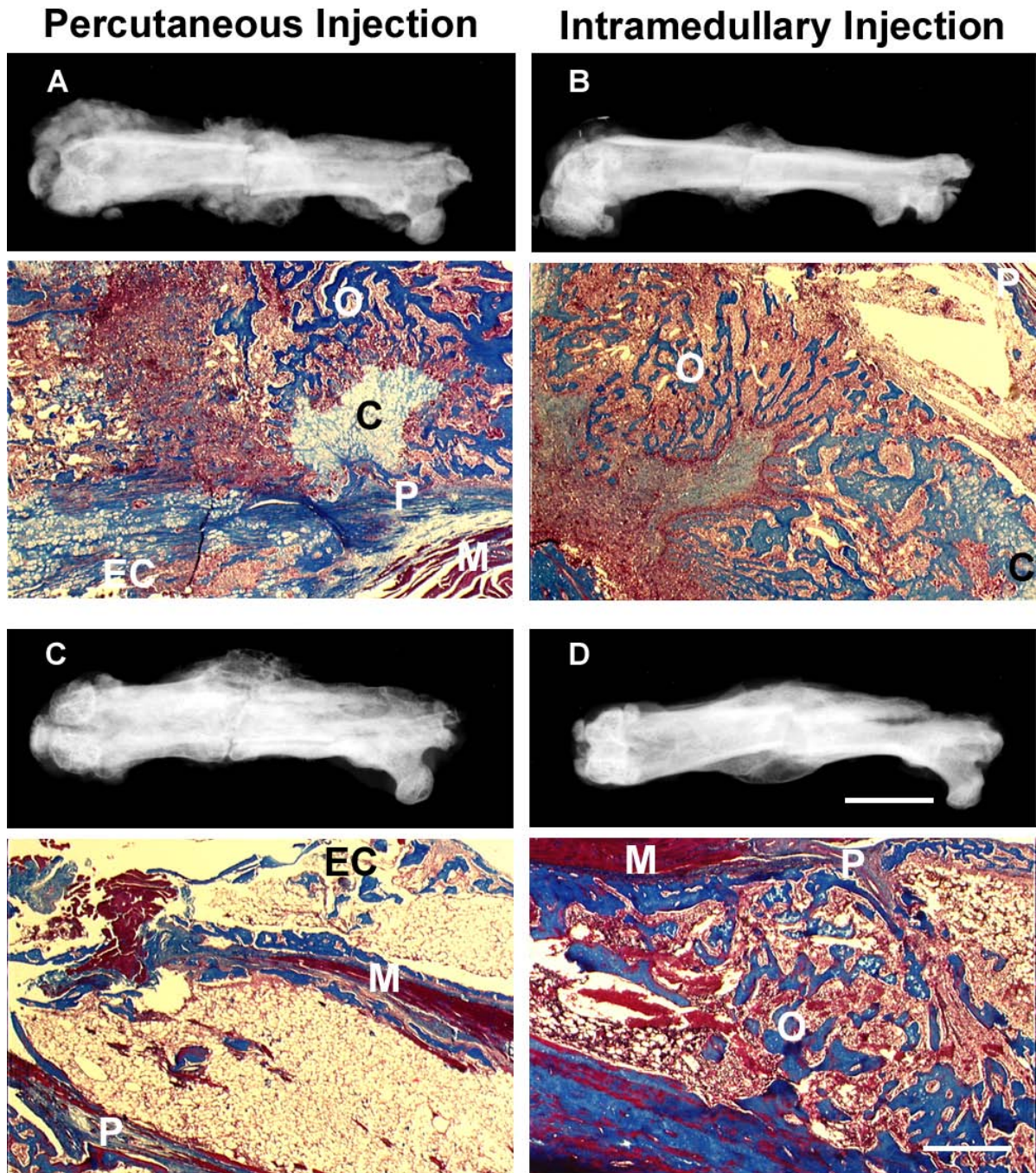
Figure 8. X-Ray and histology of the fracture callus following lateral injection (left) or catheter injection (right) at 14 days (A, B) and 28 days (C, D) healing. Scale bar = 1 cm. Trichrome stains of the fracture callus revealed ectopic (EC) bone formation outside the periosteum (P) at 14 and 28 days in post-fracture lateral injections. Bone formation was under the periosteum (P), at 14 and 28 days in post-fracture catheter injections and did not involve the muscle (M). The fracture tissues appeared normal at all healing times. Cartilage (C), Osteoid (O). Scale bar = 100 um.

pQCT comparisons that quantified the bony material of the fracture callus were not possible, because, in the case of the percutaneous injection, the bone was distributed throughout a large part of the muscles surrounding the femur. Accurate dissection that separated muscle from bony tissues proved to be impossible, and subperiosteal deposits of bone were highly variable. We have observed this effect in previous studies (Rundle et al., 2003). With respect to immunohistochemistry for transgene expression, which we have successfully used in other studies (Rundle et al., 2003), the available antibodies do not differentiate the human BMP-4 transgene protein from the endogenous rat protein, and do not yield unambiguous results. The obvious difference in bone formation around the fracture site produced by the intramedullary injection strongly supported BMP-2/4 transgene within the intended target tissues. We therefore limited the comparison of bone formation by the different injection techniques to X-ray observation, histology and torsional mechanical testing.

To determine whether the different application techniques produced an accelerated mechanical strength, the ultimate goal of bone repair, torsional mechanical strength testing was conducted on the fracture calluses. An example of the mechanical testing is shown below for one animal that received the HIV-BMP-2/4 vector-gene combination (Figure 9). The objective of fracture therapy is to enhance the return to the pre-fracture strength (ultimate load) as displayed by the unfractured contralateral femur. The ultimate load of the fractured bone (with therapy) is therefore compared to the ultimate load of the unfractured bone as a measure of its return to prefracture strength. The elastic value of the fracture represents the torsion to higher degrees of rotation on soft tissues that have limited stiffness to resist such loads.
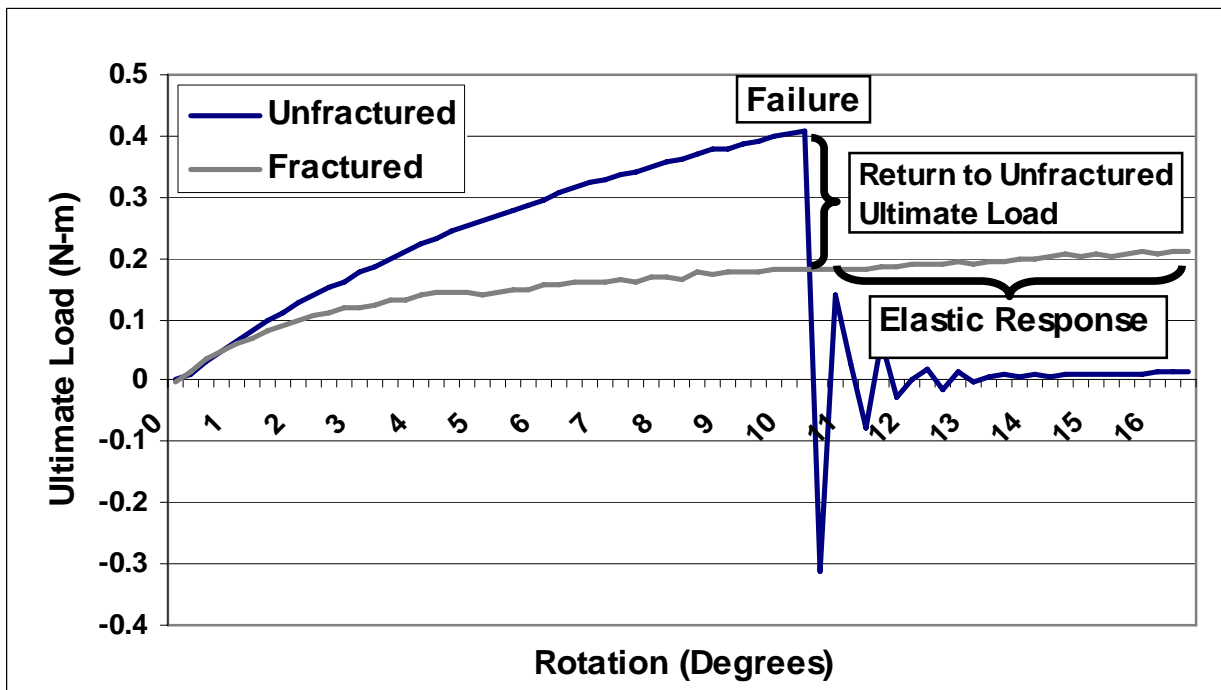

Figure 9. Illustration of the torsional mechanical testing conducted to evaluate the therapeutic value of the vectors. The ultimate load is the force value at which the bone fails, easily observed in the unfractured curve. The stiffness is calculated as the slope of the load:torsional displacement curve prior to failure.

The results of the torsional mechanical testing comparison of BMP-2/4 gene fracture therapy are presented in Figure 10. Five animals receiving the percutaneous injection and 7 animals receiving the intramedulary injection were analyzed at 28 days post-fracture. The torsional mechanical test, even with the unfractured bone, showed relatively large variations. Because of the large variations and the small sample size, our experimental design did not have sufficient statistical power to detect significant differences in the return to prefracture strength between the two methods, expressed as either the ultimate load to failure or the bone stiffness. On the hand, the lack of a significant difference may also not be entirely surprising, for although the percutaneous injection has failed to deliver a large portion of the therapy to the fracture site, it has ossified the surrounding muscle which, because it could not be dissected away, contributed to an enhanced stabilization of the femur in torsional testing. However, bone strength and stiffness following the intramedullary injection are comparable, despite the fact that it is confined to a much smaller area. In the future, we intend to include additional numbers of animals to increase statistical power to determine more definitively as to whether the all round increase in bone formation in the intramedullary injection approach, or the larger bony callus in the percutaneous injection approach, yields greater benefits with respect to bone strength.
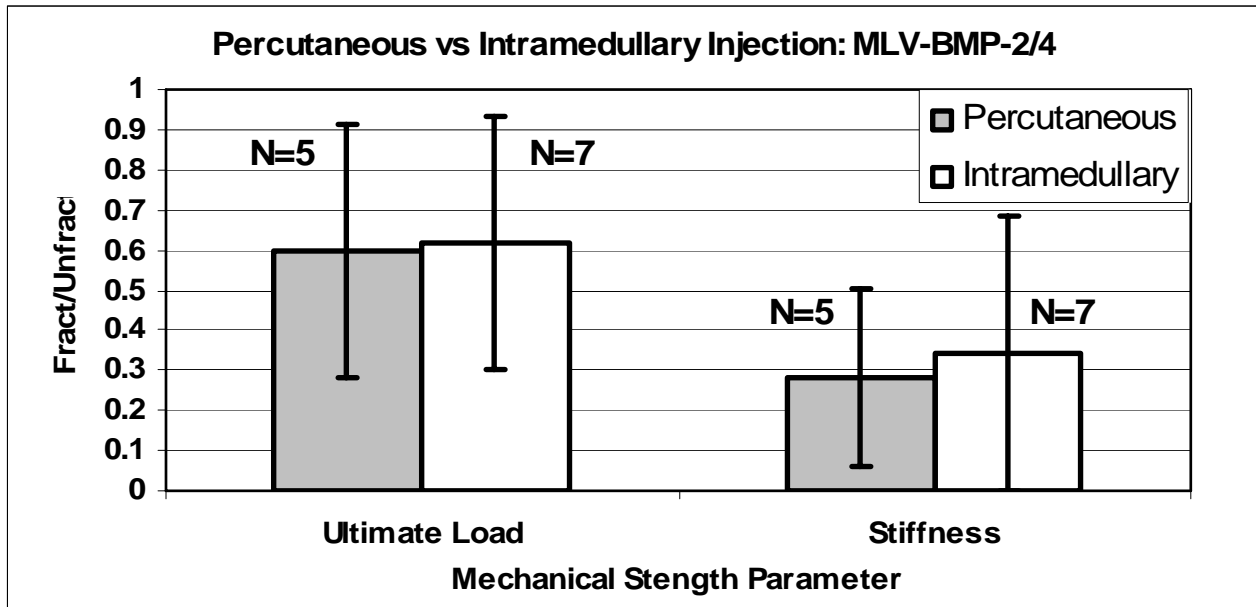
Figure 10. Results of torsional mechanical strength testing after either a percutaneous (lateral) or an intramedullary (catheter) injection of MLV-BMP-2/4 gene therapy. Data is presented as the mean ± standard deviation for the difference in torsional ultimate load between fracture therapy and unfractured contralateral femur from the same individual. Femurs were harvested at 28 days post-fracture. There were no significant differences in ultimate load to failure or the stiffness.

Conclusions:

By X-ray, histology and mechanical strength measurements, the catheter surgical modification and the intramedullary injection technique provided a more accurate delivery and expression of a highly osteogenic transgene. Transgene expression and bone formation were symmetric, and present around the entire circumference of the fracture. The ectopic bone formation produced by the traditional percutaneous injection techniques that complicate

subsequent analysis was largely avoided, and provided a more accurate evaluation of the therapeutic benefits of the test vector and gene. This study provided considerable evidence favoring the intramedullary injection of gene therapy, and accomplished the goals of this objective.

Specific Objective 3: To Compare the Superiority of the MLV-based Versus the HIV-based Vector Systems for the BMP-2/4 Transgene

Objective:

This Specific Objective compares the efficacy of the HIV-based and MLV-based vectors for fracture healing. As reported earlier, we found that bone cells demonstrated greater marker transgene expression when regulated by the non-bone-specific EF-1α promoter or the cytomegalovirus (CMV) promoter in the HIV-based vector than when regulated by the bone-specific promoters. This result suggests that more non-osteoblastic cells than osteoblastic cells were transduced by the HIV-based vectors. Moreover, even with the EF-1α or the CMV promoter, the extent and intensity of marker transgene expression in the fracture site transduced by HIV-based vectors was much lower than that in the fracture site transduced by MLV-based vector. For these reasons, we compared the MLV-based vector, with LTR-driven transgene expression, and the HIV-based vector, with CMV-driven expression, for both marker and therapeutic transgene expression. Because the return to pre-fracture mechanical strength is the definitive test of improved fracture healing, we also compared the torsional mechanical strength produced by BMP-2/4 therapeutic transgene expression from each test vector (Figure 11). Because we have been testing these applications with the MLV-based vector, which requires proliferating tissue targets for transduction, we have previously injected the fracture tissues at one day post-fracture, when cell proliferation in the wound has started. In this study, the HIV-based vector was also injected at one day post-fracture for a direct comparison with the MLV-based vector, although it does not require the actively proliferating tissues that facilitate MLV-based vector transduction at this time.

As reported in Specific Objective #2 of Technical Objective #1, we have also established an intramedullary delivery method to administer viral vectors symmetrically around the fracture site. This intramedullary delivery method allowed the transduction of cells and induced bone formation around the entire fracture site, and it was used to compare the efficacy of MLV-based vectors with HIV vectors in fracture repair.

Each vector expressed the BMP-2/4 transgene following intramedullary delivery. The BMP-2/4 gene was chosen as the transgene to develop the therapeutic delivery because of its documented ability to efficiently differentiate osteogenic precursors to bone (Peng et al., 2001). Accurate delivery of the therapeutic transgene can be easily established by its induction of cartilage and bone in any tissues transduced with the viral vectors. The vector system that exhibits the greatest therapeutic benefits as determined by a return to pre-fracture torsional mechanical strength will then be used in subsequent combination therapy with multiple transgenes.

a) MLV-based vector with BMP-2/4 therapeutic transgene.

| CMV | ‖‖‖ | Ψ | Gag | pol | BMP-2/4 | Env | LTR | ‖‖ | SV ori | SV ori |

b) MLV-based vector with β-galactosidase marker transgene.

| CMV | ‖‖‖ | Ψ | Gag | pol | β-galactosidase | Env | LTR | ‖‖ | SV ori | SV ori |

c) HIV-based vector with BMP-2/4 therapeutic transgene.

cPPT — LTR

| CMV | ‖‖ | Ψ | Gag | | | CMV | BMP-2/4 | | ‖‖ | SV ori | SV ori |

RRE — wPRE

d) HIV-based vector with β-galactosidase marker transgene.

cPPT — LTR

| CMV | ‖‖ | Ψ | Gag | | | CMV | β-galactosidase | | ‖‖ | SV ori | SV ori |
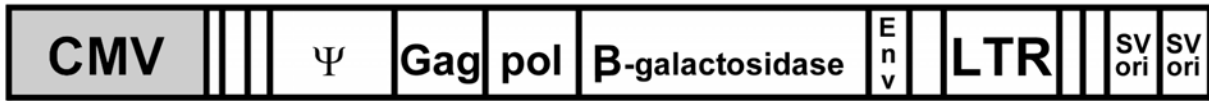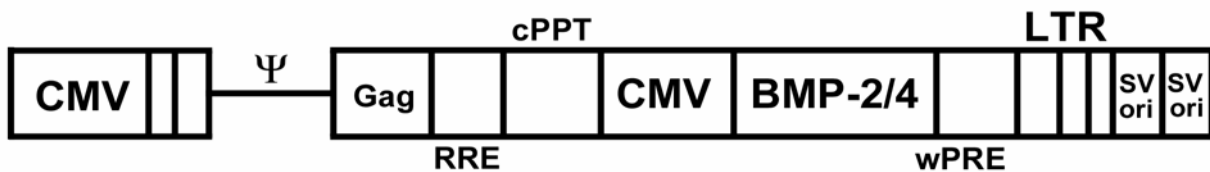
RRE — wPRE
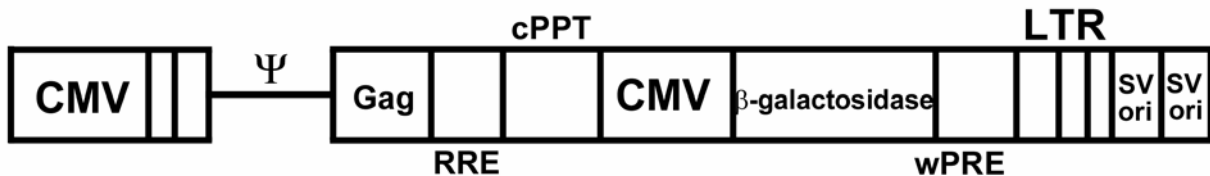
e) HIV-based vector with enhanced green fluorescent protein (EGFP) marker transgene.

cPPT — LTR

| CMV | ‖‖ | Ψ | Gag | | | CMV | EGFP | | ‖‖ | SV ori | SV ori |

RRE — wPRE
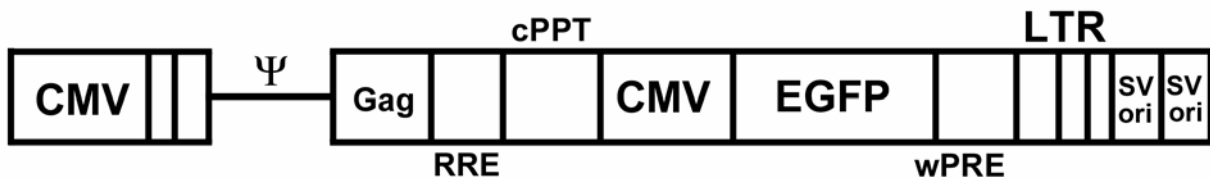
Figure 11. Gene vector constructs used in the torsional mechanical strength testing comparison between the MLV-based and HIV-based vector systems. All MLV and HIV elements present in the vector constructs are included in this diagram. The MLV-based vector utilized the viral LTR to express the BMP-2/4 therapeutic gene (a). In this vector, the CMV promoter functions only for vector production and is excised upon viral integration into the host genome. The HIV-based vector utilized the 3' CMV promoter to express the BMP-2/4 therapeutic gene (b), but in this vector the 5' CMV promoter functions only for vector production and is excised upon viral integration into the host genome.

Figure 12. Comparison of β-galactosidase marker gene expression in fractures from MLV-based vectors (A and B were duplicated from Figure 6D) or HIV-based vectors (C and D) at 7 days post-fracture. The exterior aspect of each bone (A and C) is compared with the interior of the bone when split open (B and D). Scale bar = 1 cm.

Materials and Methods:
Fracture Surgery and Intramedullary Injection:
    The fracture surgery and intramedullay injection methods were performed as described earlier in Specific Objective #2 of Technical Objective #1,

Fracture Injection:
    The therapeutic gene chosen was the BMP-2/4 hybrid gene. To most accurately establish the expression of the marker gene or therapeutic gene, the MLV-based and HIV-based vectors were adjusted to equal concentrations for intramedullary application, a procedure in which the more concentrated MLV-based vector was diluted to 1/3 of its original concentration. The delivery of vectors expressing growth factor genes to the interior of the fracture retained the therapy in the subperiosteal tissues that proliferate and differentiate to mediate fracture healing. Moreover, as reported earlier (Technical Objective #1, Specific Objective #2), the intramedullary injection distributed the β-galactosidase marker and BMP-2/4 transgene expression around the fracture circumference, indicating that the therapeutic transgene expression would be expected to be evenly distributed around the fracture and provide the greatest therapeutic effect. This approach confined transgene transduction to the periosteal cell layers and avoided gene expression in the supra-periosteal layers that do not participate in fracture healing.

Fracture Tissue Analysis:
    As reported earlier, the fracture tissues were examined by Faxitron X-ray analysis for mineralized tissues, and examined for bone formation and BMP-4 expression by histology. X-ray analysis of the fractures suggested that each viral vector appeared similar in producing bone within the periosteal fracture tissues. pQCT measurements of the bone mineral content of the fracture callus revealed no significant difference in the bone mineral content or cross-sectional

areas of the fracture callus tissues produced by either vector during fracture healing, suggesting that either viral vector system is effective in expressing gene therapy for fracture repair. Our report focuses on the comparison of the healing fracture strength produced by each vector as determined by torsional mechanical testing.
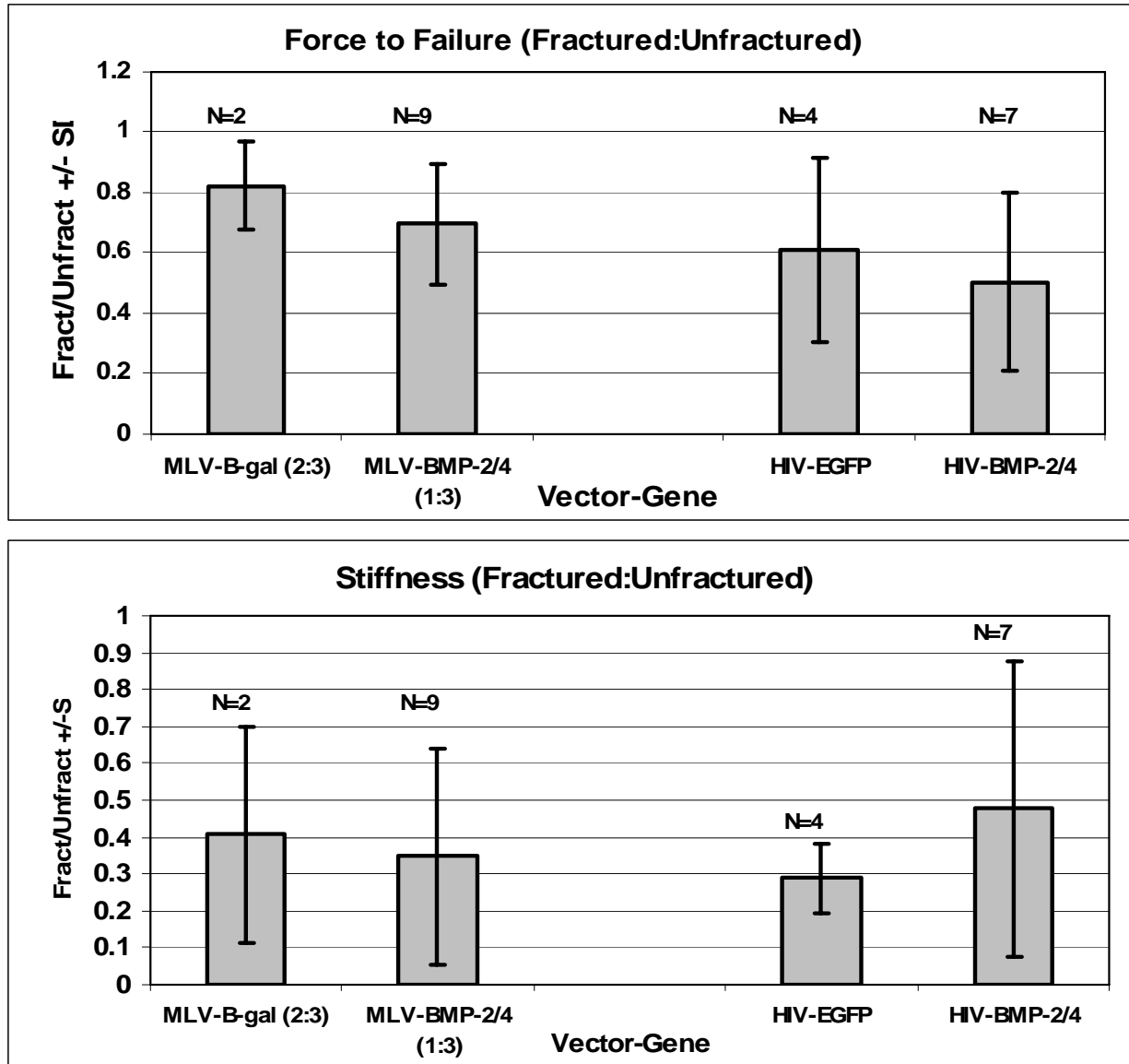
Figure 13. Comparison of the ability of the MLV-based vector expressing the BMP-2/4 therapeutic transgene with the HIV-based vector expressing BMP-2/4 transgene to promote the return to prefracture (contralateral) mechanical strength during fracture healing. The intramedullary space of the fracture was injected at one day post-fracture with 0.1 ml of 1×10^7 transforming units (tfu) MLV-based or HIV-based vectors expressing the BMP-2/4 transgene. The femurs were harvested at 28 days post-fracture. Data is presented as the mean ± standard deviation for the difference in torsional ultimate load (top) or stiffness (bottom) between the fracture therapy and the unfractured bone. Numbers of animals are indicated (N). Statistics were performed by t-Test, but there was no significant difference between the two groups.

Results:

With respect to torsional mechanical testing, two to nine individual animals were evaluated for the return to prefracture (unfractured contralateral) torsional strength following injection of either the MLV-based or the HIV-based vectors expressing the BMP-2/4 transgene (Figure 13). All tissues were harvested at 28 days healing. In agreement with the previously reported X-ray results, there was no significant difference in the ultimate load (force) produced by the expression of the therapeutic BMP-2/4 transgene from either vector. Each produced a 50% to 80% return to contralateral ultimate load, and a 30% to 50% return to contralateral stiffness, though the HIV-BMP-2/4 vector might have been required at higher concentrations, or the dilution of the MLV-BMP-2/4 vector titer to levels comparable to the HIV-BMP-2/4 vector might have reduced the effectiveness of MLV as a vector. Again, the lack of significant differences could be because of the apparent lack of sufficient statistical power of the experimental design, due to the large variation and the small sample size. Therefore, this preliminary conclusion must be confirmed with additional animals.

Conclusions:

Due to the unexpected large variation in the torsional bone strength test, our original experimental design did not have the sufficient statistical power to detect the difference in bone strength among the test groups and the respective control group. Consequently, there was no significant difference in the ability of the BMP-2/4 transgene to promote mineralized fracture tissue production in MLV-based and HIV-based vector systems. There was a difference in β-galactosidase marker gene expression, but the reason is not clear at this time and this discrepancy remains unresolved. We are still completing analysis of the histology and mechanical strength testing of the healing bone at this time.

Because the MLV-based vectors are much easier to produce in higher concentrations than the HIV-based vectors, the MLV-based vector system was chosen for our subsequent comparison between combination therapy with two different growth factor transgenes and single gene therapy (Technical Objective 1, Specific Objective 4, below).

Specific Objective 4: To Compare the Efficacy of the BMP-2/4 Transgene in the Optimized Vector System with that of the Combination of BMP-2/4 Transgene plus another Growth Factor Candidate Gene Identified by Microarray (Technical Objective #2) or another Potent Bone Growth Factor.

Objective:

To identify therapeutic gene candidates for combination therapy with the BMP-2/4 gene, we analyzed whole genome gene expression in the healing fracture tissues at 3 and 11 days post-fracture (Technical Objective #2 below). Analysis of the microarray data suggested several gene candidates that could be applied to combination therapy with our BMP-2/4 gene and MLV-based vector and whose expression was confirmed by real-time PCR analysis. However, we have also developed a highly active mutant fibroblast growth factor (FGF)-2 gene and successfully expressed it in our MLV-based vector. Several previous studies have applied exogenous FGF-2 to animal bone healing models to identify its functions in fracture repair, where it appears to increase proliferation of several cell types involved in fracture healing (Nakajima et al., 2001). Three of the four FGF receptors are expressed during fracture repair (Rundle et al., 2002), suggesting that FGF gene family members regulate healing. However, FGF-2 does not have a

classical secretion signal sequence. Its extracellular secretion is mediated by a highly inefficient, energy-dependent, non-ER/golgi pathway (Florkiewicz et al., 1995) and, as a result, the amount of secreted FGF-2 by this mechanism is low and inherently inconsistent (Moscatelli et al., 1986). These problems are largely responsible for the inconsistent efficacy of past FGF-2 gene therapy studies (Spencer et al., 2001; Hijjawi et al., 2004; Ishii et al., 2004). Accordingly, the human FGF-2 gene within our MLV-based vectors has been modified by: 1) adding the BMP2/4 hybrid secretion signaling sequence to the 5' end of the gene to enhance the transgene secretion; 2) adding an optimized Kozak sequence to promote protein translation; and 3) mutating two key cysteines (cys-70 and cys-88) to serine and asparagine respectively, to enhance protein stability. These modifications led to a marked increase in secretion and stability of functionally active FGF-2 protein in rat skin fibroblasts and marrow stromal cells (by more than 200-fold), but had no adverse effects on the biological activity or signaling mechanism of the recombinant FGF-2 protein (Chen et al., 2007). We have applied the MLV-based vector expressing our FGF-2 mutant gene to our rat femur fracture model.

In this study, we hypothesize that the BMP-2/4 will accelerate the osteogenic differentiation of osteoblastic precursor cells that have proliferated in response to FGF-2 gene expression and thereby accelerate endochondral bone formation and fracture repair. Studies were initiated that compared the effects of BMP-2/4 gene therapy with FGF-2 gene therapy when applied by intramedullary injection to the fracture tissues; we also plan to compare healing following a combined intramedullary injection of both genes expressed from their own MLV-based vector. The design of our constructs is shown schematically in Figure 14.

a) MLV-based vector with β-galactosidase marker transgene.
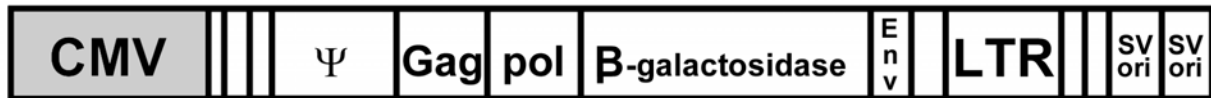
b) MLV-based vector with BMP-2/4 therapeutic transgene.

c) MLV-based vector with FGF-2 therapeutic transgene.

Figure 14. Control and therapeutic gene MLV-based vector constructs for combination gene therapy. As in Technical Objective #1, Specific Objective #2, the MLV-based vector utilizes the viral LTR to express either (a) the β-galactosidase marker gene as a non-therapeutic control gene, (b) the BMP-2/4 therapeutic gene, or (c) the FGF-2 therapeutic gene. The viral backbone and vector production is identical to that of the MLV-based vectors of Figure 11.

Figure 15. FGF-2 gene therapy expressed from the MLV-based vector at 14 days healing. (A) FGF-2 expression results in a huge fracture callus of soft tissue when compared to β-galactosidase marker gene expression (B). Scale bar = 1 cm.

The in vivo MLV-FGF-2 gene therapy produced a very large fracture callus (Figure 15) without accelerated chondrocyte maturation and endochondral bone conversion. Subsequent examination of the histology of this large fracture callus confirmed this observation, and revealed that it contained vessels highly suggestive of increased angiogenesis (Figures 16 and 17). However, when fractures were allowed to completely heal, the fracture calluses still resolved normally. These results suggest that this FGF-2 transgene increased periosteal mesenchymal cell proliferation and angiogensis, and it would be an excellent candidate for combination gene therapy in combination with an osteogenic transgene such as our BMP-2/4 gene. Because osteogenesis acts upon the soft callus tissues, BMP-2/4 gene expression would be expected to more quickly augment bone formation in the soft callus tissues that had rapidly proliferated in response to FGF-2 gene expression. Such a combination of growth factors may enhance fracture healing in this way. Consequently, this Specific Objective sought to test if the combination FGF-2 and BMP-2/4 gene therapy would yielded a better healing effect on femoral fractures than BMP-2/4 gene therapy alone.
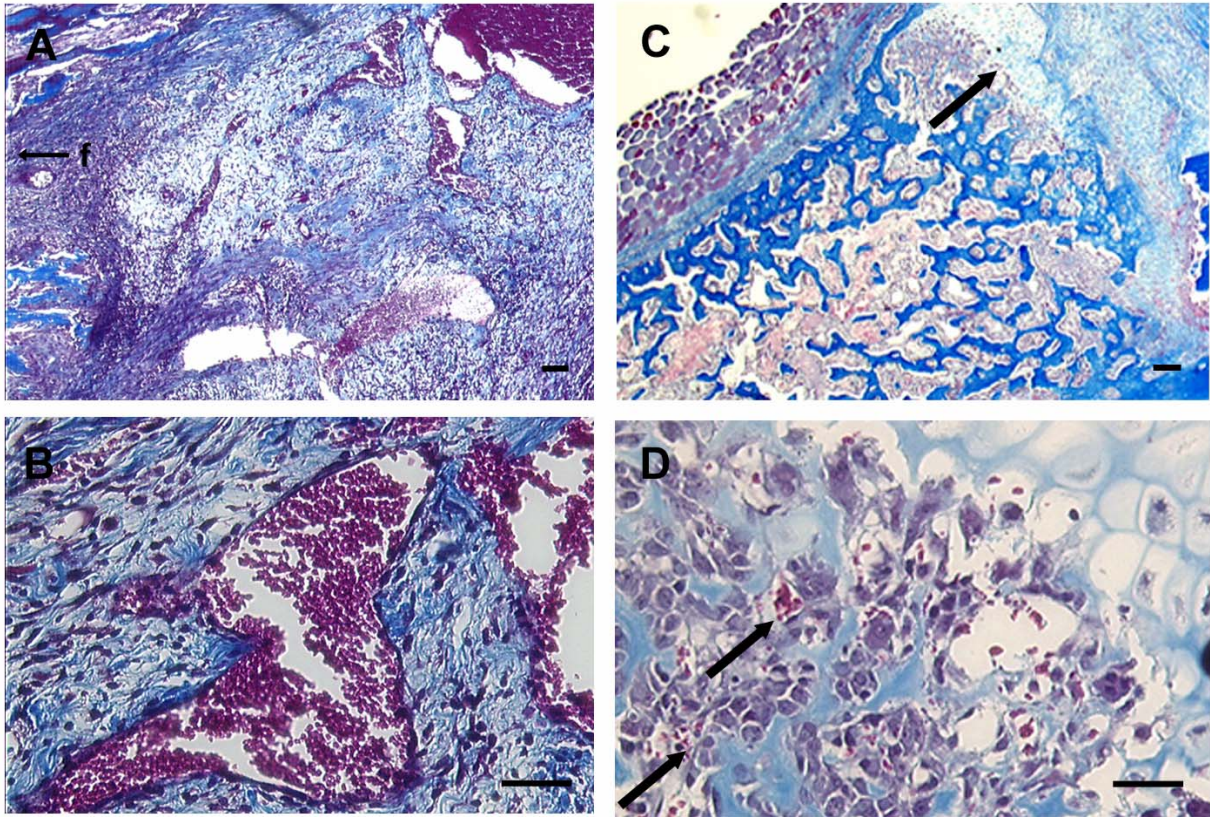
Figure 16. Bone formation in fractures expressing mutated variant of the FGF-2 gene (A, B) as compared to a wild-type FGF-2 gene (C, D) expressed from the MLV-based vector. (A) A trichrome stain of fracture tissues at 11 days post-fracture reveals several large vessels (A, upper right) with large numbers of red blood cells (B). In (C) wild-type FGF-2 gene expression provides a more normal infiltration of osteoblasts in the hypertrophic cartilage (arrow), with considerably smaller blood vessels (D, arrow). Scale bar = 100 µm. f, fracture.
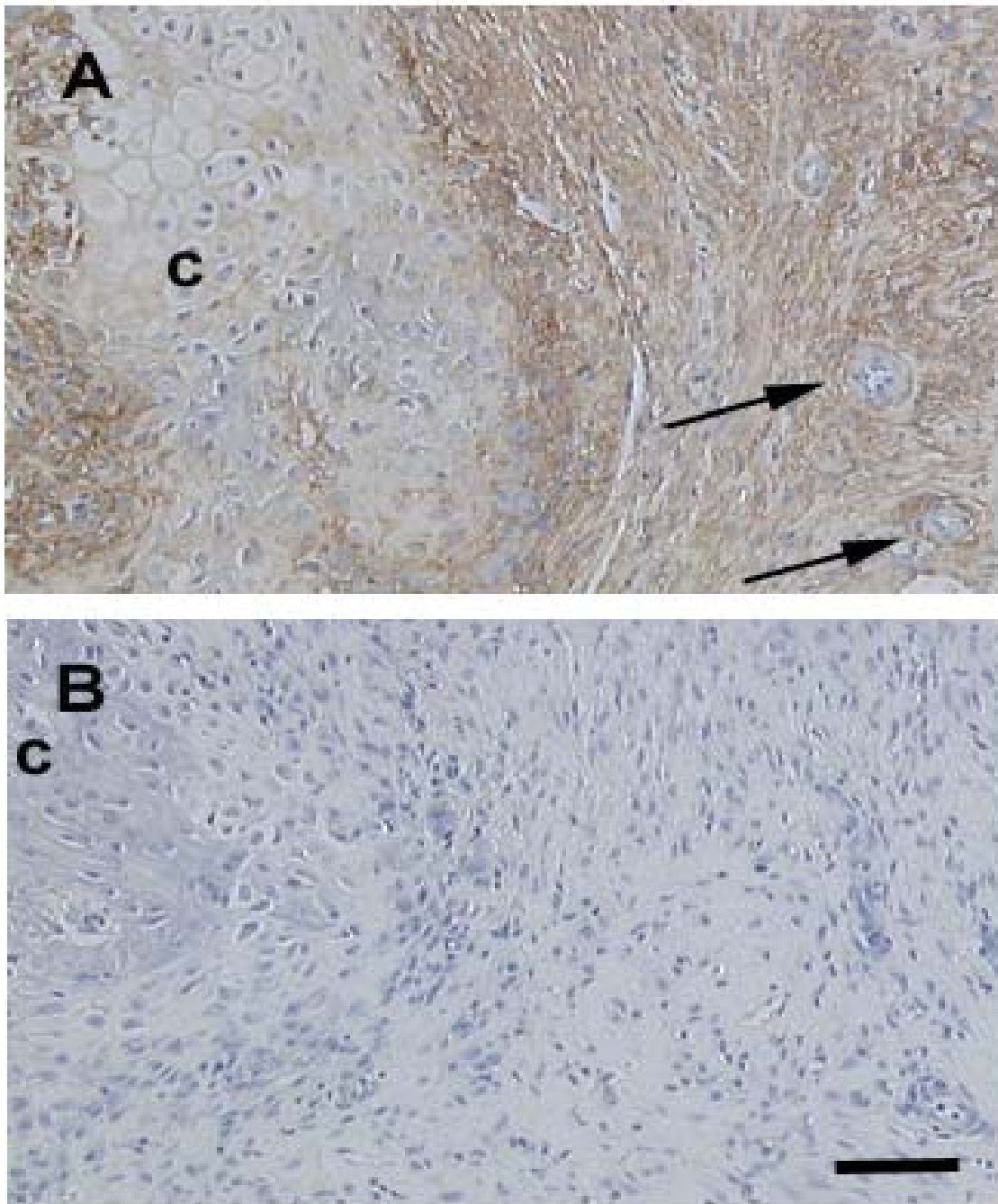
Figure 17. FGF-2 expression in fractures injected with expressing the mutated variant of the FGF-2 gene expressed from the MLV-based vector. Scale bar = 200 µm. (A) FGF-2 expression localized to the proliferating soft callus and mineralizing hard callus tissues at 11 days post-fracture, absent in only the hypertrophic chondrocytes of the cartilage (c). Sinusoid-like structures suggestive of angiogenesis are visible (arrows). (B) Omitting the anti-FGF-2 primary antibody eliminated the immunostaining.

Materials and Methods:

Fracture Surgery:

All surgical procedures were performed as described above in Technical Objective #1, Specific Objective #3.

Fracture Injection:

Following fracture surgery, groups of 4 animals each were injected with mixtures of the MLV-based vector expressing either the β-galactosidase (non-therapeutic control) gene, the BMP-2/4 gene, the modified FGF-2 gene, or a combination of the of the BMP-2/4 and modified FGF-2 genes. Each application had a total concentration of 3×10^8 transforming units (tfu). Because of the potency of FGF-2 gene expression that produced the very large fracture callus we previously observed in injections of undiluted MLV-FGF-2 preparations, a dose response was performed in which the fractures received an undiluted MLV-BMP-2/4 mixed in equal proportions (volume/volume) with dilutions of MLV-FGF-2; the diluent for each MLV-FGF-2 dilution was the MLV-β-galactosidase control gene, an approach that kept the concentration of the MLV-based vector constant.

Briefly, MLV-FGF-2 was diluted:

1) 1:1 in MLV-BMP-2/4, and 100 µl injected into the intramedullary space using the surgically implanted catheter, or

2) diluted 1:4 (0.25) in MLV-β-galactosidase, then 50 µl of this mixture mixed with 50 µl MLV-BMP-2/4, and the 100 µl total volume injected into the intramedullary space using the surgically implanted catheter, or

3) diluted 1:8 (0.125) in MLV-β-galactosidase, then 50 µl of this mixture mixed with 50 µl MLV-BMP-2/4, and the 100 µl total volume injected into the intramedullary space using the surgically implanted catheter, or

4) diluted 1:16 (0.06125) in MLV-β-galactosidase, then 50 µl of this mixture mixed with 50 µl MLV-BMP-2/4, and the 100 µl total volume injected into the intramedullary space using the surgically implanted catheter; and

5) 100 µl of each of the 3 single MLV-gene preparations was also injected into the intramedullary space using the surgically implanted catheter. The MLV-β-galactosidase marker gene preparation served as the non-therapeutic control.

Each group of animals was allowed to heal for 14 days to evaluate the callus tissues by histology, and the mineralized tissue formation by X-ray and pQCT analysis, or for 28 days to evaluate the torsional mechanical strength. These times were chosen for the highly characteristic fracture callus morphology present at 14 days post-fracture and the anticipated benefits of growth factor therapy to bone strength at 28 days.

Fracture Tissue Analysis:

Fracture tissues were examined by X-ray analysis for mineralized tissues, measured for bone mineral content by pQCT, and the histology examined for bone formation by Trichrome staining and for BMP-4 expression by immunohistochemistry. The healing fracture strength is determined by torsional mechanical testing. Tissues for mechanical testing have been available for a few months, and were finally analyzed when the Instron mechanoical testing apparatus was repaired.

Results:
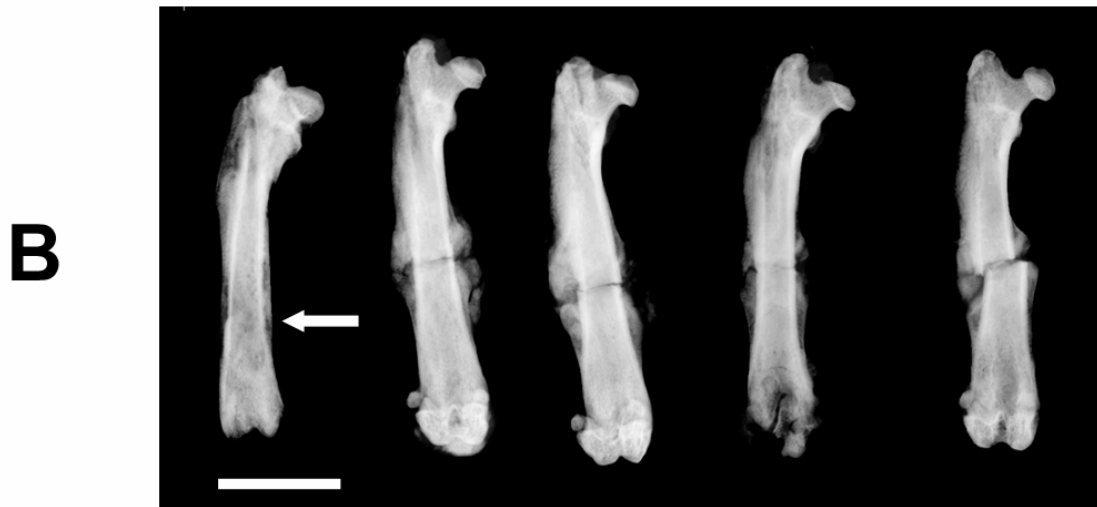
Figure 18. Combination fracture therapy using FGF-2 and BMP-2/4 transgenes at 14 days healing. (A) Gross anatomy and (B) X-ray analysis of healing fractures was performed 14 days, following fracture and the application of the different dilutions of MLV-(mutant)FGF-2 with the standard concentration of MLV-BMP-2/4. The fracture line of the most concentrated MLV-FGF-2 injection is barely visible and indicated by an arrow. The MLV-β-galactosidase marker vector-gene served as a non-therapeutic control comparison. Scale bar = 1 cm.

Examination of the gross anatomy of the healing fractures revealed that the highest concentration of MLV-FGF-2, 50 µl (undiluted) mixed and injected with 50 µl MLV-BMP-2/4, provided what appear to be highly advanced healing at 14 days, with only a very small fracture callus visible in the femur (Figure 18A) and a very faint fracture line visible in the X-ray (Figure 18B). This observation was extremely encouraging. The remaining groups with different MLV-FGF-2 dilutions (i.e., 50 µl 1/4 MLV-FGF-2 + 50 µl MLV-BMP-2/4, 50 µl 1/8 MLV-FGF-2 + 50 µl MLV-BMP-2/4, and 50 µl 1/16 MLV-FGF-2 + 50 µl MLV-BMP-2/4) appeared to produce the bone in the fracture gap, but the callus size and the increased mineralized tissue in the fracture gap at this time did not appear to facilitate healing (i.e., bony bridging of the fracture gap) beyond that of the MLV-β-galactosidase-injected control fractures.

Callus BMC — BMC (mg) +/-SD vs Gene(s): B-gal (N=6), BMP(1):FGF(1) (N=11), BMP(1):FGF(0.25) (N=5, $P<0.005$), BMP(1):FGF(0.125) (N=5), BMP(1):FGF(0.06125) (N=3)

Callus Bony Area — Area (mm^2) +/-SD vs Gene(s): B-gal (N=6), BMP(1):FGF(1) (N=11), BMP(1):FGF(0.25) (N=5, $P<0.009$), BMP(1):FGF(0.125) (N=5), BMP(1):FGF(0.06125) (N=3)
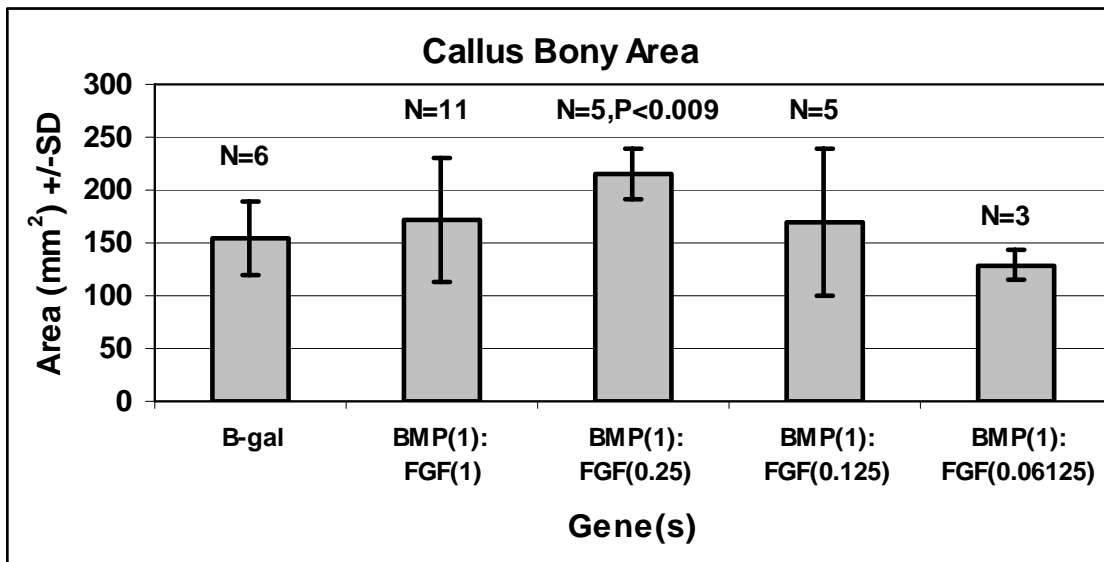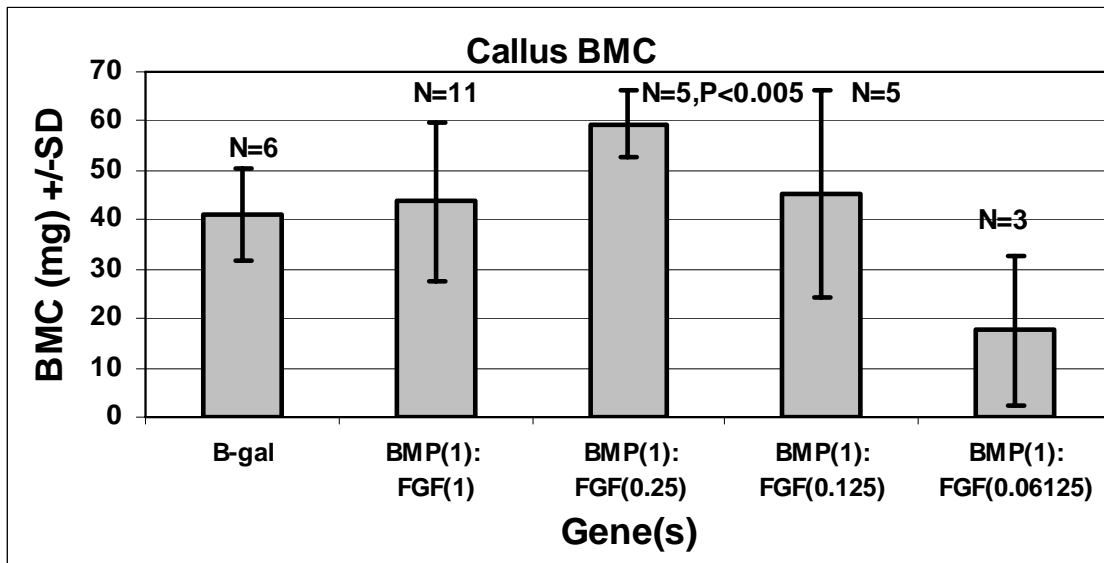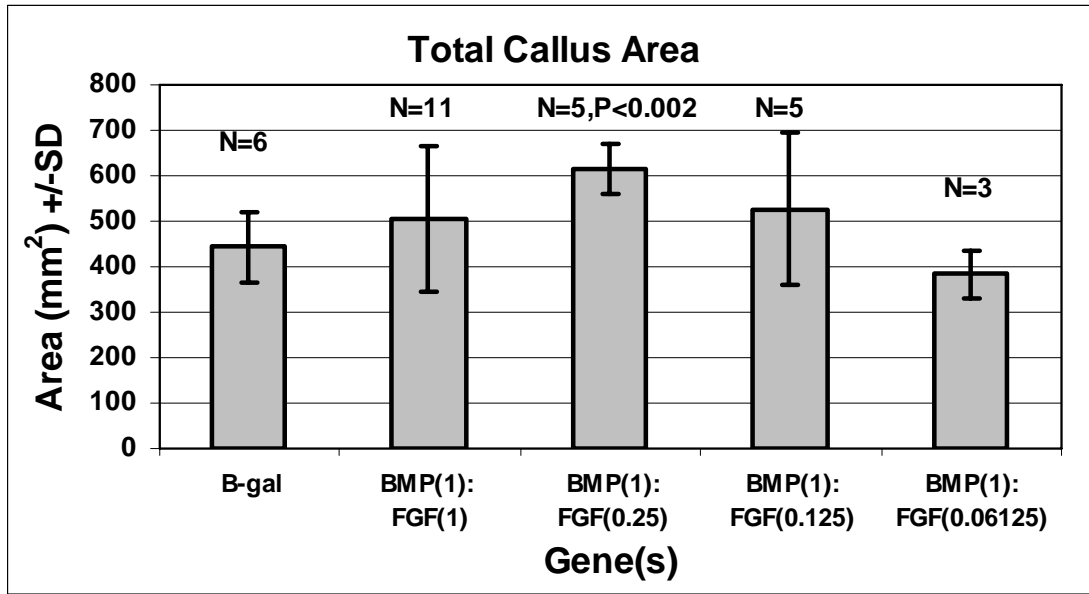
Figure 19. pQCT analysis of combination MLV-BMP-2/4 and MLV-FGF-2 gene therapy in the fracture callus at 14 days post-fracture. pQCT analysis thresholds were adjusted to measure lower density (the non-cortical fracture callus) tissues. The intramedullary space of the fracture was injected at one day post-fracture with 0.1 ml of 1 X 10^7 transforming units (tfu) MLV-based vector expressing either the BMP-2/4 or the FGF-2 transgene. Ratios of MLV-BMP-2/4:MLV-FGF-2 (Figure 18) are indicated for each injection. The pQCT parameters measured are fracture callus bone mineral content (BMC, top), cross-sectional bony area (middle) and the total callus cross-sectional area (bottom), the latter reflecting the entire callus of both bony and soft tissues. Numbers of individual animals are indicated (N). Significance between treatments was determined by t-Test relative to the β-galactosidase control.

pQCT measurements indicated that there was a biphasic effect of FGF-2 gene dosage on the development of bony (BMC and bony area) and total (total bony area) fracture callus tissues. This effect was significant at the 1:4 (0.25) dilution of MLV-FGF-2, and suggests that this concentration of FGF-2 effectively increased the proliferation of soft callus tissues for subsequent ossification through the osteogenic functions of BMP-4. Because the differences in the BMC and bony and total areas callus between each MLV-FGF-2 dilution were very similar (i.e., the BMC, bony area and total area graphs all showed the same pattern, peaking at 0.25 MLV-FGF-2 for each analysis), it appears that the amounts of soft tissue and bony tissues remained balanced and were simply augmented. We conclude that osteogenesis was not accelerated.

An examination of the mechanical testing results indicates a trend towards increased strength and stiffness at the 1:8 (0.125) and 1:16 (0.06125) MLV-FGF-2 dilutions (Figure 20). Thus, the largest fracture calluses observed at the 0.25 MLV-FGF-2 dilution did not translate into increased mechanical strength, an observation consistent with a requirement for bony bridging of the fracture gap for healing. Therefore, healing was not facilitated by the presence of more tissue in the fracture callus, even if it was bony tissue.

Force to Failure (Fractured:Unfractured)

Stiffness (Fractured:Unfractured)
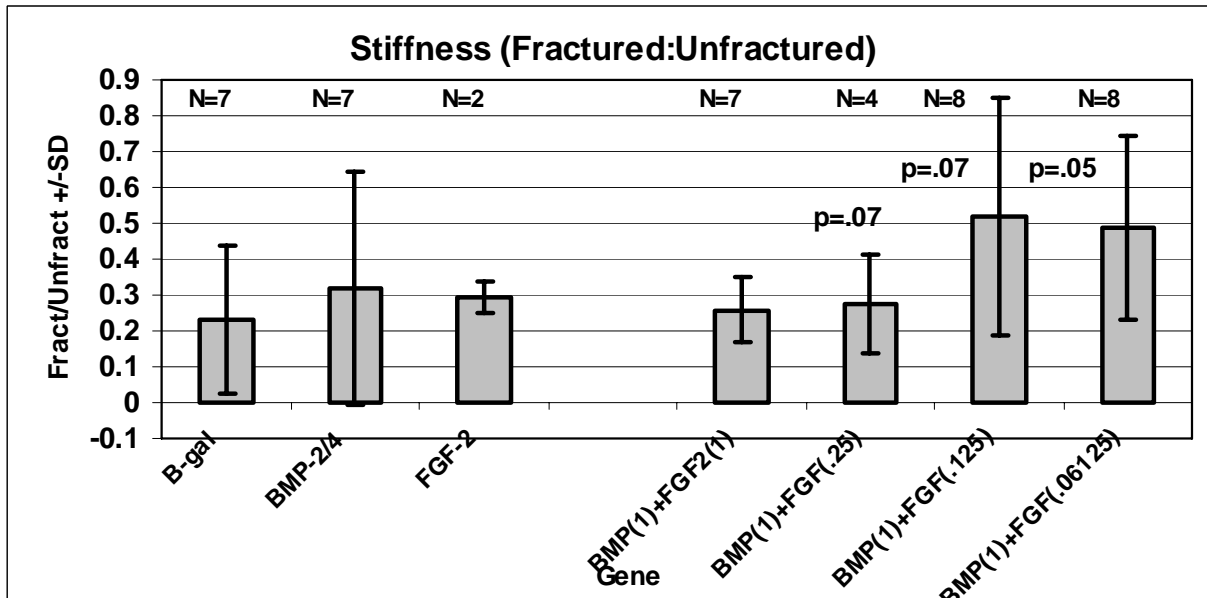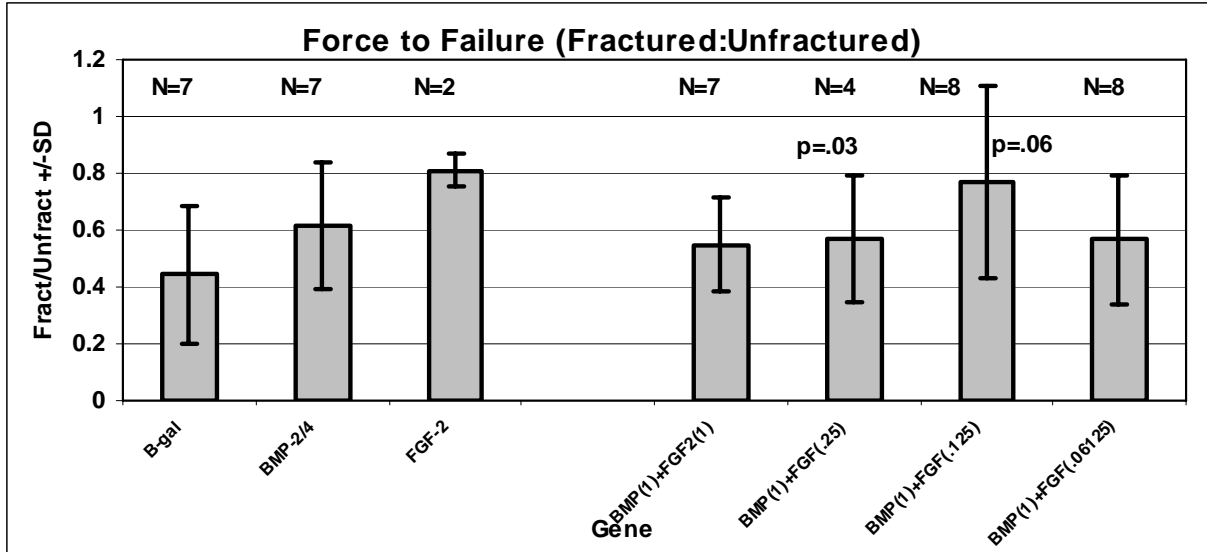
Figure 20. Torsional mechanical testing analysis of combination MLV-BMP-2/4 and MLV-FGF-2 gene therapy in the fracture callus. The intramedullary space of the fracture was injected at one day post-fracture with 0.1 ml of 1 X 10^7 transforming units (tfu) MLV-based vector expressing either the BMP-2/4 or the FGF-2 transgene. Ratios of MLV-BMP-2/4:MLV-FGF-2 (Figure 18) are indicated for each injection. The femurs were harvested at 28 days post-fracture. Data is presented as the mean ± standard deviation for the difference in torsional ultimate load and stiffness between the fracture therapy and unfractured bone. Numbers of animals are indicated (N). Significance between treatments was determined by t-Test relative to the β-galactosidase control.

The histology was also examined to characterize the tissues of the fracture callus that developed in response to this combination therapy (Figure 21).
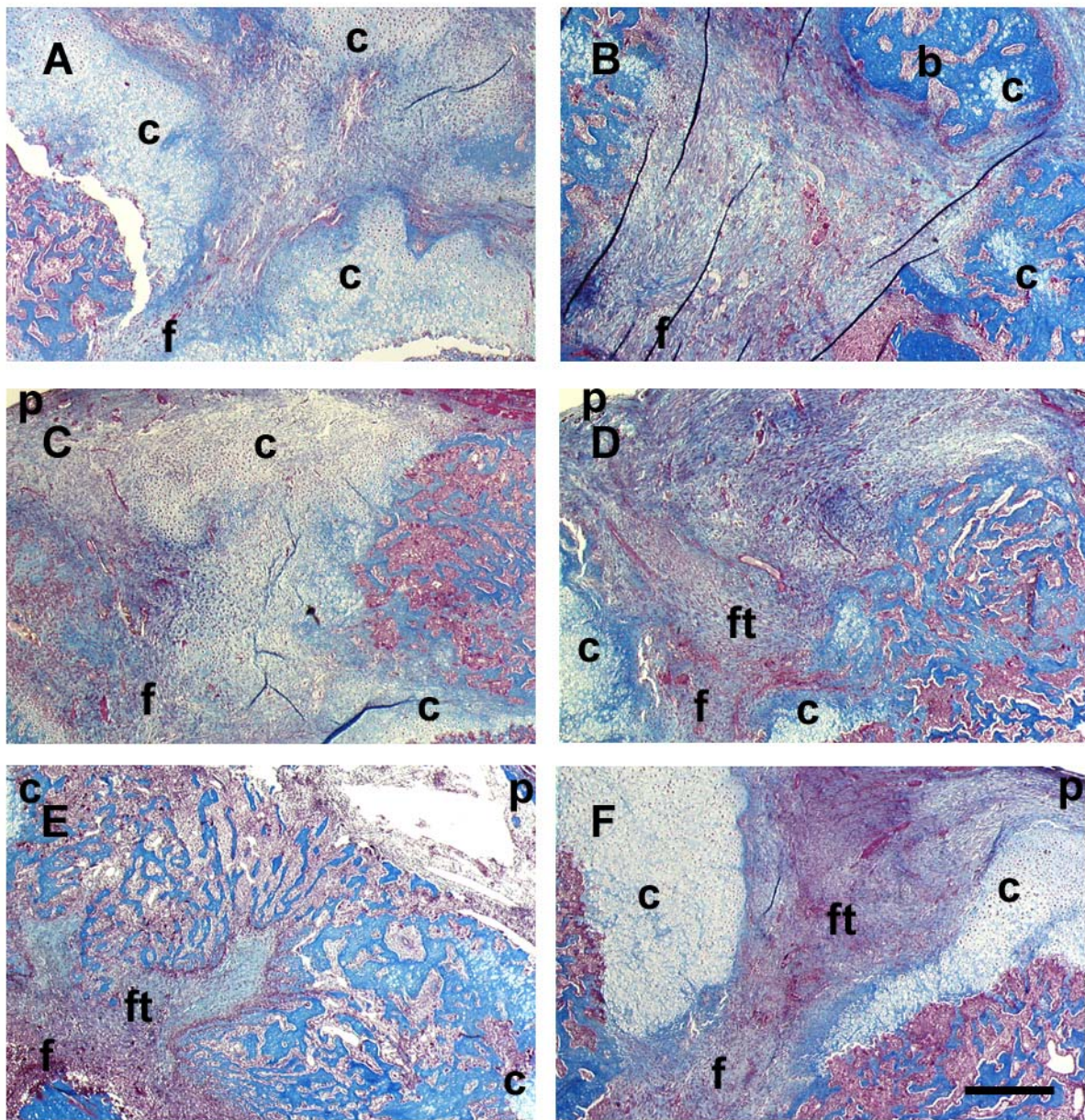
Figure 21. Trichrome stain of fracture tissues receiving combination MLV-FGF-2:MLV-BMP-2/4 gene therapy. Tissues were injected by the intramedullary technique at one day post-fracture and harvested at 14 days post-fracture. MLV-FGF-2 was diluted with MLV-BMP-2/4 (A) 1:1, (B) 1:4, (C) 1:8 and (D) 1:16. For comparison, a representative fracture receiving undiluted MLV-BMP-2/4 [from Figure 8 (B)] is presented (E), as is undiluted MLV-β-galactosidase (F). b, bone; c, cartilage; f, fracture site; ft, fibrous tissue; p, periosteum. Scale bar = 100 um.

An examination of the fracture histology (Figure 21) indicates that the FGF-2 gene therapy did indeed affect fracture repair mediated by BMP-2/4 gene therapy. The fracture cartilage appears more abundant in the fracture gap of the 1:1 and 1:8 MLV-FGF-2 dilutions than in the other treatments; it even fills the gap in the 1:8 dilution. There is less cartilage and more fibrous

tissue in the fracture gap of the 1:16 MLV-FGF-2 dilution. The 1:4 MLV-FGF-2 dilution was particularly interesting, for there was bone development within the fracture gap not observed at higher or lower FGF-2 gene dosages. These results contrast with the MLV-BMP-2/4 and MLV-β-galactosidase gene therapy treatments (each actually twice the gene dosage of the BMP-2/4 used in combination with FGF-2). There is less cartilage, but more bone and fibrous tissue (at the fracture gap) with the undiluted MLV-BMP-2/4, while the MLV-β-galactosidase control gene therapy results in a fracture gap with abundant fibrous tissue between the cartilage fronts that eventually bridge the fracture gap, as in normal healing. It therefore appears that higher FGF-2 gene dosages promote fracture cartilage development in combination therapy, and lower FGF-2 gene dosages favor fibrous tissue. However, as observed in the 1:4 MLV-FGF-2 dilution, bone formation with less abundant cartilage can also be produced by a combination of FGF-2 and BMP-2/4 gene dosages that presumably balance proliferative and osteogenic growth factor functions.

We did not localize gene expression by immunohistochemistry in this part of the study, as the observed effect on bone formation and fracture repair was the focus of this objective. Moreover, the dilution of each growth factor gene (1:4 or 1:8 for FGF-2 and 1:2 for BMP-2/4) that produced such results would be expected to produce protein not detectable by conventional immunostaining. We have effectively localized growth factor expression by FGF-2 immunostaining in Figure 17 and BMP-2/4 immunostaining (Rundle et al., 2003), but these applications examined undiluted injections of the respective growth factor genes that were easier to detect in those applications than in this one. However, the enhanced fracture bone mineral content, bony cross-sectional area and total cross-sectional area of the fracture tissues support a role for such combination gene therapy that increases the tissue abundance. The mechanical strength characteristics do not coincide with the development of the additional fracture callus, suggesting that bony bridging of the fracture callus, the hallmark of healing, has not been accelerated by the larger fracture callus. Gene therapy that promotes this bony bridging is the most desirable outcome for true bone healing.

Conclusions:

In conclusion, the studies utilizing FGF-2 gene therapy in combination with BMP-2/4 gene therapy produced differences in fracture healing as compared to either the control (non-therapeutic) injections or the single therapy injections. The development of both the hard and soft fracture callus tissues was augmented, as demonstrated by an examination of the pQCT (Figure 19) and the histology (Figure 21) results. Torsional mechanical testing analysis (Figure 20) suggested that fracture healing could be improved by combination therapy, but at growth factor gene dilutions (0.125 MLV-FGF-2) different from, though near to, those that exhibited significant differences in bone formation by pQCT and histology (0.25 MLV-FGF-2). The goals of this objective in characterizing combined gene therapy for fracture repair were completed. We conclude that these studies argue for an approach that uses combinations of transgenes in applied carefully calculated preparations or expressed from a regulated vector to promote fracture repair. Alternatively, approaches that use vectors that can provide both robust and regulated expression of the transgenes might improve fracture healing.

TECHNICAL OBJECTIVE #2: TO APPLY MICROARRAY TO STUDY FRACTURE HEALING

Our goals for this Technical Objective were to: 1) expand the analysis to include additional individual fracture samples; 2) confirm genes whose expression was changed in response to fracture repair by an independent method of expression measurement, namely real-time RT-PCR; and 3) to expand our analysis of gene expression to elucidate additional potential pathways of growth factors involved in fracture repair.

Specific Objective 1: To Extend the Number of Genes in our Current In-house Microarray Procedure

Our original in-house microarray analyses utilized only ~1,500 genes and ESTs, This Specific Objective re-evaluated the global gene expression profiling studies during fracture repair using a recently commercially available microarray containing approximately 20,000 unique genes, including all traditional growth factor genes, receptors and several genes that belong to growth factor signaling pathways.

Objective:

This study sought to identify and adapt the experimental microarray chip and analysis system best suited for the analysis of rat fracture gene expression.

Materials and Methods:

We have adopted the Agilent rat oligomer chip to analyze our fracture RNA in our microarray analysis. This chip has 20,046 unique gene targets presented as 60-base oligomers, and as such provides a more extensive number of rat gene targets than we are able to achieve with our facilities. Several major families of growth factors, signaling molecules and structural genes are represented, providing one of the most comprehensive surveys of rat gene expression currently available commercially. Most importantly, the "low-input" Agilent dye labeling system allows us to amplify the signal during fluorescent labeling of the cDNA. This approach is highly advantageous for reducing the RNA input into the system, minimizing the numbers of animals used yet maximizing the sensitivity of the microarray analysis for samples with very low amounts of tissues. This is particularly important in the unfractured but pinned control samples of the femur fracture model, which have very little tissue. This labeling system permits us to perform the analysis on these extremely limited samples without pooling the RNA from multiple individuals. We are therefore able to analyze the biological variation between multiple subjects that is not possible in pooled samples, a problem often ignored in microarray experiments. The Agilent "low input" dye labeling technique was compared with the TSA amplification technique that we have used previously, and with an analysis using no amplification. Using 2 ug of RNA for Cy3 and Cy5 dye-labeling, we compared the images following hybridization to the Agilent rat gene chip.

Results:

The scatter plots shown in Figure 22 compare total RNA labeled with the Agilent amplification protocol and the tyramide signal amplification (TSA) amplification protocol. The data was normalized identically between the arrays, since a Lowess normalization cannot be performed with fewer than 1000 spots. The plots should cluster closely around a slope of "one",

since the same "universal" RNA was labeled using the respective protocols and Cy3 and Cy5 prior to hybridization. For the Agilent low input labeling method, the linear RNA amplification did not introduce artifacts. The only data points lying outside the 2 fold lines were the ratio spikes, in controls that follow the expected ratios fairly well (top). The TSA plot (bottom) does not follow the expected slope of "one" as well, and the spike in ratio controls are not as consistent as with the Agilent labeling. Each gene's measured intensity was divided by its control channel value in each sample; if the control channel was below "10", then "10" was used as the control channel intensity. If the control channel and the signal channel were both below "10", then no data was reported. All of the genes in each sample were divided by the median of a user-specified list of positive control genes. The median of the positive control genes was calculated using only raw intensity measurements above "10". Of the genes in the positive control list, only genes marked as present were used. Positive control genes for normalization included the housekeeping genes glyceraldehyde phosphate dehydrogenase and β-actin.
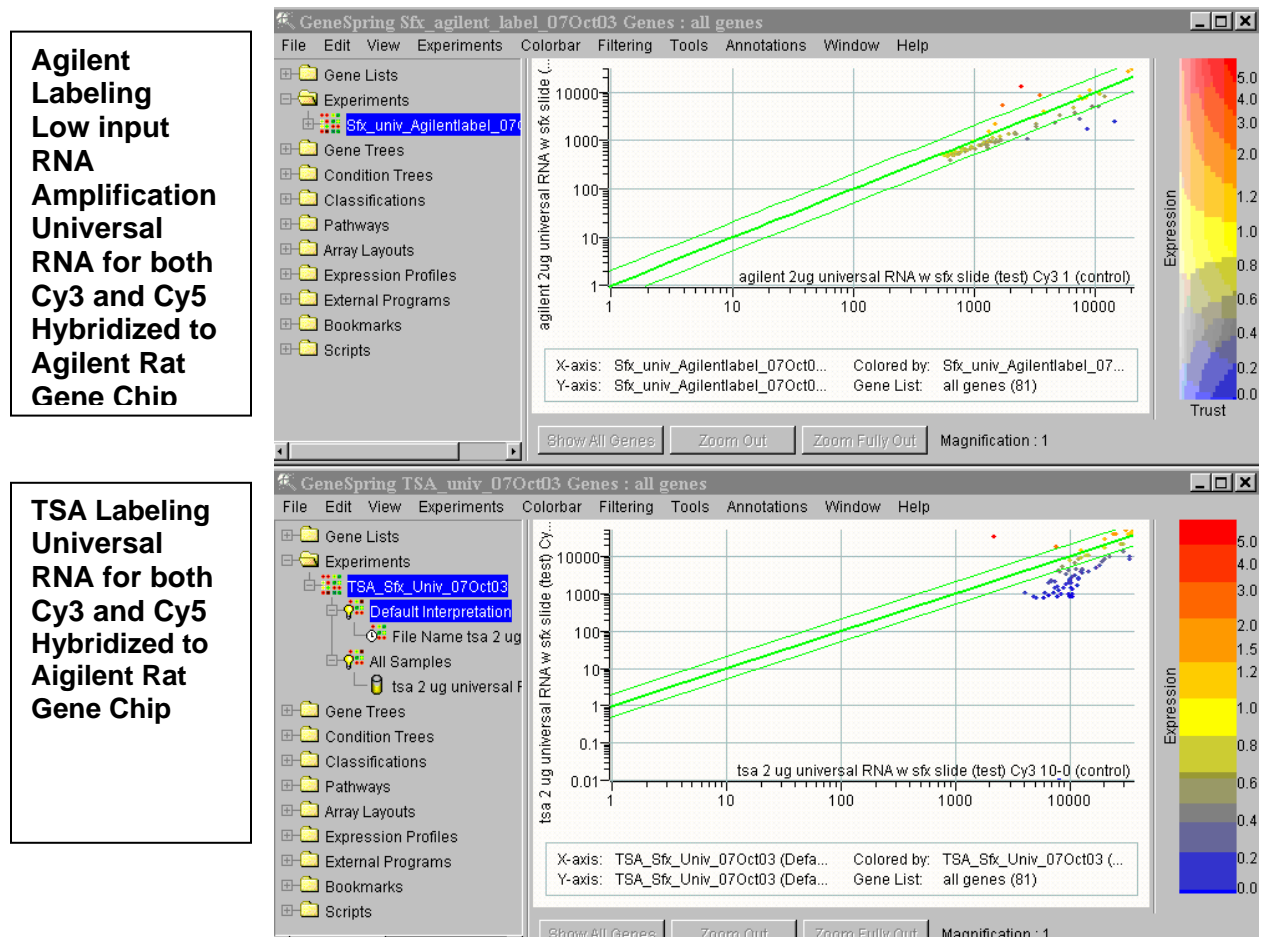
Figure 22. Scatter plot comparison of the Agilent "low input" (top) and TSA (bottom) dye labeling hybridization results on the Agilent rat gene chip.

Conclusions:

The Agilent "low input" labeling system provided the most sensitive and accurate cDNA labeling system available, and provided superior hybridization images for a reproducible analysis of gene expression. We have purchased the Agilent microarray chips that contained genes and

ESTs specific to the rat, including growth factor and their cognate receptor genes. Consequently, we will utilize the Agilent rat gene chip and dye labeling system for our future fracture microarray analysis. The objective of this study, to develop a microarray analysis that extends our initial technology toward a reliable approach for the analysis of large numbers of rat genes, has been accomplished, in that we have validated a commercial system for the comparison of gene expression in fracture tissues.

Specific Objective #2: To Apply Our Extended In-house Microarray to Study Gene Expression in the Fracture Callus at 3 Days after Fracture.

Objectives:

The microarray determination of whole genome gene expression in the normal healing fracture was initiated during the first year of this study. Microarray analysis has been especially valuable in identifying and characterizing the molecular pathways of fracture repair, as well as identifying potential therapeutic gene candidates for fracture gene therapy. To accomplish these goals, tissues were harvested for analysis at one early and one later time point in healing: 3 days and 11 days. The early time (3-day) is characteristic of the transition of the inflammatory phase and intramembranous bone formation phases and was the stated goal for this objective. We also studied the latter time point (11-day), which is characteristic of the maturation of the cartilage intermediate to endochondral bone. The early time point was to suggest gene candidates for early clinical intervention, and the addition of the 11-day data to this Technical Objective provided an additional measurement of gene expression during fracture healing. As such, it was an additional study performed in the completion of this objective.

Microarray evaluations of healing fractures have also been studied by other investigators (Hadjiargyrou et al., 2002; Meyer et al., 2003; Li et al., 2005). Our approach to the analysis of gene expression in fracture repair differed from previous microarray studies in two very important aspects: 1) Previous studies used intact bone without the Kirschner (K)-wire as control for healing fractures, which has a K-wire in the marrow space. Accordingly, the control tissues included marrow, while the fractured tissues lacked this marrow. Marrow ablation could induce inflammatory reactions that alter the expression of fracture-related genes. In our study, we used the appropriate marrow-ablated control diaphyses for comparison with the fractures (see Materials and Methods); 2) Previous studies arbitrarily used two-fold changes in expression as significant effects. Our studies included sufficient individual replicate samples that allow the appropriate application of statistics to determine significant changes. Accordingly, we believe that our experimental design is superior to those used in previous studies.

Materials and Methods:

Fracture surgery was performed using the three-point bending technique (Bonnerens and Einhorn, 1984). As indicated above, in contrast to other fracture microarray studies conducted in the past, our unfractured control femurs included an intramedullary K-wire as normally used in the fractured femurs. These controls also normalized the analysis for intramedullary bone formation induced by the K-wire in fractured femurs, which we have previously observed expected by 11 days healing. This unfractured control comparison allowed us to obtain a more accurate determination of gene expression in the periosteal tissues that mediate fracture healing.

Total RNA was isolated from individual fractured femurs at 3 days and individual fractures at 11 days healing, with the fractures compared to equal numbers of individual unfractured (control) femurs at each time point. RNA isolation was performed on pulverized fracture tissues by Trizol^{TM} purification, following the manufacturer's (Invitrogen) instructions. The purity and integrity of each RNA sample was confirmed using the Agilent Bioanalyzer.

Our approach to fracture gene expression analysis by microarray technology is shown in Figure 23. We had adopted the Agilent gene chip for these studies, which had become available in the first year of this study, and continued to use it for our expanded microarray analysis. This chip contains 60-mer oligos that represent 20,000 unique genes either derived from the rat, or homologous to rat gene sequences. The Cy3 and Cy5 labeling was performed as described in the Agilent "low input" labeling system, and the hybridization performed using equipment and procedures specified for the Agilent rat gene chip. We compared each group of fractured RNA and unfractured control RNA isolates at each time point, 3 days [corresponding to the healing phase that is immediately after the inflammatory phase but prior to the initiation of bone formation phase (Bolander 1992)] or 11 days post-fracture [corresponding to the healing phase when intramembranous and endochondral bone formation overlap (Bolander 1992)]. Because the Agilent RNA dye labeling system allowed us to analyze fracture tissues and unfractured controls for gene expression with very low amounts of RNA, we were able we were able to use individual samples to identify individual biological variations concealed in other microarray studies where the samples are pooled.

Microarray image analysis was also performed in-house, using ScanArray image analysis and Genespring expression analysis software. Lowess normalization was performed to identify differences in the Cy3 or Cy5 dye labeling efficiencies. One-way analysis of variance (ANOVA) established significant changes in expression of up-regulated genes and down-regulated genes for each group of fractured (as compared to the unfractured control) animals at 3 days healing and 11 days healing. Cluster analysis performed to classify the genes into Gene Ontology (GO) categories for further examination. With the expanded numbers of replicates in our study, we were able to rigorously analyze the changes in gene expression for statistical significance. Changes in gene expression were deemed statistically significant at $p < 0.05$.

Figure 23. Fracture Microarray Approach

K-wire, fractured femoral diaphysis	K-wire, unfractured femoral diaphysis

**Healing
3 Days or 11 Days**

RNA Isolation   **RNA Isolation**

Cy5 Label   **Cy3 Label**

**Comparison of individual pair:
Fractured vs Unfractured**

Micoarray
1 **20K Rat Oligo Chip**
2 **Low-input Hybridization**
Analysis
1 **Genespring Image Analysis**
2 **Lowess Normalization**
3 **Gene Ontology**

3 Day Analysis (n = 5 Individual Pairs)	11 Day Analysis (n = 8 Individual Pairs)

Results:

The RNA recovery from fractured and unfractured animals was routinely of sufficient quantity and quality for analysis by the Agilent low-input labeling and hybridization system on the 20,000-gene chip. Our approach successfully identified several hundred known and unknown genes, as reported for the first year of the study. Inclusion of the additional samples has improved the statistical calculations, and in the current analysis 6,555 genes displayed significant changes in expression at 3 days, 11 days or both; of these genes, 4,873 genes were known and 1,682 were unknown (Table 1). The proportions of known genes (2/3) and unknown genes (1/3) are very close to our initial analysis with fewer animals. Our fracture microarray study therefore demonstrated increased sensitivity yet remained consistent. The numbers of unknown genes with expression changes during fracture healing is especially interesting, and suggests that the molecular regulatory pathways of bone repair are indeed complex, with many remaining to be characterized. A comparison of our analysis with those of previous fracture studies again reveals that several common genes previously associated with fracture repair also displayed significant changes in expression in our study (Table 2). These results support the accuracy of our approach.

Table 1. Summary of Fracture Microarray Gene Expression Changes			
Expression Change (P<0.05)	**Known Genes**	**Unknown Genes**	**Total**
3 Days			
Up at 3 days, no change at 11 days	889	215	1104
Down at 3 days, no change at 11 days	1013	388	1401
11 Days			
Up at 11 days, no change at 3 days	904	345	1249
Down at 11 days, no change at 3 days	1206	450	1656
3 and 11 Days			
Up at both 3 and 11 days	354	96	450
Down at both 3 and 11 days	474	181	655
Biphasic			
Up at 3 days, down at 11 days	20	1	21
Down at 3 days, up at 11 days	13	6	19
Total	**4873**	**1682**	**6555**

Table 2. Comparison of selected genes with up-regulated expression in this study with previous fracture studies					
This Study					**Previous Fracture Studies**
Gene	**Accession**	**Function**	**Fold-Change (P<0.05)**		**Similar Change in Expression**
			3 Days	**11 Days**	

transforming growth factor β-2	BF420705	growth factor	**1.3**	**1.6**	[14]
transforming growth factor β-3	NM_013174	growth factor	**2.4**	**2.0**	[14, 23, 34]
fibroblast growth factor 7	NM_022182	growth factor	**1.3**	NS	[23, 34]
interleukin 6	NM_012589	inflammation	**3.5**	NS	[14, 34]
angiopoietin-2 (like)	NM_133569	angiogenesis	NS	**1.4**	[39]
mesenchymal homeobox-2	NM_017149	transcription factor	**2.5**	**2.8**	[23]
pleiotrophin/OSF-1	NM_017066	several	**2.3**	NS	[23, 34]
frizzled	NM_021266	wnt signaling	**1.5**	**1.5**	[23]
cysteine-rich protein 61	NM_031327	extracellular matrix signaling	**2.6**	**2.8**	[23, 34]
fibronectin	NM_019143	extracellular matrix	**2.4**	**2.1**	[23, 34]
tenascin	BE126741	extracellular matrix	**2.1**	**1.5**	[23, 34]
thrombospondin-2	BF408413	extracellular matrix	**1.7**	**1.8**	[23, 34]
osteonectin/SPARC	NM_012656	extracellular matrix	**1.7**	NS	[23, 34]
aggrecan	NM_022190	extrcellular matrix	NS	**5.1**	[23, 34, 39]
collagen 2α1	AA899303	cartilage maturation	**0.8**	**1.5**	[23, 34, 39]
integrin binding sialoprotein	NM_012587	mineralization	**4.0**	NS	[23, 34]
collagen 5α1	NM_134452	extracellular matrix	**2.4**	**2.1**	[23, 34]
osteocalcin/Gla	NM_012862	mineralization	NS	**2.4**	[14, 23, 34, 39]
protease nexin-1	X89963.1	extracellular matrix protease	**2.1**	**2.1**	[23, 34]

Classification of all genes with highly significant changes in expression (p<0.0002) during fracture repair into Gene Ontology (GO) categories facilitated the analysis at both 3 days and 11 days healing (Table 3). Not surprisingly, several metabolic and signaling gene categories were up-regulated at 3 days healing, when these events would be expected to be important for healing. At 11 days healing, developmental and adhesion-related genes were expressed, consistent with the tissue differentiation of the maturing fracture callus.

Table 3. Known genes with highly significant (P<0.0002) changes in the expression during fracture healing				
Accession	**Fold-Change**		**Gene Description**	**Gene Ontology Category [4]**
	3 Days	**11 Days**		
BQ209997	**5.02**	**7.80**	similar to Mouse collagenous repeat-containing 26kDa protein (CORS26).	protein metabolism
AA858962	**4.36**	**2.15**	Rat retinol-binding protein (RBP) mRNA, partial cds.	vitamin A metabolism
NM_012587	**3.97**		Rattus norvegicus integrin binding sialoprotein (Ibsp).	extracellular space
BQ211765	**3.49**		Rattus norvegicus DEXRAS1 (Dexras1) mRNA.	signal transduction
BF415205	**2.78**	**6.19**	Rat mRNA fragment for cardiac actin.	actin cytoskeleton
NM_133566	**2.29**	**1.21**	Rattus norvegicus cystatin N (LOC171096).	organogenesis and histogenesis
NM_013104	**1.97**	**4.58**	Rattus norvegicus Insulin-like growth factor binding protein 6 (Igfbp6).	extracellular space
BQ209870	**1.80**	**3.88**	similar secreted modular calcium-binding protein 2 [Mus musculus].	calcium ion binding
CA510266	**1.71**	**1.32**	similar to prefoldin 5; myc modulator-1; c-myc binding protein [Homo sapiens].	regulation of transcription, DNA dependent
NM_012488	**1.55**	**2.53**	Rattus norvegicus α-2-macroglobulin (A2m).	protease inhibitor activity/IL-1, IL-8 binding
BE329208	**1.52**	**1.43**	similar to Cricetulus griseus SREBP cleavage activating protein (SCAP), complete cds.	steroid metabolism
NM_012816	**1.41**		Rattus norvegicus α-methylacyl-CoA racemase (Amacr).	metabolism/peroxisome
NM_057197	**1.40**		Rattus norvegicus 2,4-dienoyl CoA reductase 1, mitochondrial (Decr1).	oxidoreductase
NM_031646	**1.39**		Rattus norvegicus receptor (calcitonin) activity modifying protein 2 (Ramp2).	G-protein coupled receptor signaling
NM_031050	**1.38**		Rattus norvegicus lumican (Lum).	extracellular matrix
NM_017355	**1.27**	**1.24**	Rattus norvegicus ras-related GTP-binding protein 4b (Rab4b).	vesicle-mediated transport
U56859.1	0.90	0.79	Rattus norvegicus heparan sulfate proteoglycan, perlecan domain I (RPF-I), partial cds.	cell adhesion
BF281804	0.85	0.84	similar to solute carrier family 7 member 12; isc-type amino acid transporter 2 [Mus musculus].	amino acid transport
NM_017140	0.85		Rattus norvegicus dopamine receptor D3 (Drd3).	dopamine receptor signaling pathway
BF548886	0.85	0.78	similar to Mouse T-cell antigen receptor α-chain (TCR-ATF2), partial cds.	regulation of transcription, DNA dependent
NM_013029	0.84	0.79	Rattus norvegicus Sialyltransferase 8 (GT3 α 2,8-sialyltransferase) C (Siat8c).	amino acid glycosylation
NM_012997	0.82	0.74	Rattus norvegicus Purinergic receptor P2X, ligand-gated ion channel, 1 (P2rx1).	amino acid transport
NM_031725	0.82		Rattus norvegicus secretory carrier membrane protein 4 (Scamp4).	protein transport
AA900738	0.80	0.81	similar to Rat DNA for serine dehydratase.	amino acid metabolism/gluconeogenesis

NM_133322	0.79	0.77	Rattus norvegicus potassium voltage-gated channel, KQT-like subfamily, member 2 (Kcnq2).	synaptic transmission
NM_052801	0.78	0.76	Rattus norvegicus von Hippel-Lindau syndrome (Vhl).	regulation of transcription, DNA dependent/proteolysis & peptidolysis
CB546252	0.78	0.83	similar to zinc finger protein 261; DXHXS6673E [Mus musculus].	nucleus/zinc ion binding
NM_144730	0.78	0.80	Rattus norvegicus GATA-binding protein 4 (Gata4).	regulation of transcription, DNA dependent
NM_030854		21.97	Rattus norvegicus chondromodulin-1 (Chm-1).	cell growth and maintenance/proteoglycan metabolism
BF560915		17.46	Rattus norvegicus mRNA for collagen α 1 type X, partial.	skeletal development
NM_019189		13.77	Rattus norvegicus cartilage link protein 1 (Crtl1).	hyaluronic acid binding
NM_012929		11.38	Rattus norvegicus Procollagen II α 1 (Col2α1).	skeletal development
NM_031511		6.72	Rattus norvegicus Insulin-like growth factor II (somatomedin A) (Igf2).	development
BQ210664		5.73	similar to cartilage intermediate layer protein	unknown
BQ191772		5.37	similar to mouse annexin A8.	phospholipid binding
NM_022290		5.28	Rattus norvegicus tenomodulin (Tnmd).	collagen maturation
AI576621		3.73	similar to Mouse carboxypeptidase X2, complete cds.	protein binding
AA963765		2.89	similar to osteoglycin [Mus musculus].	regulation of DNA transcription
BQ200482		1.41	similar to Mouse mRNA for acetylglucosaminyltransferase-like protein.	lipopolycaccharide biosynthesis
CB547946		1.35	similar to Mus musculus (clone pVZmSin3B) mSin3B, complete cds.	regulation of transcription, DNA dependent
AI059288		0.83	similar to Mouse B-cell activating factor (TNFSF13b, Baff), complete cds.	positive regulation of cell proliferation
CB547491		0.83	similar to Mus musculus very large G protein-coupled receptor 1 (Vlgr1, Mass1), complete cds.	G-protein coupled receptor signaling
CB545755		0.82	similar to RAD54 like (S. cerevisiae) [Mus musculus].	DNA recombination, repair
CB544611		0.82	similar to BACR7A4.19 gene product [Drosophila melanogaster].	G-protein coupled receptor signaling
CB545661		0.81	similar to BC026845_1 Mus musculus, Similar to nucleoporin 133kD, complete cds.	RNA metabolism
AW920271		0.81	similar to mouse cat eye syndrome chromosome region, candidate 5 (Cecr5), complete cds.	metabolim
BQ196556		0.80	similar to nudix (nucleoside diphosphate linked moiety X)-type motif 5 [Mus musculus].	oxidative stress response/DNA repair
AA874884		0.60	Rat heme oxygenase gene, complete cds.	oxidoreductase activity
NM_031740		0.59	Rattus norvegicus UDP-Gal:betaGlcNAc β 1,4-galactosyltransferase, polypeptide 6	glyosphingolipid biosynthesis

		(B4galt6).	
NM_053843	0.49	Rattus norvegicus Fc receptor, IgG, low affinity III (Fcgr3).	Immune response

Bold: Up-regulated

While a detailed examination of the individual genes with inflammatory functions at 3 days healing revealed several of the inflammatory genes previously observed in other fracture microarray studies, there were fewer representatives among the inflammatory cytokines and the immune response genes (Table 4). Significantly, very few of these genes were up-regulated more than 2-fold, suggesting that tight control of inflammatory gene expression is critical for bone healing. Several of these genes were also up-regulated at 11 days healing; they might perform non-inflammatory functions, because the reduction in expression of acute phase proteins between 3 days and 11 days suggests a regulated reduction in the inflammatory response. Even within the complement activation pathway, which is normally associated with inflammation, genes with negative regulatory influences on the cascade were up-regulated in expression at both 3 and 11 days healing. Several of these results are in accordance with our hypothesis that the K-wire controls normalized the analysis for the intramedullary inflammatory response. Such inflammatory gene regulation is critical for tissue repair, and an accurate description of the inflammatory gene repertoire is essential for the design of effective fracture healing therapies.

Table 4. Up-Regulated Expression of Inflammation and Immune Function Genes in Fracture Healing				
Gene		**Functions**	**Fold-Change in Expression (p<0.05)**	
Description	**Accession**		**3 Days**	**11 Days**
Growth Factors				
Platelet-derived growth factor receptor	AA925099	chemotaxis	**2.7**	**1.5**
Monocyte chemotactic protein 3	BF419899	chemotaxis	**3.3**	**1.6**
Mast cell growth factor/kit ligand	AI102098	stem cell factor, hematopoietic & mast cell growth	**1.3**	**NS**
TNFα/TNFβ	AA819277	inflammation	**NS**	**1.2**
TRAF2	BI282097	TNF inflammation	**1.1**	**NS**
TRAF4	CB546212	TNF inflammation	**1.6**	**NS**
TNF-stimulated gene 6	AF159103.1	TNF inflammation	**1.8**	**1.7**
TGFβ2	BF420705	inflammation	**1.3**	**1.6**
LTBP1	NM_021587	TGF regulation	**1.9**	**1.5**
TGFβli4	NM_013043	TGF regulation	**1.8**	**1.9**
Interleukins and Related Cytokines (www.copewithcytokines.de)				
IL1 receptor accessory protein	NM_012968	IL1 inflammation	**1.6**	**NS**

IL3 regulated nuclear factor	NM_053727	IL3 MHC, eosinphil, basophil stimulation, apoptosis inhibition	**1.4**	**NS**
IL6	NM_012589	acute phase protein induction, proliferation	**3.5**	**NS**
IL6 gp130	298242_Rn	IL6 acute phase protein induction	**1.7**	**1.4**
IL6 signal transduction protein	BF398277	IL6 acute phase protein induction	**1.5**	**1.4**
IL11 receptor α 1	221254_Rn	IL11 progenitor growth factor, acute phase protein induction	**NS**	**1.3**
IL12 p40 precursor	NM_022611	IL12 hematopoeitic response, adhesion	**NS**	**1.3**
IL18	284329_Rn	T cell activation, hematopoiesis	**1.3**	**NS**
Interferon-γ	NM_138880	immune response	**NS**	**1.4**
Interferon inducible p27-like	NM_130743	immune response	**1.4**	**1.4**
ATP dependent interferon responsive	BG373987	immune response	**NS**	**1.4**
Complement Pathway (users.rcn.com/jkimball.ma.ultranet/BiologyPages/C/Complement.html)				
Complement 1Q binding protein	NM_019259	Complement 4 activation	**1.7**	**NS**
Complement 1R	AA799803	Complement 4 activation	**1.7**	**1.4**
Complement 1S	NM_138900	Complement 4 activation	**2**	**2.6**
Complement 2	NM_172222	Complement 3 activation	**NS**	**1.4**
Complement 4	AI412156	Complement 2 activation	**NS**	**2.3**
Complement H	NM_130409	Complement 3 inhibition	**1.6**	**NS**
Complement I	NM_024157	Complement 3 inhibition	**NS**	**1.1**
CDs (www.immunologylink.com)				
CD14	NM_021744	LPS receptor	**1.4**	**NS**
CD39-like 3	AI070096	ecto-nucleoside triphosphate diphosphohydrolase	**1.5**	**NS**
CD34	AI102873	adhesion, stem cell marker	**1.6**	**1.9**
CD36	NM_054001	scavenger receptor, inflammation, angiogenesis	**1.6**	**NS**
CD81	NM_013087	T cell stimulation	**1.8**	**2.1**
CD151	NM_022523	adhesion, signaling	**1.4**	**1.3**
CD164	NM_031812	hematopoeitic-stromal interaction	**1.6**	**1.2**

NS: Not Significant

Conclusions:

We have accomplished the proposed work on microarray studies of fracture repair proposed for this objective. Microarray analysis of fracture healing by our approach has identified a number of genes or ESTs with either significant up-regulation or down-regulation in expression at days 3 and 11 days of healing. Some of the genes that we identified had been previously described by other investigators, but many had not. The expressed inflammatory gene repertoire was altered compared to previous studies, an important observation in early fracture repair, when healing is initiated. Our use of a K-wire-stabilized unfractured control bone allowed ablated the marrow, and with our statistical analysis of individual samples, allows for more sensitive detection of gene expression in the fracture tissues. The analysis of our microarray data is still on-going, and we anticipate that further examination of the data will produce additional information.

Specific Objective #3: To Evaluate the Reproducibility and To Analyze the Data from the Extended Microarray.

Objectives:

The microarray analysis of fracture healing included animals that provided final group sizes of 5 individuals (fractured and unfractured controls) at 3 days healing, and 8 individuals (fractured and unfractured controls) at 11 days healing. This analysis was used to rigorously identify and confirm differences in fracture gene expression, characterize different gene pathways that participate in fracture healing, and identify potential therapeutic gene candidates. The expression of several genes of interest was verified by real-time RT-PCR measurements of gene expression within the same fracture tissue.

Materials and Methods:

All surgical procedures and RNA isolations were performed as stated above (Technical Objective #2, Specific Objective #2). RNA labeling and hybridization to the Agilent 20,000 gene chip using the Agilent low-input system, data analysis and normalization were also performed as described above.

Changes in gene expression as determined by microarray analysis were independently confirmed by real-time RT-PCR for selected genes of interest. This confirmation was performed on some of the same fracture tissues that underwent microarray analysis, as well as additional fracture tissues at 3 and 11 days healing. Total RNA was treated with DNAse I and reverse transcribed using the Superscript III kit (Invitrogen) according to the manufacturer's specifications. Real-time RT-PCR was performed on 50 ng of cDNA using gene-specific primers and the Quantitect SYBR Green detection (Qiagen), as specified by the manufacturer. Real-time PCR was performed on a DNA Engine Opticon thermal cycler (BioRad Laboratories) at 45 seconds per step for 35 cycles and at a specific annealing temperature optimized to amplify both the gene of interest and the cyclophilin housekeeping gene with the greatest efficiencies. Each gene of interest was normalized to expression of the housekeeping gene cyclophilin for each fracture tissue, and the difference between fractured and unfractured real-time PCR cycle numbers used to calculate the fold-change in expression in the fracture for comparison to the microarray values. Examples the determination of the delta Ct (ΔCt) for two scarless wound healing genes, i.e., Protease Nexin-1 (PN-1) and Hyaluronic Acid Synthetase-1 (HAS-1), and the housekeeping gene, cyclophilin A, are shown in Figure 24. Table 5 lists the primers and annealing temperatures used for real-time PCR confirmation of the cyclophilin A gene, the genes associated with our "scarless wound healing genes" analysis, and Table 7 lists the FGF family genes and primers of our subsequent microarray analysis.
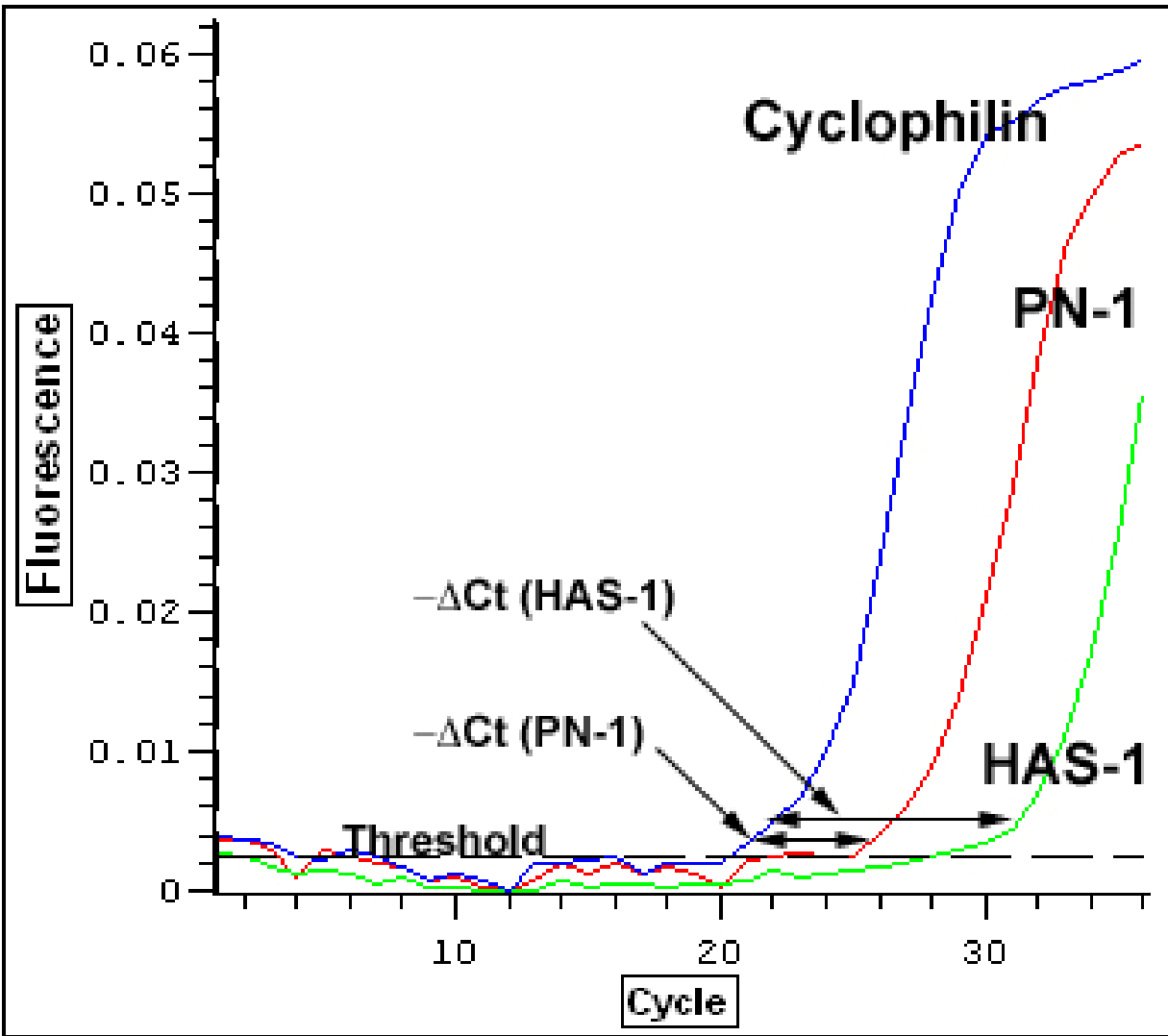
Figure 24. Illustration of real-time RT-PCR analysis, in this case protease nexin-1 (PN-1), a scarless gene that displayed changes in expression during fracture repair (Table 6), and hyaluronidase synthase-1 (HAS-1), a gene implicated in extracellular matrix cell motility. The difference in cycle number -ΔCt each gene displays relative to the normalizing housekeeping gene (cyclophilin-A) determines the magnitude of expression for each within the fracture tissue. The differences in cycle number can be within a particular tissue (-ΔCt fractured, or with therapy) can then be related to the differences in cycle number can be within a different tissue (-ΔCt, unfractured or without therapy) to obtain a normalized comparison of the differences in healing between tissues. [(-ΔCt) – (-ΔCt)].

Table 5. Real-time PCR primers and conditions for the confirmation of fracture microarray "scarless" gene expression.

Target Gene		Primers				
Gene	Accession	Position	Direction	Product	Sequence	Annealing Temp[1]
Cyclophilin	BC059141	320	Forward	192	5'-GCATACAGGTCCTGGCATCT-3'	Footnote 1

47

| | | 511 | Reverse | | 5'-TCTTGCTGGTCTTGCCATTC-3' | |

"Scarless Healing" Gene Expression Confirmation

Prx-2	NM_238327	432	Forward	227	5'-CTCGCTGCTCAAGTCTTACG-3'	56.2
		658	Reverse		5'-GGCTGTGGTGTAAGCTGAAC-3'	
TGF-β3	BC092195	1067	Forward	194	5'-CAGCATCCACTGTCCATGTC-3'	56.4
		1260	Reverse		5'-GTCGGTGTGGAGGAATCATC-3'	
Fibromodulin	NM_080698	901	Forward	232	5'-ATGGCCTTGCTACCAACACC-3'	55.2
		1132	Reverse		5'-ATAGCGCTGCGCTTGATCTC-3'	
PN-1	NM_012620	2656	Forward	267	5'-CTCCTGGTCAACCACCTTAG-3'	55.4
		2922	Reverse		5'-CCTGTGGTACACGGTGTATG-3'	
Mmp-14	NM_031056	966	Forward	330	5'-ACTTCGTGTTGCCTGATGAC-3'	56.5
		1295	Reverse		5'-TGCCATCCTTCCTCTCATAG-3'	

[1]Each annealing temperature produces the most efficient amplification of cyclophilin when compared to the gene of interest.

Results:

A microarray analysis that combined the 3-day and 11-day fracture calluses into one group identified 6,555 genes with significant changes in expression ($p < 0.05$). The increased power of the statistical analysis improved the sensitivity of the approach, and allowed a better examination of the molecular pathways involved in fracture repair.

Because, as we have indicated in the Introduction, fracture repair leads to bridging the injury with bone that is identical to the native bone but lacks scar tissue (Bolander, 1992), there might be similarities between fracture repair and scarless tissue healing. To further characterize the regenerative molecular pathways operating in fracture repair and "scarless" tissue healing, we used real-time PCR (Tables 5 and 6) to confirm the expression of several of the "scarless wound healing genes" that we described in the in the previous progress report. These genes included members of the transforming growth factor β (TGFβ) family, and other genes previously linked with fracture expression. Novel genes included Prx-2, fibromodulin and mmp-14, which have not been previously reported in microarray studies of fracture repair. The application of real-time PCR to the fracture RNA samples succeeded in confirming the expression of several of the more important scarless wound healing genes, both in the same samples analyzed by microarray and in additional samples not examined by microarray. More than 5 samples were analyzed for each of the selected genes. Real-time PCR was reproducible to a standard deviation of approximately 0.5 cycles, and was usually effective at confirming changes in expression in excess of 2-fold (1 cycle), though the magnitudes often varied from the microarray values of fold-activation. Fold-activation values of less than 2 were difficult to confirm with the sample numbers examined. Combined with the statistical approach to the analysis of several samples by microarray, however, the real-time PCR confirmation provided a more reliable characterization of the regulatory pathways of fracture repair than previous studies.

Table 6. Fracture Microarray Genes Associated With Scarless Fetal Wound Healing		
	3 Day Expression	**11 Day Expression**

Gene (Function)	Accession	Microarray (P<0.05) Fold-Change	Real-Time PCR Fold-Change[1] (n)	Microarray (P<0.05) Fold-Change	Real-Time PCR Fold-Change[1] (n)
Homeodomain					
Prx-2 (TGF-β3, PN-1 regulation)	BE118447	**4.4**	**2.2 ± 1.9 (7)**	**2.7**	**2.6 ± 1.6 (6)**
Meox-2 (cell migration)	NM_017149	**2.5**	**1.7 ± 0.6 (9)**	**2.8**	**2.5 ± 1.8 (5)**
TGF-β3-Related					
TGF-β3 (proliferation, differentiation)	NM_013174	**2.4**	**1.7 ± 0.9 (7)**	**2**	**4.3 ± 2.0 (8)**
LTBP-1 (TGF-β3 binding)	NM_021587	**1.9**	**ND**	**1.5**	ND
Fibromodulin	NM_080698	**2.3**	**2.1 ± 1.2 (8)**	**5.2**	**21.0 ± 13.2 (6)**
Other Growth Factors					
VEGF-C (angiogenesis)	NM_053653	**1.2**	ND	NS	ND
Hepatocyte Growth Factor (anti-apoptosis)	NM_017017	NS	ND	**1.4**	ND
Extracellular Matrix (ECM)					
Fibronectin-1	NM_019143	**2.4**	ND	**2.7**	ND
Collagen V (α1) (cell spreading)	NM_134452	**2.4**	ND	**2.1**	ND
ECM Matricellular (Adhesion)					
Tenascin	BE126741	**2.1**	ND	**1.5**	ND
Calpactin I Heavy Chain (Ten receptor)	NM_019905	**1.9**	ND	NS	ND
Thrombospondin-2	BF408413	**1.7**	ND	**1.8**	ND
Thrombospondin-4	X89963.1	**1.9**	ND	**3.6**	ND
Calreticulin (TSP-receptor)	NM_022399	**1.6**	ND	NS	ND
SPARC	NM_012656	**1.7**	ND	NS	ND
ECM Remodeling					
Protease Nexin-1 (ECM regulation)	X89963.1	**2.1**	**1.1 ± 0.5 (8)**	**2.1**	**12.3 ± 6.4 (8)**
Mmp-14	NM_031056	NS	**1.1 ± 0.5 (10)**	**2.1**	**4.2 ± 1.8 (9)**
TIMP-2 (Mmp-14 regulation)	NM_021989	**2.3**	ND	**1.8**	ND
NS: Not Significant; ND: Not Determined; n: number of fractured vs unfractured pairs of tissues in real-time RT-PCR; [1] mean +/- SD.					

Consequently, our microarray data strongly suggest, and our real-time PCR data support, a similarity between fetal repair and scarless healing, since both processes shared developmental gene expression pathways (Ferguson et al., 1999). Because adult bone is a tissue unique in its ability to heal without a scar, these genes immediately suggest a regulatory pathway for the regenerative characteristics of bone repair that might be applicable to healing in other tissues.

Additional growth factor pathways were also examined to further elucidate the molecular pathways that regulate fracture healing. The fibroblast growth factor (FGF) family is of particular interest, because the members of this family are generally thought to be highly potent mediators of cell proliferation, a critical early step in tissue repair.

Table 7. Real-time PCR primers and conditions for the confirmation of FGF-related fracture microarray gene expression.

Target Gene		Primers				Annealing Temp[1]
Gene	Accession	Position	Direction	Product	Sequence	
Cyclophilin	BC059141	320	Forward	192	5'-GCATACAGGTCCTGGCATCT-3'	Footnote 1
		511	Reverse		5'-TCTTGCTGGTCTTGCCATTC-3'	
FGF Gene Family Expression Confirmation						
FGF-13		290	Forward	249	5'-TCTTCGAGTCGTGGCTATTC-3'	54.3
		538	Reverse		5'-GCAGGCTTGTTCTTCTTGAC-3'	
JIP-2a		216	Forward	262	5'-CCATGCAGCTGGTACTGAAG-3'	60.0
		477	Reverse		5'-AGGTCCATCTGCAGCATCTC-3'	
FGFR-5		1404	Forward	216	5'-AACGCAGTGGTGACAAGGAC-3'	54.3
		1619	Reverse		5'-GACATGCTGGTGCTGATGAG-3'	

1: Each annealing temperature produces the most efficient amplification of cyclophilin when compared to the gene of interest.

While we found FGF7 expression to be up-regulated in the microarray analysis (1.3-fold at 3 days), in agreement with other studies (Hadjiargyrou et al., 2002; Li et al., 2005), there was an unexpected absence of other FGFs. An exception was FGF-13, which was up-regulated 2.3-fold at 11 days healing; lacking a signal sequence, FGF-13 might act intracellularly or upon release from damaged cells. Subsequent real-time PCR analysis with gene-specific primers (Table 7) confirmed the microarray study and established that FGF-13 and its intracellular link to the JNK signaling pathway, JNK interacting protein (JIP)-2a were significantly up-regulated in expression during endochondral bone formation (FGF-13: 6.7, $p<0.0005$; JIP-2a: 6.4-fold, $p<0.0004$). Other members of this pathway are regulated through phosphorylation, rather than transcriptionally, and would not be detected in gene expression studies. Interestingly, FGF receptor 5 (FGFR5), a truncated FGF receptor variant that lacks a kinase signaling domain, was also significantly up-regulated in expression at 11 days healing (2.1-fold), an observation confirmed by real-time PCR (3.1-fold up-regulated in expression, $p<0.0001$). FGFR5 might act as a dominant negative receptor in growth factor regulation, binding extracellular FGFs and maximizing the effect of intracellular FGF signaling mediated by FGF-13 through JIP-2a.

We continued to search for molecular pathways that might regulate the response of the fracture tissues to FGF-2 expression. The wnt pathway has recently become the focus of considerable study in fracture repair, for its diverse effects related to chondrocyte proliferation and differentiation (Zhong et al., 2006), as well as on FGF-2-related proliferation of endothelial cells in angiogenesis (Holnthoner et al., 2002). Because our previous results with FGF-2 gene therapy suggested that this growth factor affects both angiogenesis and chondrogenesis (Figures 17 and 21, respectively), and other FGFs were observed in the microarray analysis of fracture repair, we further investigated wnt-related pathway components whose genes were expressed in the microarray analysis of fracture repair.

Table 8. Gene Ontology microarray analysis of Wnt-related gene expression during fracture healing			
Accession	Fold-change	P-value	Description

3 Days			
GO:0016055(Wnt receptor signaling pathway) (2)			
NM_021266	1.39	0.005	Rattus norvegicus frizzled homolog 1, (Drosophila) (Fzd1), mRNA.
BQ209192	1.68	0.003	similar to AF454755_1 Mus musculus vitrin (Vit) mRNA; vitreous protein
GO:0007222(frizzled signaling pathway) (1)			
NM_022542	1.39	0.012	Rattus norvegicus rhoB gene (Arhb), mRNA.
GO:0007166(cell surface receptor linked signal transduction)			
NM_021266	1.39	0.005	Rattus norvegicus frizzled homolog 1, (Drosophila) (Fzd1), mRNA.
11 Days			
None			
3 and 11 Days Combined			
GO:0016055(Wnt receptor signaling pathway) (6)			
BF398114	1.17	0.044	Rat GSK-3beta interacting protein Axil mRNA, complete cds.
NM_031820	1.15	0.037	Rattus norvegicus dishevelled 1 (Dvl1), mRNA.
BE108187	1.18	0.021	similar to Mouse LDL receptor-related protein 6 (Lrp6) mRNA, complete cds.
NM_053624	0.78	0.009	Rattus norvegicus paired-like homeodomain transcription factor 1 (Pitx1), mRNA.
NM_021266	1.39	0.001	Rattus norvegicus frizzled homolog 1, (Drosophila) (Fzd1), mRNA.
BQ209192	1.68	0	similar to AF454755_1 Mus musculus vitrin (Vit) mRNA; vitreous protein.
GO:0030111(regulation of Wnt receptor signaling pathway) (1)			
BF398114	1.17	0.044	Rat GSK-3beta interacting protein Axil mRNA, complete cds.
GO:0030178(negative regulation of Wnt receptor signaling pathway) (1)			
BF398114	1.17	0.044	Rat GSK-3beta interacting protein Axil mRNA, complete cds.
GO:0007275(development)			
NM_021266	1.39	0.001	Rattus norvegicus frizzled homolog 1, (Drosophila) (Fzd1), mRNA.
GO:0007222(frizzled signaling pathway) (5)			
BQ209021	0.86	0.049	similar to Protein:NP_031511 ras homolog D; aplysia ras-related homolog D
BF398114	1.17	0.044	Rat GSK-3beta interacting protein Axil mRNA, complete cds.
NM_057132	1.42	0.014	Rattus norvegicus plysia ras-related

			homolog A2 (Arha2), mRNA.
BF523425	0.77	0.012	unknown function
NM_022542	1.39	0.011	Rattus norvegicus rhoB gene (Arhb), mRNA.
GO:0007166(cell surface receptor linked signal transduction)			
NM_021266	1.39	0.001	Rattus norvegicus frizzled homolog 1, (Drosophila) (Fzd1), mRNA.

In agreement with other studies that have characterized wnt pathway components as expressed early in fracture repair (Zhong et al., 2006), several wnt-related genes displayed upregulated expression that was either confined to early healing, at 3 days, or began at 3 days and continued through later healing, at 11 days. Wnt signaling molecules themselves were not represented. However, elements of the both the canonical wnt pathway (such as frizzled) and the non-canonical wnt pathway (such as LRP6) were observed. The most highly upregulated gene was a homolog of vitrin, an extracellular protein with angiogenic functions related to von Willebrand Factor. It is therefore possible that our FGF-2 gene therapy has affected chondrogenesis and angiogenesis through wnt-related mechanisms.

At the present time, we continue to analyze the microarray gene expression data to functionally classify the genes with changes in expression, characterize gene pathways important in fracture healing and identify gene candidate(s) for our fracture therapy.

Conclusions

Using a 20,000 rat gene chip and appropriate controls that normalized marrow RNA input among multiple replicates at two healing times, we analyzed whole genome expression in fracture tissues among multiple replicate animals, using unfractured controls that normalized marrow RNA input. This approach allowed us to more accurately identify some 6,555 genes with significant changes during fracture healing. We have identified and confirmed growth factor, structural, and transcription factor genes that participate in developmentally related (scarless wound healing) pathways and that must also contribute to the complex regulation of bone repair. Our microarray analysis was reliable: 1) The expression of several well-known genes, notably FGF-7 (up-regulated 1.3-fold in early fracture repair), compared well with previous studies (Hadjiargyrou et al., 2002; Li et al., 2005), though differences with these studies were also observed; 2) Several of the genes, especially those associated with scarless wound healing, had their expression changes in fracture healing confirmed by an independent measurement, specifically real-time RT-PCR. The latter results demonstrate that fracture repair is similar to fetal tissue development and repair, and that the regenerative qualities of bone repair can be used to elucidate therapies for improved wound healing of skeletal and nonskeletal tissues. We also expanded the microarray analysis and confirmation to a subset of the FGF gene family that might modulate fracture healing through intracellular pathways, and examined the expression of wnt-related genes that might interact with FGF pathways and explain the effects of the FGF-2 transgene observed in our gene therapy studies.

The high number of unknown genes and ESTs that displayed changes in expression during fracture healing suggests remaining pathways that are undiscovered as of this time are important in bone repair. Further characterization of such gene expression pathways should facilitate the molecular understanding of normal and impaired fracture repair. Thus, while we have accomplished the aims of this objective to analyze and confirm the microarray gene expression

results, much remains to be learned from the microarray analysis of gene expression in fracture healing.

An added Specific Objective #4: To evaluate the functional role of one or more Expressed Sequence Tags (ESTs) with altered expression during fracture healing by inhibition or augmentation of its expression *in vitro,* followed by identification of the resulting changes cellular phenotype and gene expression.

Objectives:

Because the nature and functions of genes coded by ESTs have not been identified, understanding the functions of ESTs whose expression was upregulated during fracture repair could yield information concerning novel genes or pathways. Accordingly, during this funding period, we have added a Specific Objective to assess potential functions of one or more ESTs with altered expression during fracture healing. To further investigate the possible functions of the large numbers of unknown genes and ESTs in the regulation of fracture repair, we inhibited the expression of at least one of those ESTs in rat bone cells *in vitro* by siRNA gene knockdown technology (Kim et al., 2005; Solias et al., 2005). We then determined the response of periosteal-derived cells to the inhibition of EST expression by measuring the expression of bone formation marker genes in those cells by real-time RT-PCR. These studies should allow an effective characterization of the effects of expression of an unknown gene on bone cells.

Materials and Methods:

Several ESTs that displayed significant changes in expression in fracture tissues at 3 days and 11 days were identified in the microarray analysis. RNA was purified from several primary and transformed cell lines that represented mesenchymal, chondrocytic and osteoblastic stages of bone cell development (Table 9).

Table 9. PCR Confirmation of Fracture EST Expression in Cell Lines for siRNA Studies								
		PCR Expression					**Microarray Expression**	
EST	**Product**	**Normal Cells**		**Transformed Lines**			**Fracture Tissues**	
		RMS	**RCOB**	**Rat-1**	**RCS**	**ROS17.2/8**	**3 Days**	**11 Days**
BQ209715	**253**	+	+	+	+	+	1.87[a]	0.73[a]
BF283714	299	-	-	-	-	-	NS	2.29
CORS26	137	-	-	+	-	+	5.02	7.88
AP2M1	117	-	-	-	-	-	NS	0.8
BGLAP1	147	+	+	+	+	+	0.36	NS
CHM-1	153	+	+	-	-	-	NS	21.97
AW528046	168	-	+	-	+	+	2.81	NS
CB546087	322	+	-	+	-	+	4.6	4.83
CB545954	381	+	+	+	+	+	3.33	2.66
CB547532	153	-	-	-	-	-	3.51	1.93
BU758349	**146**	+	+	+	+	+	**2.57**	**NS**
BM390058	483	-	-	-	-	-	2.31	3.32
RMS: rat marrow stromal cells; RCOB: rat calvarial osteoblasts; Rat-1: rat fibroblasts; RCS: rat chondrosarcoma; ROS: rat osteosarcoma								
Product: +; No product: -								
Bold: Candidate for siRNA inhibition; [a]Confirmed by Real-Time PCR in fracture tissues								

Total RNA was isolated from periosteal cell cultures by the Trizol^{TM} method, and cDNA prepared as previously described for the microarray analysis. PCR primers were designed to the selected ESTs and real-time RT-PCR performed on the cDNAs for 35 cycles at a 55°C annealing temperature. The products evaluated for the number of cell lines expressing each, in the fracture microarray at 3 days, 11 days or both.

The EST BQ209715 showed the greatest changes in expression in the fracture microarray, was expressed in most bone-derived cell lines, and had its expression during fracture healing confirmed by real-time RT-PCR. This EST was chosen for siRNA-mediated inhibition of its expression in bone cell cultures *in vitro*. One other EST was chosen for comparison; however, this previously unknown EST (CB545954) was recently searched against the NCBI database, and was found to be RNA polymerase III. As such it is probably not of great interest in the study of regulation in fracture repair. The EST BU758349 was substituted in its place, as it was expressed in several primary and transformed bone cell lines. Like EST BQ209715, this EST remains unidentified. The periosteal-derived cells were analyzed for the effects of specific inhibition of the expression of these ESTs by siRNA technology.

siRNA oligomer duplexes were designed to each of these ESTs (Table 10) and engineered into a proprietary murine leukemia virus (MLV)-based vector (Imgenex) for transduction and selection of transduced cell populations through the viral vector neomycin resistance gene. A random oligomer duplex with no homology to any gene served as the negative control in the transduction and gene expression studies. All inhibitory sequences were blunt-end hairpin duplexes of 25mer oligos identified as having potential and specific siRNA activity through multiple algorithms available from different commercial suppliers of siRNA-related services (Ambion, Imgenex, Integrated DNA Technologies). The length of the targeting sequence was chosen 25 bases for its greater potential for the specific target sequence inhibition, as well as its limited potential for the induction of viral-related cellular responses.

Table 10. siRNA sequences for inhibition of EST expression

BQ209715

  Xho1   Sense   Loop   Antisense
5'-tcga-TGCTAAGTCTGATTGCTAAGGTATT-ttcaagaga-AATACCTTAGCAATCAGACTTAGCA-ttttt-3'
3'-   ACGATTCAGACTAACGATTCCATAA-aagttctct-TTATGGAATCGTTAGTCTGAATCGT-aaaaa-gatc-5'
         Antisense   Loop   Sense   Poly-A Xba-1

BU758349

  Xho1   Sense   Loop   Antisense
5'-tcga-CACAGGTGCTCTAGGAAATATAGCC-ttcaagaga-GGCTATATTTCCTAGAGCACCTGTG-ttttt-3'
3'-   GTGTCCACGAGATCCTTTATATCGG-aagttctct-CCGATATAAAGGATCTCGTGGACAC-aaaaa-gatc-
5'   Antisense   Loop   Sense   Poly-A Xba-1

Control

  Xho1   Sense   Loop   Antisense
5'-tcga-TCAGTCACGTTAATGGTCGTTGCAT-ttcaagaga-ATGCAACGACCATTAACGTGACTGA-ttttt-3'
3'-   AGTCAGTGCAATTACCAGCAACGTA-aagttctct-TACGTTGCTGGTAATTGCACTGACT-aaaaa-gatc-
5'   Antisense   Loop   Sense   Poly-A Xba-1

Periosteal-derived bone cells were isolated by collagenase II digestion of rat femurs that were carefully cleaned of soft tissues. Four individual periosteal cell cultures from different animals were prepared, transduced with the MLV-siRNA-EST vectors, and cultured in the presence of 400 µg/ml G418 (neomycin) for the selection of transduced cells. All cell cultures were at less than 5 passages of culture age at time of RNA harvest. Post-transduction and near confluence in culture, total RNA was isolated from each cell culture and the cDNA analyzed by real-time RT-PCR for changes in the expression of bone cell marker genes, as previously described. The genes and their primer sequences used for real-time RT-PCR are listed in Table 11. RNA preparation and reverse transcription of cDNA were performed as previously described. Changes in the expression of bone cell-related genes were determined by real-time RT-PCR comparison of the individual bone cell preparations from each animal that were transduced with the MLV-siRNA vector expressing the specific EST siRNA (BQ209715 or BU758349) versus the negative control EST.

Table 11. Real-time PCR primers and conditions for the analysis of inhibition of EST expression.

Target Gene		Primers				
Gene	Accession	Position	Direction	Product	Sequence	Annealing Temp[1]
Housekeeping						
Cyclophilin	BC059141	320	Forward	192	5'-GCATACAGGTCCTGGCATCT-3'	Footnote 1
		511	Reverse		5'-TCTTGCTGGTCTTGCCATTC-3'	
ESTs						
	BQ209715	351	Forward	120	5'-AAGCGGCCAGGACTTAACTT-3'	56.0
		470	Reverse		5'-TCGCACAGCTTAACCTGGAA-3'	
	BU758349	178	Forward	146	5'-TGAAGTAGCGCAGGTCCTGA-3'	56.0
		323	Reverse		5'-CCACCTCTGGCAATGGTAAC-3'	
siRNA Activity						
Dicer	XM_001069041	1477	Forward	451	5'-CGTGTCCTGGAGTGATTCTG-3'	56.0
		1857	Reverse		5'-ATTAGAGATCGGCGCTCGTG-3'	
Bone–related Gene Expression						
Alk Phos	XM_001069041	1737	Forward	224	5'-GGATTCCTGCTGCCGTTGTT-3'	48.0
		1960	Reverse		5'-GAGGGACTGGCTCTGACTAT-3'	
Osteocalcin	NM_013414	27	Forward	279	5'-CGGTGCAGACCTAGCAGACA-3'	56.0
		306	Reverse		5'-CCAATGTGGTCCGCTAGCTCG-3'	
Osteopontin	NM_012881	697	Forward	244	5'-CTTGTCCTCATGGCTGTGAA-3'	56.0
		940	Reverse		5'-GAAGACCAGCCATGAGTCAAG-3'	
Osteonectin	NM_012656	1233	Forward	277	5'- AGTGTCTCACTGGCTGTGTT-3'	56.0
		1508	Reverse		5'- AGTCGTTGACCTAGGCTACC -3'	
Col 2α1	NM_012929	2103	Forward	292	5'- TGGCACTCCTGGTACTGATG -3'	56.0
		2394	Reverse		5'-GCCTCGAGCTCCAGTACTTC-3'	
Col 10α1	XM_001053056	833	Forward	408	5'-TGCCTCTTGTCAGTGCTAAC-3'	56.0
		1240	Reverse		5'-AGAAGGACGAGTGGACATAC-3'	

Wnt-1	XM_001062385	772	Forward	202	5'-AATCCTGCACCTGCGACTAC-3'	56.0
		973	Reverse		5'-TGGCGCATCTCAGAGAACAC-3'	
Wnt-10b	XM_001062326	805	Forward	220	5'-GGCCAAGTTGTTGCAGCTTC-3'	56.0
		1024	Reverse		5'-GTTGTGGATCCGCATTCTCG-3'	
Osterix	XM_001037632	635	Forward	500	5'-CATCCATGCAGGCATCTCAC-3'	56.0
		1134	Reverse		5'-AAGCCTTGCCGTACACCTTG-3'	

1: Each annealing temperature produces the most efficient amplification of cyclophilin when compared to the gene of interest.

Results

A total of 10 ESTs that displayed significant changes in expression in the fracture microarray were analyzed for expression in a number of different primary and transformed bone cell lines (Table 7). Of these, two whose functions remain unknown at this time (BQ209715 and BU758349), but that were expressed in all lines and/or displayed significant changes during fracture repair were selected for the analysis of the effect of their inhibition in rat periosteal-derived bone cell culture.

The results of the inhibition of expression of these ESTs are presented in Figure 25. Of all the genes tested (Table 9), only the extracellular matrix genes osteonectin and osteopontin were expressed in transduced bone cells, but changes induced by culture with viral vector-trandsduced sequences were highly variable.
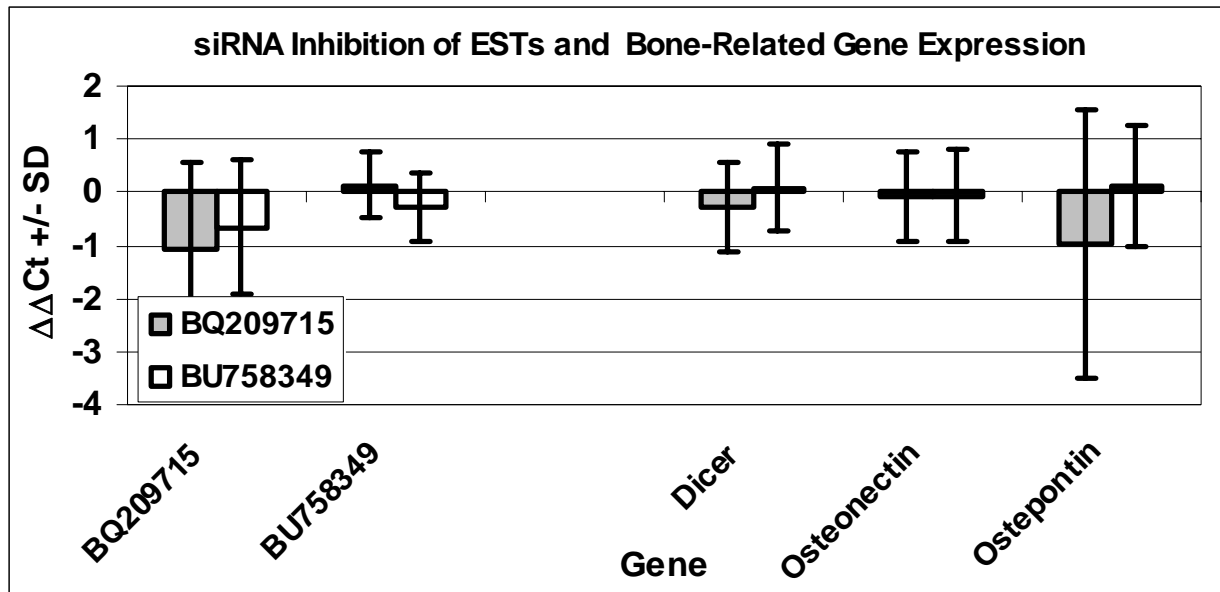

Figure 25. Analysis of siRNA-mediated inhibition of EST gene expression in periosteal-derived cells *in vitro*. MLV-mediated siRNA inhibition of expression of the ESTs BQ209715 and BU758349, as well as numerous bone-related genes, was determined in periosteal-derived cells *in vitro* by real-time RT-PCR. Differences in gene expression are presented as $\Delta\Delta$Ct: the difference in cycle number for a gene of interest between the siRNA-treated cells $(\Delta Ct)_{siRNA}$ normalized to the cyclophilin housekeeping gene, versus the control sequence siRNA-treated cells $(\Delta Ct)_{control\ siRNA}$, also normalized to the cyclophilin A housekeeping gene.

Changes in the expression of the individual ESTs in response to siRNA inhibition were difficult to establish (Figure 25). Expression of the ESTs BQ209715 and BU758349, as well as the bone-related genes osteonectin and osteopontin, were easily detectable, but revealed no significant differences in expression indicative of inhibition by siRNA function. The enzyme "dicer," an effector of siRNA-related transcript digestion (and the attendant inhibition of gene expression) also displayed high expression without differences in expression relative to the control cells. Most of the bone-related genes in Table 9 exhibited no detectable expression. Thus, it appears as though the inhibition of expression of these two ESTs by the siRNA approach failed to specifically reduce the function of either EST and did not modulate bone-related gene expression, but instead induced a non-specific response of the siRNA-related cell machinery, such as "dicer".

Conclusions:

Despite best attempts at sequence design, the siRNA sequences derived from these two ESTs failed to definitively inhibit the expression of these ESTs. We conclude that they were not consistently expressed in bone-derived cells or that our siRNA effects were too limited or nonspecific. Likewise, real-time RT-PCR expression measurements detected only osteonectin and osteopontin expression in the periosteal-derived cells, confirming their bone formation potential but offering little insight into molecular control of fracture healing, at least in this *in vitro* model. The very short length of the ESTs limited approaches using different oligos from different regions of the EST for inhibition: an approach that would be expected to be more successful for a gene with a longer target sequence. We nevertheless completed this objective for EST analysis, and even extended the analysis to an additional EST. Future siRNA applications will utilize pools of siRNA sequences from genes with more sequence information to improve targeting and enhance inhibition.

KEY RESEARCH ACCOMPLISHMENTS

1. We have completed the comparison of MLV-based and HIV-based vector systems the expression of therapeutic transgenes for fracture repair. Mechanical testing confirmed no differences between vectors.

2. We have completed the comparison studies of single and combination gene therapy in fracture repair using two therapeutic genes (BMP-2/4 and FGF-2) expressed from the MLV-based vector and applied using our novel surgical techniques.

3. We have performed an extensive and rigorously controlled microarray analysis on the RNA from multiple individual animal subjects during early (inflammatory) and late (endochondral bone formation) stages of fracture repair.
   a) Several hundred known and unknown genes are being classified into functional categories to better understand the molecular pathways of fracture repair.
   b) The expression of genes with possible therapeutic was independently confirmed by real-time RT-PCR. This confirmation included genes expressed in "scarless" fetal wound healing that could be adopted for novel wound therapies in other tissues.

c) This analysis identified genes expressed in novel pathways of gene regulation for fracture repair, one of which involves the members of the FGF family of growth factors whose expression was confirmed, and another that involves the wnt family of signaling molecules.

4. Studies that utilized siRNA technology to study the effects of inhibition expression in bone cell lines of one or two ESTs that were expressed in the healing fracture tissues were completed, and yielded information on this approach applicable to future studies.

REPORTABLE OUTCOMES

Publications
1. Rundle CH, Wang H, Yu H, Chadwick RB, Davis EI, Wergedal JE, Lau K-HW, Mohan S, Ryaby JT, Baylink DJ. (2006) Microarray analysis of gene expression during the inflammation and endochondral bone formation stages of rat femur fracture repair. Bone 38: 521-529.

Abstracts
1. Rundle CH,Wang H, Yu H, Chadwick RB, Tesfai J, Lau K-HW, Mohan S, Ryaby JT, Baylink DJ. (2005) Microarray analysis of fracture repair identifies the homeodomain transcription factor Prx-2 and other genes that imply similarities between bone repair and scarless fetal tissue healing. Abstract presented at the 51st Annual Meeting of the Orthopaedic Research Society, Washington, DC.
2. Rundle CH,Wang H, Yu H, Chadwick RB, Tesfai J, Lau K-HW, Mohan S, Ryaby JT, Baylink DJ. (2004) Whole Genome Expression Profiling of Fracture Healing Under Rigorous Experimental Design Reveals Novel Pathways: Pleiotrophin and Meox2 in Fracture Healing. Abstract presented at the 26th Annual Meeting of the American Society for Bone and Mineral Research, Seattle, WA.

CONCLUSIONS

The development of highly effective gene therapy approaches to musculoskeletal injuries requires the optimization of the components and techniques for the accurate assessment of therapeutic benefits. We have optimized conditions for the accurate evaluation of therapeutic transgene candidates by modifying a standard *in vivo* fracture model to compare and evaluate viral vector and therapeutic gene combinations. We have also performed microarray analysis of global gene expression in the normal healing fracture callus to characterize the molecular pathways of fracture healing at early (3 days) and later (11 days) healing times. We have identified potential therapeutic gene candidates among the several hundred known and unknown genes with a significant increase or decrease in expression. The application of combinations of therapeutic genes to enhance fracture repair healing has altered fracture healing and suggested future approaches for clinical applications of gene therapy in bone repair.

REFERENCES

1. AAOS: American Academy of Orthopedic Surgeons Symposium (2007) J. Am. Acad. Orthorp. Surg. In Press.
2. Andrew JG, Hoyland J, Freemont AJ, Marsh D. (1993) Insulinlike growth factor gene expression in human fracture callus. Calcif. Tissue Int. 53: 97-102.
3. Andrew JG, Hoyland JA, Freemont AJ, Marsh, DR. (1995) Platelet-derived growth factor expression in normally healing human fractures. Bone 16: 455-460.
4. Apte SS, Fukai N, Beier DR, Olsen BR. (1997) The matrix metalloproteinase-14 (MMP-14) gene is structurally distinct from other MMP genes and is co-expressed with the TIMP-2 gene during mouse embryogenesis. J. Biol. Chem. 272: 25511-25517.
5. Ashburner M, Ball CA, Blake JA, Botstein D, Butler H, Cherry JM, Davis AP, Dolinski K, Dwight SS, Eppig JT, Harris MA, Hill DP, Issel-Tarver L, Kasarskis A, Lewis S, Matese JC, Richardson JE, Ringwald M, Rubin GM, Sherlock G. (2000) Gene ontology: tool for the unification of biology. The Gene Ontology Consortium. Nature Genet. 25: 25-29.
6. Barnes, GL, Kostenuik PJ, Gerstenfeld LC, Einhorn TA. (1999) Growth factor regulation of fracture repair. J. Bone Miner. Res. 14: 1805-1815.
7. Baumann H, Gauldie J. (1994) The acute phase response. Immunol. Today 15: 74-80.
8. Beasley LS, Einhorn TA. (2000) Role of growth factors in fracture healing. In: Canalis E, editor. Skeletal growth factors. Philadelphia, PA: Lippencott, Williams and Wilkins p. 311-322.
9. Blanck, R.R. (1999) Army "Answers the call". U.S. Medicine 35: 28.
10. Bolander ME. (1992) Regulation of fracture repair by growth factors. Proc. Soc. Exp. Biol. Med. 200: 165-170.
11. Bonnarens F, Einhorn TA. (1984) Production of a standard closed fracture in laboratory animal bone. J. Orthop. Res. 2: 97-101.
12. Bullard KM, Longaker MT, Lorenz HP. (2003) Fetal wound healing: Current biology World J. Surg. 27: 54-61.
13. Chen, S-T, Gysin R, Kapur S, Baylink DJ, Lau K-HW. (2007) Modifications of the fibroblast growth factor-2 gene led to a marked enhancement in sectetion and stability of the recombinant fibroblast growth factor-2 protein. J. Cell Biochem. 100: 1493-1508.
14. Cho T-J, Gerstenfeld LC, Einhorn TA. (2000) Differential temporal expression of members of the transforming growth factor B superfamily during murine fracture healing. J. Bone Miner. Res. 17: 513-520.
15. Clark DA, Coker R. (1998) Transforming growth factor-beta (TGF-beta). Int. J. Biochem. Cell Biol. 30: 293-298.
16. Dang CM, Beanes SR, Lee H, Zhang X, Soo C, Ting KD. (2003) Scarless fetal wounds are associated with an increased matrix metalloproteinase-to-tissue-derived inhibitor of metalloproteinase ratio. Plastic Reconstr. Surg. 111: 2273-2285.
17. Dinarello CA. (2003) Proinflammatory cytokines. Chest 118: 503-508.
18. Dinarello CA. (2002) The IL-1 family and inflammatory diseases. Clin. Exp. Rheumatol. 20: S1-S13.
19. Einhorn TA. (1995) Enhancement of fracture healing. J. Bone Jt. Surg. 77-A: 940-956.
20. Febbraio M, Hajjar DP, Silverstein RL. (2001) CD36: A class B scavenger receptor involved in angiogenesis, athersclerosis, inflammation, and lipid metabolism. J. Clin. Invest. 108: 785-791.

21. Ferguson C, Aplern E, Miclau T, Helms J. (1999) Does adult fracture repair recapitulate embryonic skeletal formation? Mech. Dev. 87: 57-66.
22. Florkiewicz R, Majack RA, Buechler RD, Florkiewicz E. (1995) Quantitative export of FGF-2 occurs through an alternative, energy-dependent, non-ER/Golgi pathway. J. Cell Physiol. 162: 388-399.
23. Hadjiargyrou M, Lombardo F, Zhao S, Ahrens W, Joo J, Ahn H, Jurman M, White DM, Rubin CT. (2002) Transcriptional profiling of bone regeneration. Insight into the molecular complexity of wound repair. J. Biol. Chem. 277: 30177-30182.
24. Hijjawa J, Mogford JE, Chandler LA, Cross KJ, Said H, Sosnowski BA, Mustoe TA. (2004) Platelet-derived growth factor B, but not fibroblast growth factor 2, plasmid DNA improves survival of ischemic myocutaneous flaps. Arch. Surg. 139: 142-147.
25. Holnthoner W, Pillinger M, Groger M, Wolff K, Ashton, AW, Albanese C, Neumeister P, Pestell RG, Petzelbauer P. (2002) Fibroblast growth factor-2 induces Lef/Tcf-dependent transcription in human endothelial cells. J. Biol. Chem. 277: 45847-45853.
26. Ibelgaufts H. (2003) COPE: Horst Ibelgaufts' Cytokines Online Pathfinder Encyclopaedia www.copewithcytokines.de.
27. Ishii S, Koyama H, Miyata T, Nishikage S, Hamada H, Miyatake S, Shigematsu H. (2004) Appropriate control of ex vivo gene therapy delivering basic fibroblast growth factor promotes successful and safe development of collateral vessels in rabbit model of hind limb ischemia. J. Vasc. Surg. 39: 629-638.
28. Iwane M, Kurokawa T, Sasada R, Seno M, Nakagawa S, Igarashi K. (1987) Expression of cDNA encoding human basic fibroblast growth factor in E. coli. Biochem. Biophys. Res. Commun. 146: 470-477.
29. Janeway CA, Jr, Travers P, Walport M, Schlomchik MJ. (2003) In: Janeway CA, Jr. editor. Immunobiology: the immune system in health and disease, fifth edition. New York, NY: Garland Publishing; Appendix 2.
30. Jones FS, Meech R, Edelman DB, Oakey RJ, Jones PL. (2001) Prx1 controls vascular smooth muscle cell proliferation and tenascin-C expression and is upregulated with Prx2 in pulmonary vascular disease. Circulation Res. 89: 131-138.
31. Kim D-H, Behlke MA, Rose SD, Chang M-S, Choi S, Rossie JJ. (2005) Synthetic dsRNA dicer substrates enhance RNAi potency and efficacy. Nature Biotech. 23: 222-226.
32. Kimball, JW. (2005) Biology Pages. users.rcn.com/jkimball.ma.ultranet/BiologyPages/C/Complement.html.
33. Kohama K, Nonaka K, Hosokawa R, Shum L, Ohishi M. (2002) Tgf-beta-3 promotes scarless repair of cleft lip in mouse fetuses. J. Dent. Res. 81: 688-694.
34. Li X, Quigg RJ, Zhou J, Ryaby JT, Wang H. (2005) Early signals for fracture healing. J. Cell. Biochem. 95: 189-205.
35. Mackie EJ, Halfter W, Liverani D. (1988) Induction of tenascin in healing wounds. J. Cell Biol. 107: 2757-2767.
36. Mankoo BS, Skuntz S, Harrigan I, Grigorieva E, Candia A, Wright CV, Arnheiter H, Pachnis V. (2003) The concerted action of Meox homeobox genes is required upstream of genetic pathways essential for the formation, patterning and differentiation of somites. Development 130: 4655-4664.
37. Mannaioni PF, Di Bello MG, Masini E. Platelets and inflammation: Role of platelet-derived growth factor, adhesion molecules and histamine. (1997) Inflamm. Res. 46: 4-18.

38. Menten P, Wuyts A, van Damme J. (2001) Monocyte chemotactic protein-3. Eur. Cytokine Net. 12: 554-560.

39. Meyer RA, Jr, Meyer MH, Tenholder M, Wondracek S, Wasserman R, Garges P. (2003) Gene expression in older rats with delayed union of femoral fractures. J. Bone Joint Surg. 85-A: 1243-1254.

40. Moscatelli D, Presta M, Joseph-Silvestein J, Rifkin DB. (1986) Both normal and tumor cells produce basic fibroblast growth factor. J. Cell. Physiol. 129: 273-276.

41. Murphy-Ullrich JE. (2001) The de-adhesive activity of matricellular proteins: Is intermediate cell adhesion an adaptive state? J. Clin. Invest. 107: 785-790.

42. Nakajima F, Ogasawara A, Goto K, Moriya H, Ninomiya Y, Einhorn TA, Yamazaki M. (2001) Spatial and temporal gene expression in chondrogenesis during fracture healing and the effects of basic fibroblast growth factor. J. Orthop. Res. 19: 935-944.

43. Nilsson G, Butterfield JH, Nilsson K, Siegbahn A. (1994) Stem cell factor is a chemotactic factor for human mast cells. J. Immunol. 153: 3717-3723.

44. Ono I, Yamashita T, Hida T, Jin HY, Ito Y, Hamada H, Akasaka Y, Ishii T, Jimbow K. (2004) Local administration of hepatocyte growth factor gene enhances the regeneration of dermis in acute incisional wounds. J. Surg. Res. 120: 47-55.

45. Peng H, Chen S-T, Wergedal JE, Polo JM, Yee J-K, Lau K-HW, Baylink DJ (2001) Development of an MFG-based retroviral vector system for secretion of high levels of functionally active human BMP4. Mol. Therapy 4: 95-104.

46. Rifkin DB. (2005) Latent transforming growth factor-beta (TGF-beta) binding proteins: orchestrators of TGF-beta availability. J. Biol. Chem. 280: 7409-7412.

47. Rossignol P, Ho-Tin-Noe B, Vranckx R, Bouton MC, Meilhac O, Lijnen HR, Guillin MC, Michel JB, Angles-Cano E. (2004) Protease nexin-1 inhibits plasminogen activation-induced apoptosis of adherent cells. J. Biol. Chem. 279: 10346-10356.

48. Roth JJ, Sung JJ, Granick MS, Solomon MP, Longaker MT, Rothman VL, Nicosia RF, Tuszynski GP. (1999) Thrombospondin 1 and its specific cysteine-serine-valine-threonine-cysteine-glycine receptor in fetal wounds. Ann. Plast. Surg. 42: 553-563.

49. Rundle CH, Miyakoshi N, Sheng MH-C, Ramirez E, Wergedal JE, Lau K-HW, Baylink DJ. (2002) Expression of fibroblast growth factor receptor genes in fracture repair. Clin. Orthop. Rel. Res. 403: 253-263.

50. Rundle CH, Miyakoshi N, Kasukawa Y, Chen S-T, Sheng MH-C, Wergedal JE, Lau K-HW, Baylink DJ. (2003) In vivo bone formation in fracture repair induced by direct retroviral-based gene therapy with bone morphogenetic protein-4. Bone 32: 591-601.

51. Scott KK, Norris RA, Potter SS, Norrington DW, Baybo MA, Hicklin DM, Kern MJ. (2003) GeneChip microarrays facilitate identification of Protease Nexin-1 as a target gene of the Prx2 (S8) homeoprotein. DNA Cell Biol.22: 95-105.

52. Solias D, Lerner C, Burchard J, Ge W, Linsley PS, Paddison PJ, Hannon GJ, Cleary MA. (2005) Synthetic shRNAs as potent RNAi triggers. Nature Biotech. 23: 227-231

53. Soo C, Hu F-Y, Zhang X, Wang Y, Beanes SR, Lorenz HP, Hedrick MH, Mackool RJ, Plaas A, Kim S-J, Longaker MT, Freymiller E, Ting K. (2000) Differential expression of fibromodulin, a transforming growth factor-B modulator, in fetal skin development and scarless repair. Am. J. Pathol. 157: 423-433.

54. Soo C, Beanes SR, Hu F-Y, Zhang X, Dang C, Chang G, Wang Y, Nishimura I, Freymiller E, Longaker MT, Lorenz HP, Ting K. (2003) Ontogenetic transition in fetal wound

transforming growth factor-B regulation correlates with collagen organization. Am. J. Pathol. 163: 2459-2476.

55. Spencer B, Agarwala S, Gentry L, Brandt CR. (2001) HSV-1 vector-delivered FGF2 to the retina is neuroprotective but does not preserve functional responses. Mol. Ther. 3: 746-756.

56. White P, Thomas DW, Fong S, Stelnicki E, Meijlink F, Largman C, Stephens P. (2003) Deletion of the homeobox gene Prx-2 affects fetal but not adult fibroblast wound healing responses. J. Invest. Dermatol. 120: 135-144.

57. Witzenbichler B, Kureishi Y, Luo Z, Le Roux A, Branellec D, Walsh K. (1999) Regulation of smooth muscle cell migration and integrin expression by the Gax transcription factor. J. Clin. Invest. 104: 1469-1480.

58. Zhong N, Gersch RP, Hadjiargyrou M. (2006) Wnt signaling activation during bone regeneration and the role of dishevelled in chondrocyte proliferation and differentiation. Bone 39: 5-16.

Appendices

Rundle C, Wang H, Yu H, Chadwick R, Davis E, Wergedal J, Lau KH, Mohan S Ryaby J, Baylink. Microarray analysis of gene expression during the inflammation and endochondral bone formation stages of rat femur fracture repair.   Bone 38: 521-529.

Microarray analysis of gene expression during the inflammation and endochondral bone formation stages of rat femur fracture repair

Charles H. Rundle[a], Hali Wang[c], Hongrun Yu[a], Robert B. Chadwick[a], Emile I. Davis[a],
Jon E. Wergedal[a,b], K.-H. William Lau[a,b,*], Subburaman Mohan[a,b],
James T. Ryaby[c], David J. Baylink[a,b]

[a] *Musculoskeletal Disease Center, Jerry L. Pettis V. A. Medical Center, Loma Linda, CA 92357, USA*
[b] *Departments of Medicine and Biochemistry, Loma Linda University, Loma Linda, CA 92354, USA*
[c] *Research and Development, Orthologic Corporation, 1275 Washington St., Tempe, AZ 85281, USA*

Abstract

Microarray analysis of gene expression was performed in the healing femur fractures of 13-week-old male rats during the inflammatory stage of repair, at 3 days post-fracture, and the endochondral bone formation stage of repair, at 11 days post-fracture. Multiple replicate pairs of fracture tissues paired with unfractured tissues, and unfractured control bones that had the stabilizing K-wire were introduced. This approach normalized the marrow contributions to the RNA repertoire. We identified 6555 genes with significant changes in expression in fracture tissues at 3 days and 11 days healing. The repertoire of growth factor genes expressed was also surprisingly restricted at both post-fracture intervals. The large number of Expressed Sequence Tags (ESTs) expressed at both post-fracture times indicates that several molecular pathways yet to be identified regulate fracture repair. The number of genes expressed during immune responses and inflammatory processes was restricted with higher expression largely during the early post-fracture analysis. Several of the genes identified in this study have been associated with regulation of cell and extracellular matrix interactions during scarless healing of fetal skin wounds. These observations suggest that these genes might also regulate the scarless healing characteristic of bone regeneration by similar mechanisms.
© 2005 Elsevier Inc. All rights reserved.

Keywords: Fracture healing; Microarray; Inflammation; Endochondral; Scarless

Introduction

Several million long bone fractures occur annually in the United States, approximately 10% of which display impaired healing [17]. Traditional surgical and non-surgical interventions can facilitate healing, but society would achieve considerable humanitarian and economic benefits from any improvements in fracture treatments. Such improvements would be realized through an understanding of bone repair.

Bone repair requires the regulated expression of diverse families of genes that coordinate complex interactions among various cell types. Endochondral bone repair proceeds through ordered stages of inflammation, intramembranous bone formation, chondrogenesis, endochondral bone formation and finally remodeling [8]. Fracture callus formation eventually results in the bridging of the fracture and the restoration of skeletal integrity. However, bone is unique in that it is one of the very few adult tissues normally capable of healing without a scar, and in this respect, bone repair is a truly regenerative process. Although the molecular pathways that regulate bone repair remain largely unknown, studies of gene expression in endochondral bone repair have established that several extracellular matrix components and growth factor gene families that play significant roles in tissue development are also expressed during the different stages of fracture repair ([1,2,12,22], reviewed by [5,7]). These observations suggest that the molecular regulation of fracture

---

repair is complex but probably recapitulates some aspects of skeletal morphogenesis [19]. If developmental genes regulate both fracture repair and bone regeneration, then these pathways can be characterized by identification of the genes expressed during fracture repair.

Microarray analysis of gene expression offers the opportunity for a global survey of gene expression during fracture repair and the elucidation of the molecular pathways of bone regeneration. Previous examinations of genome-wide gene expression in rodent fracture healing have demonstrated that gene expression in fracture healing is indeed complex and have also been very helpful in identifying known and novel genes that are expressed in fracture healing and elucidating the molecular pathways of bone repair. These studies have generally examined up-regulated genes from a cDNA-subtracted library [20] throughout normal fracture repair or up-regulated and down-regulated genes during very restricted periods in normal fracture repair [28] or in restricted repertoires of genes in the normal fracture model [35]. Models of impaired fracture healing [21,33], determinations of response to fracture therapy [46] or alternative bone healing models [38] have also been utilized. Previous studies have generally analyzed pooled RNA samples, an approach that homogenizes individual biological variations. Additionally, microarray analysis usually uses an arbitrary threshold of 1.5- or 2-fold to identify significant changes in gene expression relative to control tissues. Their design has also utilized unfractured control bones without the stabilizing pin, which incorporates the substantial contributions of the marrow component into the RNA repertoire for examination of gene expression from the control bone, but not from the fractured bone. Each of these variables can affect the interpretation of the results.

The objective of this study was to use whole genome microarray gene analysis to identify the genes expressed in fracture repair of the rat femur at two stages: (1) at 3 days, immediately after the inflammatory phase but prior to bone formation, and (2) at 11 days, when intramembranous and endochondral bone formation overlap [8]. However, two important factors distinguish our approach from previous microarray studies using the rodent fracture model. The unfractured femurs used for the control comparison had the stabilizing Kirschner wire introduced into the intramedullary cavity, which controlled for bone formation induced by the pin in the absence of a fracture, as well as for marrow contributions to the RNA repertoire. We also utilized the Agilent Technologies (Palo Alto, CA) 20,000 gene chip and low-input hybridization system that allowed the examination of gene expression during healing in individual animals without sample pooling and took biological variation into account. This approach allowed us to apply statistical analysis to corroborate the arbitrary thresholds normally used to define significant changes in gene expression between fractured and unfractured bone. The identification of gene expression changes under these conditions of analysis should provide more accurate insights on the molecular pathways that regulate the bone repair and regeneration and suggest potential therapeutic pathways to enhance the healing of bone injuries.

Materials and methods

Femur fractures were produced in 13-week-old male Sprague–Dawley rats (Harlan, Indianapolis, IN) by the three-point bending technique [9]. Thirteen-week-old rats were used in this study because (a) as young adults, these animals had passed the period of most rapid adolescent bone growth that might affect interpretations of gene expression in fracture healing, and (b) the fracture healing ability of younger animals is expected to be more effective than older animals. A 1.14-mm diameter stabilizing Kirschner (K)-wire was inserted in both fractured and unfractured control femurs to ablate the marrow equally in each bone. This approach normalized the substantial contributions of the marrow to the fracture RNA repertoire and controlled for marrow gene expression unrelated to fracture healing and gene expression due to K-wire induction of bone formation in the marrow.

RNA was purified from the fracture diaphyses at two post-fracture healing times: 3 days, between the inflammation and intramembranous bone formation stages, and 11 days, during the endochondral bone formation stage. These post-fracture times were sufficiently separated to provide an examination of very different stages of bone healing and identify the molecular pathways that regulate each stage. Briefly, the diaphysis was isolated from the fractured femur and from an unfractured control femur with a K-wire at each post-fracture time. The bone was pulverized while cooled with liquid nitrogen, and the RNA was isolated using Trizol (Invitrogen, Carlsbad, CA) according to the manufacturer's directions. Total RNA was further purified by RNeasy columns (Qiagen, Valencia, CA) according to the manufacturer's specifications, quantified by Nanodrop (Agilent) and its integrity confirmed by Bioanalyzer (Agilent).

Microarray analysis was performed using the Agilent low-input labeling system and the Cy-5 or Cy-3 labeled RNA applied to the rat 20,000 oligomer microarray chip (Agilent). The low-input system allowed the use of low RNA recoveries from the control tissues and avoided pooling samples that could conceal individual variations in gene expression. Individual fracture tissues were randomly paired with individual K-wire stabilized but unfractured tissues: 5 pairs of tissues were compared at 3 days healing, and 8 pairs of tissues were compared at 11 days healing. Microarray image segmentation analysis was performed using ImaGene software (BioDiscovery, El Segundo, CA), that used an internal statistical analysis of the signal intensity of the spot and immediate surrounding area to flag each spot as present, empty, negative or marginal. Gene expression results were based upon spots flagged as present as well as those flagged as present or marginal. Lowess normalization and statistical analysis were performed using the Genespring software package (Agilent). Changes in gene expression at $P < 0.05$ were deemed significant.

Changes in gene expression as determined by microarray analysis were independently confirmed by real-time RT-PCR for selected genes of interest. This confirmation was performed on some of the same fracture tissues that underwent microarray analysis, as well as additional fracture tissues at 3 and 11 days healing. Total RNA was treated with DNAse I (Invitrogen) and reverse transcribed using the Superscript III kit (Invitrogen) according to the manufacturer's specifications. Real-time RT-PCR was performed on 50 ng of cDNA using gene-specific primers (Integrated DNA Technologies, Coralville, IA) and the Quantitect sybr green detection (Qiagen) as specified by the manufacturer. Real-time PCR was performed on a DNA Engine Opticon thermal cycler (Biorad Laboratories, Hercules, CA) at 45 s per step for 35 cycles at annealing temperatures optimized to amplify the gene of interest and the housekeeping gene (Table 1). Each gene of interest was normalized to expression of the housekeeping gene cyclophilin for each fracture tissue.

Results

Microarray analysis of fracture calluses at 3 days and 11 days post-fracture identified 6555 genes with significant changes in expression ($P < 0.05$), 67% (4873) of which were known genes and 33% (1682) of which were unidentified genes and ESTs (Table 2).

Table 1
Real-time PCR primers and conditions for the detection of scarless wound healing gene expression

Target gene		Primers				Annealing temperature [a]
Name	Accession	Position	Direction	Product	Sequence	
Cyclophilin	BC059141	320	Forward	192	5′-GCATACAGGTCCTGGCATCT-3′	
		511	Reverse		5′-TCTTGCTGGTCTTGCCATTC-3′	
Fibromodulin	NM_080698	901	Forward	232	5′-ATGGCCTTGCTACCAACACC-3′	55.2
		1132	Reverse		5′-ATAGCGCTGCGCTTGATCTC-3′	
Meox-2	NM_017149	569	Forward	301	5′-GTCCTGTGCTCCAACTCTTC-3′	53.7
		869	Reverse		5′-GGTCTAGGTTCACCGCTATC-3′	
Mmp-14	NM_031056	966	Forward	330	5′-ACTTCGTGTTGCCTGATGAC-3′	56.5
		1295	Reverse		5′-TGCCATCCTTCCTCTCATAG-3′	
PN-1	NM_012620	2656	Forward	267	5′-CTCCTGGTCAACCACCTTAG-3′	55.4
		2922	Reverse		5′-CCTGTGGTACACGGTGTATG-3′	
Prx-2	NM_238327	432	Forward	227	5′-CTCGCTGCTCAAGTCTTACG-3′	56.2
		658	Reverse		5′-GGCTGTGGTGTAAGCTGAAC-3′	
TGF-β3	BC092195	1067	Forward	194	5′-CAGCATCCACTGTCCATGTC-3′	56.4
		1260	Reverse		5′-GTCGGTGTGGAGGAATCATC-3′	
HAS-1 [b]	NM_172323	1543	Forward	219	5′-CTGGCTGCTAACTATGTACC-3′	54.5
		1761	Reverse		5′-TCTGCACAGTCTCCTTACAC-3′	

[a] Each annealing temperature produces the most efficient amplification of cyclophilin and in the gene of interest.
[b] Hyaluronic acid synthetase-1.

An examination of the known genes that were significantly up-regulated or down-regulated revealed that several are associated with fracture healing in previous fracture expression analyses, including several extracellular molecules and members of selected growth factor gene families (Table 3). The increases in expression of these genes corresponded generally to those gene expression changes in previous studies at similar post-fracture healing times, though there were differences in magnitude of expression between studies. The changes in gene expression among other genes did vary between studies; different genes compared well with one study but not with another (data not shown).

A "Gene Ontology" classification [4] of the genes with statistically significant changes in expression was performed for 3 days healing, 11 days healing and both 3 and 11 days healing

Table 2
Summary of fracture microarray gene expression changes

Expression change ($P < 0.05$)	Known Genes	Unknown Genes	Total
3 days			
Up at 3 days, no change at 11 days	889	215	1104
Down at 3 days, no change at 11 days	1013	388	1401
11 days			
Up at 11 days, no change at 3 days	904	345	1249
Down at 11 days, no change at 3 days	1206	450	1656
3 and 11 days			
Up at both 3 and 11 days	354	96	450
Down at both 3 and 11 days	474	181	655
Biphasic			
Up at 3 days, down at 11 days	20	1	21
Down at 3 days, up at 11 days	13	6	19
Total	4873	1682	6555

(Table 4). Because there were 4873 known genes with significantly altered expression at $P < 0.05$, only those genes with changes in expression at $P < 0.0002$ were included. Even at this very high level of statistical significance, this list revealed some TGFβ-related genes, developmental transcription factors, extracellular matrix and adhesion genes, and provided an initial analysis from which to further examine and functionally associate genes with less significant levels of expression.

The up-regulated inflammatory and immune genes were further examined (Table 5). Relatively few inflammatory genes were significantly up-regulated in expression, those that were observed at 3 days post-fracture, corresponding to the established inflammatory phase of fracture repair [8]. B cell, T cell and major histocompatibility genes were notably absent. Members of the complement pathway were present, but the cascade ended before C3a activation, suggesting regulation of innate immunity and the inflammatory response. Relatively few interleukins and Cluster of Differentiation (CD) antigens were represented, and some of those could have non-inflammatory or non-immune functions [24].

To determine whether regenerative molecular pathways are common in fracture repair and tissue development, we examined growth factor genes and transcription factors involved in skeletal development at 3 and 11 days healing (Table 6). Developmental factor and homeodomain transcription factor genes showed statistically significant and greater fold-changes in expression during fracture repair. This analysis included TGF-β3, and the paired box transcription factor Prx-2, not previously described in fracture healing. A further examination of genes related to TGF-β3 and Prx-2 revealed several growth factors and extracellular matrix genes previously described in studies of scarless wound healing in fetal skin. Real-time PCR measurements of changes in expression of some of these genes generally confirmed their up-regulation in expression during fracture repair, although there was a

Table 3
Comparison of selected genes with up-regulated expression in this study with previous fracture studies

This study					Previous fracture studies
Gene	Accession	Function	Fold-change ($P < 0.05$)		Similar change in expression
			3 days	11 days	
Transforming growth factor β-2	BF420705	Growth factor	1.3	1.6	[12]
Transforming growth factor β-3	NM_013174	Growth factor	2.4	2.0	[12,20,28]
Fibroblast growth factor 7	NM_022182	Growth factor	1.3	NS	[20,28]
Interleukin 6	NM_012589	Inflammation	3.5	NS	[12,28]
Angiopoietin-2 (like)	NM_133569	Angiogenesis	NS	1.4	[33]
Mesenchymal homeobox-2	NM_017149	Transcription factor	2.5	2.8	[20]
Pleiotrophin/OSF-1	NM_017066	Several	2.3	NS	[20,28]
Frizzled	NM_021266	wnt signaling	1.5	1.5	[20]
Cysteine-rich protein 61	NM_031327	Extracellular matrix signaling	2.6	2.8	[20,28]
Fibronectin	NM_019143	Extracellular matrix	2.4	2.1	[20,28]
Tenascin	BE126741	Extracellular matrix	2.1	1.5	[20,28]
Thrombospondin-2	BF408413	Extracellular matrix	1.7	1.8	[20,28]
Osteonectin/SPARC	NM_012656	Extracellular matrix	1.7	NS	[20,28]
Aggrecan	NM_022190	Extracellular matrix	NS	5.1	[20,28,33]
Collagen 2α1	AA899303	Cartilage maturation	0.8	1.5	[20,28,33]
Integrin binding sialoprotein	NM_012587	Mineralization	4.0	NS	[20,28]
Collagen 5α1	NM_134452	Extracellular matrix	2.4	2.1	[20,28]
Osteocalcin/Gla	NM_012862	Mineralization	NS	2.4	[12,20,28,33]
Protease nexin-1	X89963.1	Extracellular matrix protease	2.1	2.1	[20,28]

NS—not significant.

difference in the magnitude of expression noted for some genes (Table 6).

Discussion

Our global analysis of fracture tissue gene expression recognized many genes important in fracture repair, underscoring the complexity of the fracture repair process (Table 2). The numbers of genes with significant changes in expression at 3 or 11 days indicated that relatively few genes were common to both the inflammatory–intramembranous bone formation and endochondral bone formation stages of fracture repair, and different molecular pathways of gene expression regulate different phases of bone healing. The large number of unknown genes and ESTs identified by our analysis also implies that novel, yet-to-be identified molecular pathways play significant roles in the regulation of fracture repair, and that bone regeneration will need to be characterized by a detailed examination of gene expression in bone healing.

An examination of the known genes that displayed significant changes in expression either up-regulated or down-regulated at 3 and 11 days healing revealed representatives of several growth factor gene families observed in previous studies of gene expression in fracture repair (Table 2). With respect to the collagens and growth factors, we generally found agreement with previous studies [12] and in comparable clusters by Hadjiargyrou et al. [20] and at 3 days post-fracture with the later time point examined by Li et al. [28]. Among the growth factors observed at the earliest time point in healing fractures in younger rats [33], only one vascular endothelial growth factor (VEGF) isoform was represented, though the same extracellular matrix molecules were expressed. Differences in fracture gene expression between studies were common, and it appears that

variations in experimental approaches, in addition to biological variation in the regulation of fracture healing, can affect interpretations of gene expression changes.

Several Gene Ontology categories were represented that suggested important regulatory pathways at each time, even at a high level of significance (Table 4). The cell proliferation and protein metabolism categories were well represented at 3 days healing, as required for the subsequent proliferation of periosteal mesenchymal cells of the early soft callus. Several members of the skeletal development, cell adhesion and extracellular matrix categories were present at 11 days healing, consistent with the maturation of the various callus tissues during endochondral bone formation. This classification provided an insight into important molecular pathways of fracture repair that could be further characterized by an analysis of functionally related genes with less significant changes in expression.

Despite the importance of the inflammatory reaction early in fracture healing, the expression of inflammatory genes in fracture healing has not been well characterized. The marrow can be a major source of RNA and inflammatory gene expression resulting from damage produced by K-wire stabilization of the fractured bone. Our fracture controls included the K-wire that ablated the marrow to the same degree as the fracture, normalizing the marrow repertoire to allow for more sensitive detection of inflammatory gene expression in the periosteum, whose vessels constitute the major blood supply to the fracture [11]. Several inflammatory and immune-related genes were observed to be down-regulated in expression at 3 days post-fracture by Li et al. [28]. However, conflicting results were presented showing an up-regulation of inflammatory and immune genes in the cDNA-subtracted library microarray analysis performed by Hadjiargyrou et al. [20], suggesting that

Table 4
Known genes with highly significant ($P < 0.0002$) changes in the expression during fracture healing

Accession	Fold-change		Gene description	Gene ontology category [4]
	3 days	11 days		
BQ209997	**5.02**	**7.80**	Similar to mouse collagenous repeat-containing 26-kDa protein (CORS26)	Protein metabolism
AA858962	**4.36**	**2.15**	Rat retinol-binding protein (RBP) mRNA, partial cds	Vitamin A metabolism
NM_012587	**3.97**		*Rattus norvegicus* integrin binding sialoprotein (Ibsp)	Extracellular space
BQ211765	**3.49**		*Rattus norvegicus* DEXRAS1 (Dexras1) mRNA	Signal transduction
BF415205	**2.78**	**6.19**	Rat mRNA fragment for cardiac actin	Actin cytoskeleton
NM_133566	**2.29**	**1.21**	*Rattus norvegicus* cystatin N (LOC171096)	Organogenesis and histogenesis
NM_013104	**1.97**	**4.58**	*Rattus norvegicus* Insulin-like growth factor binding protein 6 (Igfbp6)	Extracellular space
BQ209870	**1.80**	**3.88**	Similar secreted modular calcium-binding protein 2 [*Mus musculus*]	Calcium ion binding
CA510266	**1.71**	**1.32**	Similar to prefoldin 5; myc modulator-1; c-myc binding protein [*Homo sapiens*]	Regulation of transcription, DNA dependent
NM_012488	**1.55**	**2.53**	*Rattus norvegicus* α-2-macroglobulin (A2m)	Protease inhibitor activity/IL-1, IL-8 binding
BE329208	**1.52**	**1.43**	similar to *Cricetulus griseus* SREBP cleavage activating protein (SCAP), complete cds	Steroid metabolism
NM_012816	**1.41**		*Rattus norvegicus* α-methylacyl-CoA racemase (Amacr)	Metabolism/peroxisome
NM_057197	**1.40**		*Rattus norvegicus* 2,4-dienoyl CoA reductase 1, mitochondrial (Decr1)	Oxidoreductase
NM_031646	**1.39**		*Rattus norvegicus* receptor (calcitonin) activity modifying protein 2 (Ramp2)	G-protein-coupled receptor signaling
NM_031050	**1.38**		*Rattus norvegicus* lumican (Lum)	Extracellular matrix
NM_017355	**1.27**	**1.24**	*Rattus norvegicus* ras-related GTP-binding protein 4b (Rab4b)	Vesicle-mediated transport
U56859.1	0.90	0.79	*Rattus norvegicus* heparan sulfate proteoglycan, perlecan domain I (RPF-I), partial cds	Cell adhesion
BF281804	0.85	0.84	Similar to solute carrier family 7 member 12; isc-type amino acid transporter 2 [*Mus musculus*]	Amino acid transport
NM_017140	0.85		*Rattus norvegicus* dopamine receptor D3 (Drd3)	Dopamine receptor signaling pathway
BF548886	0.85	0.78	Similar to mouse T cell antigen receptor α-chain (TCR-ATF2), partial cds	Regulation of transcription, DNA dependent
NM_013029	0.84	0.79	*Rattus norvegicus* sialyltransferase 8 (GT3 alpha 2,8-sialyltransferase) C (Siat8c)	Amino acid glycosylation
NM_012997	0.82	0.74	*Rattus norvegicus* Purinergic receptor P2X, ligand-gated ion channel, 1 (P2rx1)	Amino acid transport
NM_031725	0.82		*Rattus norvegicus* secretory carrier membrane protein 4 (Scamp4)	Protein transport
AA900738	0.80	0.81	Similar to rat DNA for serine dehydratase	Amino acid metabolism/gluconeogenesis
NM_133322	0.79	0.77	*Rattus norvegicus* potassium voltage-gated channel, KQT-like subfamily, member 2 (Kcnq2)	Synaptic transmission
NM_052801	0.78	0.76	*Rattus norvegicus* von Hippel-Lindau syndrome (Vhl)	Regulation of transcription, DNA dependent/proteolysis and peptidolysis
CB546252	0.78	0.83	Similar to zinc finger protein 261; DXHXS6673E [*Mus musculus*]	Nucleus/zinc ion binding
NM_144730	0.78	0.80	*Rattus norvegicus* GATA-binding protein 4 (Gata4)	Regulation of transcription, DNA dependent
NM_030854		**21.97**	*Rattus norvegicus* chondromodulin-1 (Chm-1)	Cell growth and maintenance/proteoglycan metabolism
BF560915		**17.46**	*Rattus norvegicus* mRNA for collagen α 1 type X, partial	Skeletal development
NM_019189		**13.77**	*Rattus norvegicus* cartilage link protein 1 (Crtl1)	Hyaluronic acid binding
NM_012929		**11.38**	*Rattus norvegicus* Procollagen II α 1 (Col2a1)	Skeletal development
NM_031511		**6.72**	*Rattus norvegicus* insulin-like growth factor II (somatomedin A) (Igf2)	Development
BQ210664		**5.73**	Similar to cartilage intermediate layer protein	Unknown
BQ191772		**5.37**	Similar to mouse annexin A8	Phospholipid binding
NM_022290		**5.28**	*Rattus norvegicus* tenomodulin (Tnmd)	Collagen maturation
AI576621		**3.73**	Similar to mouse carboxypeptidase X2, complete cds	Protein binding
AA963765		**2.89**	Similar to osteoglycin [*Mus musculus*]	Regulation of DNA transcription
BQ200482		**1.41**	Similar to mouse mRNA for acetylglucosaminyltransferase-like protein	Lipopolysaccharide biosynthesis
CB547946		**1.35**	Similar to *Mus musculus* (clone pVZmSin3B) mSin3B, complete cds	Regulation of transcription, DNA dependent
AI059288		0.83	Similar to mouse B cell activating factor (TNFSF13b, Baff), complete cds	Positive regulation of cell proliferation
CB547491		0.83	Similar to *Mus musculus* very large G-protein-coupled receptor 1 (Vlgr1, Mass1), complete cds	G-protein-coupled receptor signaling
CB545755		0.82	Similar to RAD54 like (*S. cerevisiae*) [*Mus musculus*]	DNA recombination, repair
CB544611		0.82	Similar to BACR7A4.19 gene product [*Drosophila melanogaster*]	G-protein-coupled receptor signaling
CB545661		0.81	Similar to BC026845_1 *Mus musculus*, similar to nucleoporin 133kD, complete cds	RNA metabolism
AW920271		0.81	Similar to mouse cat eye syndrome chromosome region, candidate 5 (Cecr5), complete cds	Metabolism
BQ196556		0.80	Similar to nudix (nucleoside diphosphate linked moiety X)-type motif 5 [*Mus musculus*]	Oxidative stress response/DNA repair
AA874884		0.60	Rat heme oxygenase gene, complete cds	Oxidoreductase activity
NM_031740		0.59	*Rattus norvegicus* UDP-Gal:betaGlcNAc beta 1,4-galactosyltransferase, polypeptide 6 (B4galt6)	Glyosphingolipid biosynthesis
NM_053843		0.49	*Rattus norvegicus* Fc receptor, IgG, low affinity III (Fcgr3)	Immune response

Bold: up-regulated.

Table 5
Up-regulated expression in fracture in inflammation and immune function genes

Gene		Functions	Fold-Change in expression (P < 0.05)	
Description [Reference]	Accession		3 days	11 days
Growth factors				
Platelet-derived growth factor receptor [31]	AA925099	Chemotaxis	2.7	1.5
Monocyte chemotactic protein 3 [32]	BF419899	Chemotaxis	3.3	1.6
Mast cell growth factor/kit ligand [36]	AI102098	Stem cell factor, hematopoietic and mast cell growth	1.3	NS
TNFα/TNFβ [15]	AA819277	Inflammation	NS	1.2
TRAF2	BI282097	TNF inflammation	1.1	NS
TRAF4	CB546212	TNF inflammation	1.6	NS
TNF-stimulated gene 6	AF159103.1	TNF inflammation	1.8	1.7
TGFβ2 [13]	BF420705	Inflammation	1.3	1.6
LTBP1	NM_021587	TGF regulation	1.9	1.5
TGFβli4	NM_013043	TGF regulation	1.8	1.9
Interleukins and related cytokines (www.copewithcytokines.de) [23]				
IL1 receptor accessory protein [16]	NM_012968	IL1 inflammation	1.6	NS
IL3 regulated nuclear factor	NM_053727	IL3 MHC, eosinphil, basophil stimulation, apoptosis inhibition	1.4	NS
IL6 [6]	NM_012589	Acute phase protein induction, proliferation	3.5	NS
IL6 gp130	298242_Rn	IL6 acute phase protein induction	1.7	1.4
IL6 signal transduction protein	BF398277	IL6 acute phase protein induction	1.5	1.4
IL11 receptor alpha 1	221254_Rn	IL11 progenitor growth factor, acute phase protein induction	NS	1.3
IL12 p40 precursor	NM_022611	IL12 hematopoeitic response, adhesion	NS	1.3
IL18	284329_Rn	T cell activation, hematopoiesis	1.3	NS
Interferon-γ	NM_138880	Immune response	NS	1.4
Interferon inducible p27-like	NM_130743	Immune response	1.4	1.4
ATP-dependent interferon responsive	BG373987	Immune response	NS	1.4
Complement pathway (users.rcn.com/jkimball.ma.ultranet/BiologyPages/C/Complement.html) [26]				
Complement 1Q binding protein	NM_019259	Complement 4 activation	1.7	NS
Complement 1R	AA799803	Complement 4 activation	1.7	1.4
Complement 1S	NM_138900	Complement 4 activation	2	2.6
Complement 2	NM_172222	Complement 3 activation	NS	1.4
Complement 4	AI412156	Complement 2 activation	NS	2.3
Complement H	NM_130409	Complement 3 inhibition	1.6	NS
Complement I	NM_024157	Complement 3 inhibition	NS	1.1

Table 5 (*continued*)

Gene		Functions	Fold-Change in expression (P < 0.05)	
Description [Reference]	Accession		3 days	11 days
CDs [24]				
CD14	NM_021744	LPS receptor	1.4	NS
CD39-like 3	AI070096	Ecto-nucleoside triphosphate diphosphohydrolase	1.5	NS
CD34	AI102873	Adhesion, stem cell marker	1.6	1.9
CD36 [18]	NM_054001	Scavenger receptor, inflammation, angiogenesis	1.6	NS
CD81	NM_013087	T cell stimulation	1.8	2.1
CD151	NM_022523	Adhesion, signaling	1.4	1.3
CD164	NM_031812	Hematopoeitic-stromal interaction	1.6	1.2

NS—not significant.

the repertoire of expressed genes can be affected by marrow contributions to the fracture model.

In this study, the up-regulation of the platelet-derived growth factor (PDGF) receptor gene implicated PDGF genes during inflammation. The mast cell growth factor, monocyte chemotactic protein 3 [32] and members of the tumor necrosis factor family [15] displayed up-regulated expression, which was higher at 3 days post-fracture (Table 5) and consistent with inflammatory functions in healing. Most notably, in comparison to previous microarray studies [20,28], the T cell receptor, immunoglobulin genes and major histocompatibility genes displayed no significant changes during early and later fracture healing. Though 3 days is probably too early for the adaptive immune response, if immune genes were functional in fracture repair, their expression would be observed by 11 days post-fracture. In agreement with previous studies [20], the innate immunity complement genes were up-regulated; however, the complement cascade ceased expression at C3a, the initial immune effector complement component, probably through expression of C3 inhibitors (Table 5). As with growth factor expression, the repertoire of interleukins and CD antigens were similar to other studies with some variations in individual members. The inflammatory mediators interleukin IL-1 [16] and IL-6 [6] and their related components, also observed in other studies, were up-regulated in early fracture healing. Other interleukins and CD antigens were up-regulated later in healing and could be assigned non-inflammatory and non-immune functions. We conclude that marrow gene expression could affect interpretations of microarray analysis in fracture repair.

Bone is the only adult tissue that is capable of healing without scar formation [10], and an examination of fracture gene expression from previous studies (Table 3) in combination with a more detailed analysis of our Gene Ontology list (Table 4) identified growth factors and developmental genes previously associated with scarless fetal skin repair that might also regulate bone regeneration during fracture healing (Table 6). The genes previously associated with scarless fetal skin wound

Table 6
Fracture microarray genes associated with scarless fetal wound healing

Gene (function) [Reference]	Accession	3-day expression		11-day expression	
		Microarray ($P < 0.05$)	Real-time PCR	Microarray ($P < 0.05$)	Real-time PCR
		Fold-change	Fold-change [a] (n)	Fold-change	Fold-change [a] (n)
Homeodomain					
Prx-2 (TGF-β3, PN-1 regulation) [10,43]	BE118447	4.4	2.2 ± 1.9 (7)	2.7	2.6 ± 1.6 (6)
Meox-2 (cell migration) [48]	NM_017149	2.5	1.7 ± 0.6 (9)	2.8	2.5 ± 1.8 (5)
TGF-β3-related					
TGF-β3 (proliferation, differentiation) [13]	NM_013174	2.4	1.7 ± 0.9 (7)	2	4.3 ± 2.0 (8)
LTBP-1 (TGF-β3 binding) [39]	NM_021587	1.9	ND	1.5	ND
Fibromodulin [23,44]	NM_080698	2.3	2.1 ± 1.2 (8)	5.2	21.0 ± 13.2 (6)
Other growth factors					
VEGF-C (angiogenesis) [10]	NM_053653	1.2	ND	NS	ND
Hepatocyte Growth Factor (anti-apoptosis) [37]	NM_017017	NS	ND	1.4	ND
Extracellular matrix (ECM) [10]					
Fibronectin-1	NM_019143	2.4	ND	2.7	ND
Collagen V (*a*1) (cell spreading)	NM_134452	2.4	ND	2.1	ND
ECM matricellular (adhesion) [34]					
Tenascin [13,25,29]	BE126741	2.1	ND	1.5	ND
Calpactin I Heavy Chain (Ten receptor)	NM_019905	1.9	ND	NS	ND
Thrombospondin-2	BF408413	1.7	ND	1.8	ND
Thrombospondin-4	X89963.1	1.9	ND	3.6	ND
Calreticulin (TSP-receptor)	NM_022399	1.6	ND	NS	ND
SPARC	NM_012656	1.7	ND	NS	ND
ECM remodeling					
Protease Nexin-1 (ECM regulation) [41]	X89963.1	2.1	1.1 ± 0.5 (8)	2.1	12.3 ± 6.4 (8)
Mmp-14 [14]	NM_031056	NS	1.1 ± 0.5 (10)	2.1	4.2 ± 1.8 (9)
TIMP-2 (Mmp-14 regulation) [3]	NM_021989	2.3	ND	1.8	ND

NS—not significant; ND—not determined; n—number of fractured vs. unfractured pairs of tissues in real-time RT-PCR.

[a] mean ± SD.

healing are diverse in function, but those identified to date influence the turnover or adhesion of cells and extracellular matrix components [10]. The genes associated with scarless wound healing and not observed in previous studies might have displayed less dramatic changes in expression that we were able to detect with the statistical approach afforded by the multiple replicates in our study.

Due to their extensively documented regulation during tissue development, the homeodomain transcription factors are obvious candidates for the regulation of bone regeneration. The paired-related homeodomain transcription factor Prx-2 has been previously associated with scarless wound healing [47] and displayed significant increases in expression in fracture healing. Tenascin-C [25] and the plasmin inhibitor protease nexin (PN)-1 [43] have been identified as possible target genes of Prx-2 expression; they also displayed significant increases in expression in fracture healing. Prx-2-mediated changes in the extracellular matrix components through tenascin and PN-1 expression could bind and alter TGF-β3 availability. Consequently, our findings support the involvement of Prx-2 in fracture healing, suggesting a similarity of molecular pathways in both fracture healing and scarless healing in fetal tissues. The expression of the mesenchymal homeodomain transcription

factor Meox-2 was also up-regulated during fracture healing. Its role is not well defined, but it has been shown to affect cell migration during developmental somitogenesis [30,48]. Meox-2 expression might therefore regulate bone regeneration by balancing cell adhesion and migration.

Growth factor genes involved in skeletal development and previously associated with scarless fetal wound healing were identified. TGF-β3 gene expression was especially notable in this respect [27,45], as it was increased 2-fold throughout fracture healing. The TGFs are pleiotropic growth factors that could exert varied effects on inflammation, proliferation, differentiation and apoptosis in the healing fracture [13]. The TGFs could also be differentially regulated post-transcriptionally by specific extracellular matrix components, such as latent TGF binding protein (LTBP)-1 [39] and fibromodulin [44]. Other growth factor genes expressed in scarless fetal wound healing that were also up-regulated in fracture healing included the angiogenic VEGF-C gene [10] and the apoptosis inhibitor hepatocyte growth factor [37].

The up-regulation of tenascin expression immediately suggested that additional matricellular genes could modulate cell–matrix adhesion and de-adhesion [34]. The expression of the matricellular genes and their respective receptors was up-
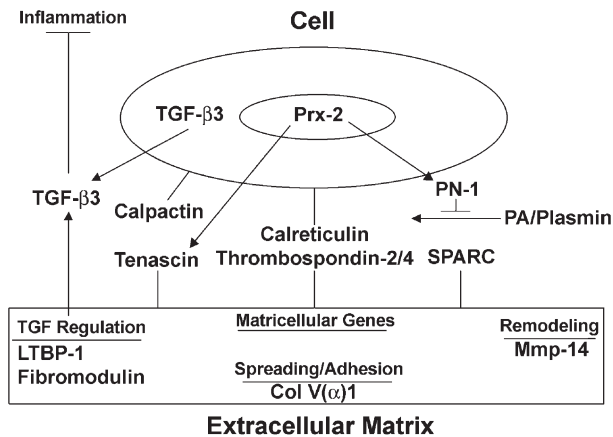
Fig. 1. A model for bone regeneration regulation by scarless fetal wound healing genes. TGF-β3 exerts pleiotropic effects, including inhibition of inflammation. Cell motility and cell–matrix adhesion are mediated by the matricellular genes and their receptors, whose digestion by plasmin is inhibited by PN-1.

regulated throughout fracture healing (Table 6). Although only thrombospondin-1 has been associated with fetal wound healing [42], these genes are critical in regulating the cell–matrix interactions implicated in scarless wound healing by other genes expressed in fetal skin repair. The extracellular matrix composition might also affect expression of the remodeling genes, such as matrix metalloproteinase (mmp)-14, observed in both scarless wound healing [14] and during endochondral bone formation in this study.

These results suggest that a similar set of genes that regulate normal tissue healing and scarless wound healing are differentially expressed during the inflammatory and endochondral stages of fracture repair. These include genes that modulate cell–matrix interactions and extracellular matrix organization at different times during healing, such as the matricellular genes. Other genes regulate these genes transcriptionally or posttranscriptionally; examples are Prx-2 and PN-1 inhibition of plasmin [41] and the pleiotropic effects TGF-β3, which might include the inhibition of inflammation (Fig. 1). The expression of these common genes implies that the molecular pathways of fracture repair mediate bone regeneration by mechanisms similar to scarless fetal wound healing.

We examined gene expression during the normal repair of a simple femur fracture with the elimination of scar tissue from the healing bone. This model does not address impaired healing, such as fracture non-unions, in which fibrous tissue is retained within the fracture gap without healing of the injured bone. Fracture non-unions can result from several causes beyond the scope of this study, including severe trauma to the bone, often with extensive comminution or a large interfragmentary gap, interruption of the periosteal blood supply and nerves, as well as infection associated with trauma (reviewed in [40]). Nevertheless, even in the absence of very severe trauma, a fracture nonunion that results simply from a large interfragmentary gap or excessive motion of the fracture tissues implicates the extracellular matrix as an important mediator of tissue repair.

In conclusion, we identified 6555 genes with significant changes in expression in fracture tissues at 3 days and 11 days

healing using the Agilent rat 20,000 gene chip. Our approach took advantage of multiple replicates of fracture tissues paired with unfractured tissues with the K-wire introduced into the bone to examine gene expression at these critical times of fracture healing. The induction and resolution of the inflammatory phase of early fracture healing are important for the transition from inflammation to repair; it immediately affects the deposition and resolution of the extracellular matrix and ultimately affects osteogenesis in bone and scar production in injured tissues. A profile of inflammatory gene expression during the early stages of fracture repair identified fewer inflammatory mediators of fracture healing than in previous microarray studies. The intramedullary K-wire also causes intramedullary damage to the bone that might increase osteogenic activity outside of the fracture callus and affect femoral gene expression during endochondral bone repair. Several of the genes identified during early and later fracture healing have been associated with regulation of the extracellular matrix during scarless healing of fetal skin wounds. A comparison of gene expression in fracture repair by microarray analysis with fetal scarless wound healing would present an ideal opportunity to ascertain additional genes that regulate bone regeneration. The expression of genes that regulate the regenerative qualities of bone repair can be used to elucidate therapies for improved wound healing of both skeletal and nonskeletal tissues.

References

[1] Andrew JG, Hoyland J, Freemont AJ, Marsh D. Insulinlike growth factor gene expression in human fracture callus. Calcif Tissue Int 1993;53:97–102.
[2] Andrew JG, Hoyland JA, Freemont AJ, Marsh DR. Platelet-derived growth factor expression in normally healing human fractures. Bone 1995;16:455–60.
[3] Apte SS, Fukai N, Beier DR, Olsen BR. The matrix metalloproteinase-14 (MMP-14) gene is structurally distinct from other MMP genes and is co-expressed with the TIMP-2 gene during mouse embryogenesis. J Biol Chem 1997;272:25511–7.
[4] Ashburner M, Ball CA, Blake JA, Botstein D, Butler H, Cherry JM, et al. Gene ontology: tool for the unification of biology. The Gene Ontology Consortium. Nat Genet 2000;25:25–9.
[5] Barnes GL, Kostenuik PJ, Gerstenfeld LC, Einhorn TA. Growth factor regulation of fracture repair. J Bone Miner Res 1999;14:1805–15.
[6] Baumann H, Gauldie J. The acute phase response. Immunol Today 1994;15:74–80.
[7] Beasley LS, Einhorn TA. Role of growth factors in fracture healing. In:

Canalis E, editor. Skeletal growth factors. Philadelphia, PA: Lippencott, Williams and Wilkins; 2000. p. 311–22.

[8] Bolander ME. Regulation of fracture repair by growth factors. Proc Soc Exp Biol Med 1992;200:165–70.

[9] Bonnarens F, Einhorn TA. Production of a standard closed fracture in laboratory animal bone. J Orthop Res 1984;2:97–101.

[10] Bullard KM, Longaker MT, Lorenz HP. Fetal wound healing: current biology. World J Surg 2003;27:54–61.

[11] Chanavaz M. Anatomy and histophysiology of the periosteum: quantification of the periosteal blood supply to the adjacent bone with ^{85}Sr and gamma spectrometry. J Oral Implantol 1995;21:214–9.

[12] Cho T-J, Gerstenfeld LC, Einhorn TA. Differential temporal expression of members of the transforming growth factor B superfamily during murine fracture healing. J Bone Miner Res 2000;17:513–20.

[13] Clark DA, Coker R. Transforming growth factor-β (TGF-β). Int J Biochem Cell Biol 1998;30:293–8.

[14] Dang CM, Beanes SR, Lee H, Zhang X, Soo C, Ting KD. Scarless fetal wounds are associated with an increased matrix metalloproteinase-to-tissue-derived inhibitor of metalloproteinase ratio. Plastic Reconstr Surg 2003;111:2273–85.

[15] Dinarello CA. Proinflammatory cytokines. Chest 2000;118:503–8.

[16] Dinarello CA. The IL-1 family and inflammatory diseases. Clin Exp Rheumatol 2002;20:1–13.

[17] Einhorn TA. Enhancement of fracture healing. J Bone Jt Surg 1955;77-A: 940–56.

[18] Febbraio M, Hajjar DP, Silverstein RL. CD36: A class B scavenger receptor involved in angiogenesis, atherscrosis, inflammation, and lipid metabolism. J Clin Invest 2001;108:785–91.

[19] Ferguson C, Aplern E, Miclau T, Helms J. Does adult fracture repair recapitulate embryonic skeletal formation? Mech Dev 1999;87:57–66.

[20] Hadjiargyrou M, Lombardo F, Zhao S, Ahrens W, Joo J, Ahn H, et al. Transcriptional profiling of bone regeneration. Insight into the molecular complexity of wound repair. J Biol Chem 2002;277: 30177–82.

[21] Hatano H, Siegel HJ, Yamagiwa H, Bronk JT, Turner RT, Bolander ME, et al. Identification of estrogen-related genes during fracture healing, using DNA microarray. J Bone Miner Metab 2004;22:224–35.

[22] Hiltunen A, Hannu TA, Vuorio E. Regulation of extracellular matrix genes during fracture healing in mice. Clin Orthop Relat Res 1993;297:23–7.

[23] Ibelgaufts H. COPE: Horst Ibelgaufts' Cytokines Online Pathfinder Encyclopaedia 2003; www.copewithcytokines.de.

[24] Janeway Jr CA, Travers P, Walport M, Schlomchik MJ. In: Janeway Jr AC, editor. Immunobiology: The Immune System in Health and Disease. Fifth ed. New York (NY): Garland Publishing; 2001. Appendix 2.

[25] Jones FS, Meech R, Edelman DB, Oakey RJ, Jones PL. Prx1 controls vascular smooth muscle cell proliferation and tenascin-C expression and is upregulated with Prx2 in pulmonary vascular disease. Circ Res 2001;89:131–8.

[26] Kimball JW. Biology Pages 2005; users.rcn.com/jkimball.ma.ultranet/ BiologyPages/C/Complement.html.

[27] Kohama K, Nonaka K, Hosokawa R, Shum L, Ohishi M. Tgf-β-3 promotes scarless repair of cleft lip in mouse fetuses. J Dent Res 2002;81:688–94.

[28] Li X, Quigg RJ, Zhou J, Ryaby JT, Wang H. Early signals for fracture healing. J Cell Biochem 2005;95:189–205.

[29] Mackie EJ, Halfter W, Liverani D. Induction of tenascin in healing wounds. J Cell Biol 1988;107:2757–67.

[30] Mankoo BS, Skuntz S, Harrigan I, Grigorieva E, Candia A, Wright CV, et al. The concerted action of Meox homeobox genes is required upstream of genetic pathways essential for the formation, patterning and differentiation of somites. Development 2003;130:4655–64.

[31] Mannaioni PF, Di Bello MG, Masini E. Platelets and inflammation: role of platelet-derived growth factor, adhesion molecules and histamine. Inflamm Res 1997;46:4–18.

[32] Menten P, Wuyts A, van Damme J. Monocyte chemotactic protein-3. Eur Cytokine Netw 2001;12:554–60.

[33] Meyer Jr RA, Meyer MH, Tenholder M, Wondracek S, Wasserman R, Garges P. Gene expression in older rats with delayed union of femoral fractures. J Bone Jt Surg 2003;85-A:1243–54.

[34] Murphy-Ullrich JE. The de-adhesive activity of matricellular proteins: is intermediate cell adhesion an adaptive state? J Clin Invest 2001;107: 785–90.

[35] Nakazawa T, Nakajima A, Seki N, Okawa A, Kato M, Moriya H, et al. Gene expression of periostin in the early stage of fracture healing detected by cDNA microarray analysis. J Orthop Res 2004;22:520–5.

[36] Nilsson G, Butterfield JH, Nilsson K, Siegbahn A. Stem cell factor is a chemotactic factor for human mast cells. J Immunol 1994;153:3717–23.

[37] Ono I, Yamashita T, Hida T, Jin HY, Ito Y, Hamada H, et al. Local administration of hepatocyte growth factor gene enhances the regeneration of dermis in acute incisional wounds. J Surg Res 2004;120:47–55.

[38] Pacicca DM, Patel N, Lee C, Salisbury K, Lehmann W, Carvalho R, et al. Expression of angiogenic factors during distraction osteogenesis. Bone 2003;33:889–98.

[39] Rifkin DB. Latent transforming growth factor-β (TGF-β) binding proteins: orchestrators of TGF-β availability. J Biol Chem 2005;280:7409–12.

[40] Rodriguez-Merchan EC, Forriol F. Nonunion: general principles and experimental data. Clin Orthop 2004;419:4–12.

[41] Rossignol P, Ho-Tin-Noe B, Vranckx R, Bouton MC, Meilhac O, Lijnen HR, et al. Protease nexin-1 inhibits plasminogen activation-induced apoptosis of adherent cells. J Biol Chem 2004;279:10346–56.

[42] Roth JJ, Sung JJ, Granick MS, Solomon MP, Longaker MT, Rothman VL, et al. Thrombospondin 1 and its specific cysteine–serine–valine–threonine–cysteine–glycine receptor in fetal wounds. Annu Plast Surg 1999;42:553–63.

[43] Scott KK, Norris RA, Potter SS, Norrington DW, Baybo MA, Hicklin DM, et al. GeneChip microarrays facilitate identification of Protease Nexin-1 as a target gene of the Prx2 (S8) homeoprotein. DNA Cell Biol 2003;22:95–105.

[44] Soo C, Hu F-Y, Zhang X, Wang Y, Beanes SR, Lorenz HP, et al. Differential expression of fibromodulin, a transforming growth factor-B modulator, in fetal skin development and scarless repair. Am J Pathol 2000;157:423–33.

[45] Soo C, Beanes SR, Hu F-Y, Zhang X, Dang C, Chang G, et al. Ontogenetic transition in fetal wound transforming growth factor-β regulation correlates with collagen organization. Am J Pathol 2003;163:2459–76.

[46] Wang H, Li X, Tomin E, Doty SB, Lane JM, Carney DH, et al. Thrombin peptide (TP508) promotes fracture repair by up-regulating inflammatory mediators, early growth factors, and increasing angiogenesis. J Orthop Res 2005;23:671–9.

[47] White P, Thomas DW, Fong S, Stelnicki E, Meijlink F, Largman C, et al. Deletion of the homeobox gene Prx-2 affects fetal but not adult fibroblast wound healing responses. J Invest Dermatol 2003;120:135–44.

[48] Witzenbichler B, Kureishi Y, Luo Z, Le Roux A, Branellec D, Wash K. Regulation of smooth muscle cell migration and integrin expression by the Gax transcription factor. J Clin Invest 1999;104:1469–80.